

**Study on Adsorptive Separation of Toxic Heavy  
Metals from Aquatic Environment**

HOANG ANH VIET

THE UNIVERSITY OF KITAKYUSHU  
Graduate School of Environmental Engineering

2021

# PREFACE

This dissertation work was performed under the supervision of Professor Dr. Syouhei Nishihama and Professor Dr. Kazuharu Yoshizuka at Department of Chemical and Environmental Engineering, Graduate School of Environmental Engineering, The University of Kitakyushu from 2016 to 2021.

The objective is the separation of toxic heavy metals from aquatic environment, using adsorption technique. The adsorptive separation of heavy metals was operated in both of batchwise adsorption and chromatographic adsorption to elucidate selectivity and removal efficiency.

The author hopes that the results in this dissertation could contribute to develop separation of heavy metals from aqueous environment in water treatment and wastewater treatment.

HOANG Anh Viet  
Department of Chemical and Environmental Engineering  
Graduate School of Environmental Engineering  
The University of Kitakyushu

## Table of Contents

<b>Chapter 1. General Introduction</b> .....	1
1.1. Heavy metals.....	1
1.1.1. Source of heavy metals .....	1
1.1.2. Impact of heavy metals on human health.....	5
1.1.3. Methodologies for heavy metals removal .....	7
1.2. Adsorption technique .....	9
1.2.1. Batchwise Adsorption .....	9
1.2.2. Column adsorption.....	11
1.2.3. Adsorbents.....	11
1.3. Objective .....	12
<b>Chapter 2. Adsorptive Removal of Arsenic from Aquatic Environment</b> .....	14
2.1. Introduction .....	14
2.2. Experimental .....	15
2.2.1. Reagents .....	15
2.2.2. Batchwise adsorption .....	15
2.2.3. Column adsorption .....	16
2.3. Results and discussion.....	17
2.3.1. Batchwise adsorption .....	17
2.3.1.1. Effect of pH on arsenic adsorption.....	17
2.3.1.2. Adsorption isotherm.....	19
2.3.1.3. Kinetic study .....	23
2.3.1.4. Desorption process .....	26
2.3.2. Chromatographic removal of arsenic .....	27
2.3.2.1. Removal of arsenic from single solution and mixed solution.....	27
2.3.2.2. Effect of space velocity on arsenic removal .....	29
2.3.2.3. Repeated use of adsorption column .....	31
2.4. Conclusion.....	32
<b>Chapter 3. Reductive Adsorption of Chromium(VI) by Coal-based Activated Carbon</b>	
3.1. Introduction .....	33
3.2. Experimental .....	34

3.2.1.	Reagents .....	34
3.2.2.	Batchwise experiment .....	34
3.2.3.	Column Experiment .....	35
3.3.	Results and discussion.....	36
3.3.1.	Batchwise adsorption .....	36
3.3.1.1.	Effect of pH on reductive adsorption .....	36
3.3.1.2.	Adsorption isotherm.....	39
3.3.1.3.	Thermodynamic adsorption .....	41
3.3.1.4.	Kinetic study .....	45
3.3.2.	Chromatographic operation.....	48
3.4.	Conclusion.....	52
<b>Chapter 4.</b>	<b>Selective Adsorption of Lead(II) from Aqueous Environment.....</b>	<b>53</b>
4.1.	Introduction .....	53
4.2.	Experimental .....	54
4.2.1.	Reagents .....	54
4.2.2.	Batchwise adsorption .....	55
4.2.3.	Column adsorption .....	56
4.3.	Results and discussion.....	56
4.3.1.	Batchwise adsorption .....	56
4.3.1.1.	Effect of pH.....	56
4.3.1.2.	Adsorption isotherm.....	63
4.3.1.3.	Adsorption kinetics .....	67
4.3.1.4.	Desorption process .....	70
4.3.2.	Chromatographic separation .....	70
4.4.	Conclusion.....	73
<b>Chapter 5.</b>	<b>General Conclusion.....</b>	<b>75</b>
<b>References Cited.....</b>		<b>77</b>
<b>List of Publication .....</b>		<b>85</b>
<b>Acknowledgement .....</b>		<b>86</b>

# Chapter 1. General Introduction

## 1.1. Heavy metals

Heavy metals are defined as elements having a high atomic weight between 63.5 and 200.6 and high density [1,2], which tend to accumulate in living organism, causing various disease and disorders [3,4]. The main modes of contaminant access to organisms is through food, drinking and the atmosphere [5]. Industrial, agricultural, and domestic wastes contribute to environmental pollution, which cause adverse harm to living organisms. Studies have reported that heavy metals are found naturally but have been altered by human production to increase the number in the environment. Natural activities such as weathering and volcanic actions have been reported to significantly contribute to heavy metal contamination. Environmental pollution can occur through metal corrosion, atmospheric deposition, soil erosion of metal ions and leaching of heavy metals, sediment resuspension, and metal evaporation from water resources to soil and groundwater. Although heavy metals are naturally occurring elements that are found throughout the earth's crust, anthropogenic activities are also importance sources of environmental pollution. Especially, rapid development of industrial has serious contribute to release of toxic heavy metals discharged into environment. Heavy metals enter the environment through various industrial activities such as metal plating facilities, mining operations, fertilizer industries, tanneries, batteries, paper industries [1,4].

Heavy metals, such as arsenic, selenium, chromium, lead, cadmium, copper, zinc, mercury, cobalt, and nickel, are high toxicity even in minor quantity. They may enter the human body through eating food, drinking water, or absorption through the skin when they come in contact directly with human in industrial, agricultural, manufacturing and residential settings. The toxic heavy metals considered here are arsenic (As), chromium (Cr), lead (Pb), zinc (Zn), cadmium (Cd), and copper (Cu), due to their common present in water environment, their widespread use in industrial activities and their impact on human health.

### 1.1.1. Source of heavy metals

Heavy metals can emanate from both natural and anthropogenic processes and end up in different environmental compartments, such as soil, water, air, and their interface. The natural sources of heavy metals in the environment are usually from the rocks and processes by which they formed, and which affected them after lithification. Under different and certain environmental conditions, natural emissions of heavy metals occur such as rock weathering,

volcanic eruptions, forest fires, sea-salt sprays and wind-borne soil particles. Anthropogenic processes, such as industrial, agricultural, mining, and metallurgical processes, wastewater, and runoff, also cause pollutants to the environment. Some important anthropogenic sources which significant contribute to the heavy metals contamination in the environment include automobile exhaust which releases lead; battery manufacturing which releases lead, zinc, cadmium, and copper; insecticide and rodenticide which releases arsenic; chromium plating which releases chromium and lead; smelting which releases arsenic, copper, and zinc [6]. Human activities are main cause of environmental pollution, due to the everyday manufacturing of goods to obtain the demands of the large population. The most common heavy metals which present in the environment, are arsenic, lead, zinc, copper, cadmium, and chromium.

### **Arsenic**

Arsenic is a ubiquitous element found in the atmosphere, soils and rocks, natural water, and organisms. In natural, arsenic exists in more than 200 ores including elemental arsenic, sulfides, arsenide, oxides, arsenite, and arsenate, which arsenopyrite  $FeAsS$  is the most common arsenic ore mineral. It is generally accepted that arsenopyrite, together with the other dominant arsenic sulfide minerals realgar and orpiment, are only formed under high temperature conditions in the earth's crust. Arsenic is introduced into water by the dissolution of mineral and concentration in groundwater [7]. Geothermal water also contains relatively high contents of arsenic as a result of the leaching of arsenic from rocks, which occurs predominantly in the geothermal reservoir at high temperatures [8]. High level of arsenic concentration have reported in water environment in many countries of Vietnam, Japan,

Table 1.1 The source and concentration level of arsenic in several countries

Location	Concentration ( $\mu\text{g L}^{-1}$ )	Arsenic source	References
Bangladesh	10 – 1000	Well waters	[12]
Kyushu, Japan	<10 – 3230	Geothermal water	[8]
Nepal	8 – 2660	Drinking water	[13]
Hanoi, Vietnam	0 – 3050	Groundwater	[14]
Chile	100 – 1000	Groundwater	[12]
Inner Mongolia, China	1 – 2400	Groundwater	[15]
Ron Phibun, Thailand	4.8 – 583	River	[16]
Cordoba, Argentina	7 – 114	River	[17]

Taiwan, China, India, and Poland [9–11], and causing of many health problems. Table 1.1 shows the source and concentration level of arsenic in several countries [8,12–17]. In water environment, arsenic exists as arsenate, As(V), and arsenite, As(III), in the forms of arsenic acid ( $\text{H}_3\text{AsO}_4$ ) and arsenous acid ( $\text{H}_3\text{AsO}_3$ ). As(III) is often found in reducing conditions as geothermal water and groundwater, whereas As(V) exist in oxidizing conditions as surface water. The arsenic species predominates depends on the pH of the solution. The most dominant species in natural waters are anionic forms as shown in Eqs. (1-1) – (1-3) for As(V) and Eqs. (1-4) – (1-6) for As(III) [18].



## Chromium

Chromium is a natural occurring element present in earth's crust with valence states ranging from chromium(II) to chromium(VI). Chromium compounds are most stable in trivalent (Cr(III)) form and hexavalent form (Cr(VI)). Chromium may enter the environment from natural and anthropogenic sources. The largest release of chromium occurs from industrial establishments, including electroplating, tannery facilities, chromate production, and chrome-plating. The increase in the environmental concentrations of chromium has been linked to wastewater release of chromium, mainly from chrome-plating industry. The characteristics of chrome-plating industry wastewater are given in Table 1.2 [19]. The concentration of Cr(VI) in wastewater ( $5722 \text{ mg L}^{-1}$ ) was much larger than the effluent standard limitation guidelines by Japan Ministry of the Environment  $0.5 \text{ mg L}^{-1}$  ( $9.62 \text{ } \mu\text{mol L}^{-1}$ ) [20]. In aqueous solutions, Cr(VI) occurs as five anionic forms (Eqs. (1-7) – (1-10)) [21], while Cr(III) occurs as nonionic and cationic forms (Eqs. (1-11) – (1-14)) [22,23].



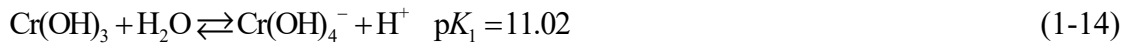
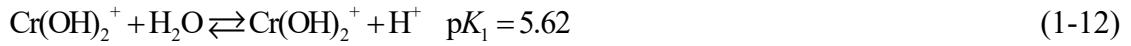
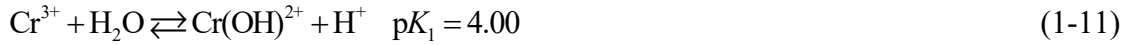


Table 1.2 Characteristics of chrome plating industry wastewater [19]

pH	Concentration (mg L <sup>-1</sup> )					
	TSS	Fe	Pb	Cu	Cr(VI)	F
2.09	112.0	79.5	1.095	28.3	5722	–

TSS: Total suspended solids

## Lead

Lead is a naturally occurring bluish-gray metal present in small amounts in the earth's crust. Lead has many industrial, agricultural, and domestic application. Anthropogenic activities, such as battery manufacturing, paints, smelting, and paper industries, are therefore main sources of lead release in high concentration [24]. Lead is currently used for production of lead-acid batteries. The amounts of lead available from spent batteries, as well as from batteries manufacturing wastewater, are therefore still increasing. In manufacturing battery wastewater discharge, other toxic heavy metals, such as copper (Cu), zinc (Zn), and cadmium (Cd), are existed, together with lead, at high concentration, as shown in Table 1.3 [25]. High level of Pb was contaminated in industrial wastewater, while the maximum concentration of Pb for effluent should be 0.1 mg L<sup>-1</sup> (4.83 μmol L<sup>-1</sup>) [20]. In aqueous solution, lead mainly exists in the form of Pb<sup>2+</sup> in acidic region, while exists in the other forms of Pb(OH)<sup>+</sup>, Pb(OH)<sub>2</sub> and Pb(OH)<sub>3</sub><sup>-</sup> in alkali region, as shown in Eqs. (1-15) – (1-17) [26].

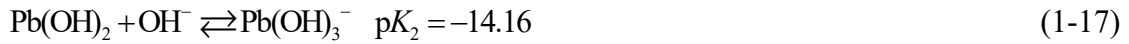


Table 1.3 Characteristics of battery manufacturing industry wastewater [25]

pH	Concentration (mg L <sup>-1</sup> )					
	TSS	Pb	Cd	Zn	Cu	Sulfate
4.1	30.0	190.0	135.0	19.0	8.5	260.0

TSS: Total suspended solids

### 1.1.2. Impact of heavy metals on human health

Heavy metals are non-degradable and can bio-accumulate in the main system of human body. Under normal circumstances, human body can tolerate trace amounts of metals without experiencing severe health problems. Many heavy metals are trace elements that are essential for human health, such as arsenic, zinc, copper, chromium, and nickel, although these metals will become toxic when their concentration exceeds their permissible limit in the ecosystem. Human may directly get in contact with heavy metals by consuming contaminated food stuff and drinking water through inhalation of air as dust fumes or occupation exposure at workplace. In human body, most of heavy metals are distributed through blood to tissue [27]. The main mechanism of heavy metal toxicity includes the generation of free radical to cause oxidative stress and damage of biological molecules, such as enzymes, proteins, lipids, and nucleic acid. Heavy metals can damage and alter the functioning of organs of brain, kidney, liver, blood, and lungs. Their toxicity can either be acute effects and chronic effects. Chronic long-term exposure of heavy metals can progressively lead to muscular, physical, and neurological degenerative process, even cancer and death. Various health effects of some heavy metals are highlighted in Figure 1.1 [4,28], and detailed are shown as following.

The toxicity of arsenic is highly influenced by its oxidation and solubility, and depends on exposure dose and duration [1]. Inorganic arsenic has been confirmed as a carcinogenic, the various effect of arsenic poisoning on human health includes keratosis, melanosis, dorsum, cancer and even death, depending on the quantity consumed. The lethal dose of arsenic in acute poisoning ranges from 100 mg to 300 mg or 0.6 mg arsenic per 1 kg of weight per day [29]. At

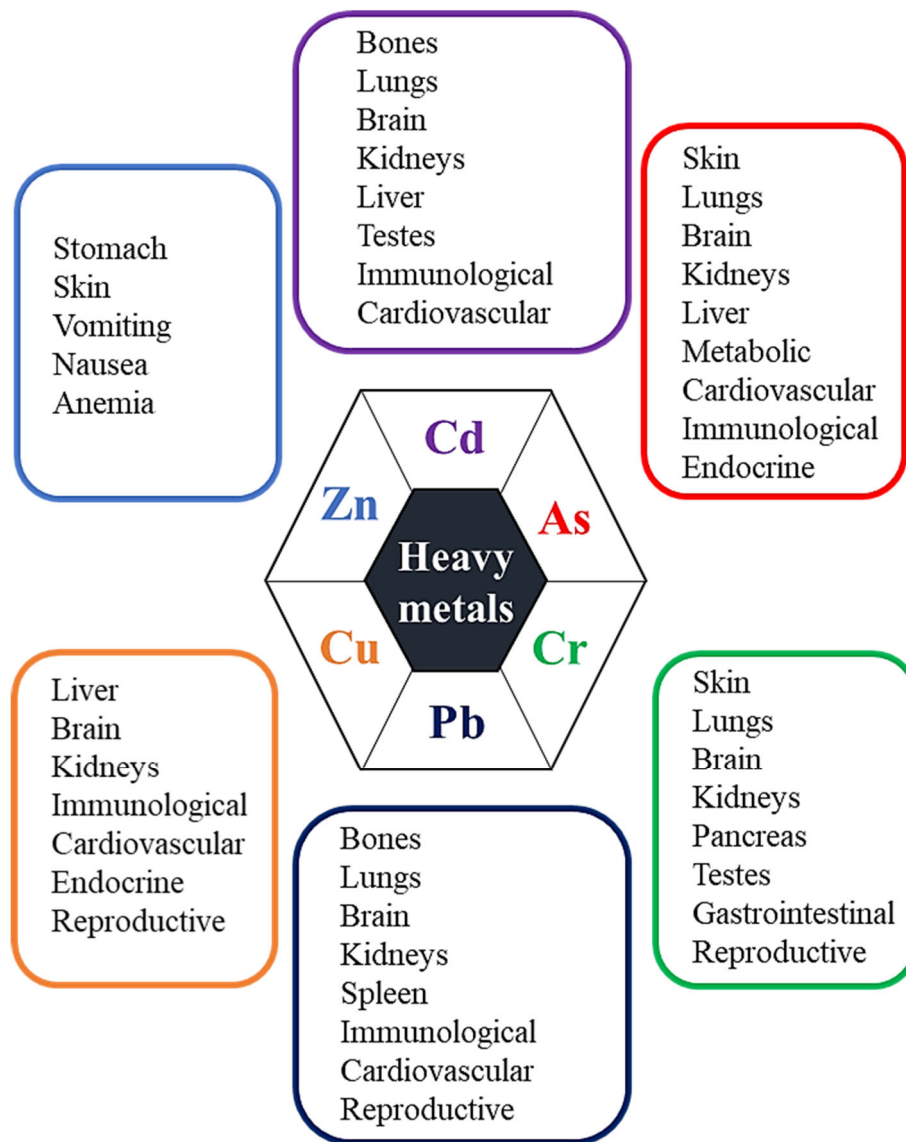


Figure 1.1 Main organs and systems affected by environmental or occupational exposure to heavy metals [4,27].

low level of arsenic in long-term uptake, however, chronic exposure to inorganic As causes several disorders upon different biological systems like endocrine system, renal system, pulmonary disease, peripheral vascular disease, and reproductive system which ultimately lead to cancer [10]. As shown in Table 1.1, arsenic has been found in natural water at high level exceeding the World Health Organization limitation guideline for drinking water of  $10 \mu\text{g L}^{-1}$  ( $0.133 \mu\text{mol L}^{-1}$ ) [20]. The major arsenicosis regions are presently found in many countries such as Bangladesh [9,30], Vietnam, Myanmar, Cambodia [14], Thailand [16], Nepal [13], and China [31].

Chromium is a naturally occurring element, and stable in trivalent form and hexavalent form in environment. Cr(VI) species has been considered as one of top 16th hazardous

substances, according to The Agency for Toxic Substances and Diseases Registry classified, due to their toxic and carcinogenic profile [32]. Whereas Cr(III) is an essential nutrient that plays a role in protein metabolism by potentiating the action of insulin [1,33]. The limitation of exposure of Cr(III) is  $5000 \mu\text{g L}^{-1}$  for an 8 h-workday and 40 h-workweek [34]. However, breathing a high level of Cr(VI) can cause nose irritations and nosebleeds [34]. Occupational and environmental exposure to Cr(VI)-containing compounds is known to cause multiorgan toxicity such as skin rashes, upset stomachs and ulcers, respiratory problems, weakened immune systems, kidney and liver damage, the alteration of genetic material, lung cancer, and death [1,34].

Lead is a naturally occurring element in the environment, but anthropogenic activities such as battery manufacturing contribute to the release of high concentrations. Lead can cause many human health problems including damage to the central nervous system, kidney, liver and brain function with many toxic symptoms such as anemia, insomnia, headache, dizziness, irritability, weakness of muscles and hallucination [4]. Cadmium has been confirmed as a probable human carcinogen. Long-term exposure at a low level of cadmium results in kidney, stomach, liver and lung dysfunction, while a high level of exposure will result in death [1,4].

Zinc and copper are trace elements that are essential for human and animal. It is necessary for the physiological function of living organisms. However, the excessive ingestion of zinc brings about serious toxicological concerns, such as stomach cramps, skin irritations, vomiting, nausea and anemia [4,28]. Also, too much of copper can cause eminent health problems, such as vomiting, cramps, convulsions, or even death [4].

### 1.1.3. Methodologies for heavy metals removal

Recently, many studies have investigated the removal of heavy metals contaminated in water/wastewater. The technologies that are currently in use include chemical precipitation, membrane filtration, solvent extraction, oxidation/reduction, and adsorption [35–37]. The choice of suitable technique depends on factors of economic cost, efficiency, and environmental impact. The conventional techniques for heavy metals removal are following:

Chemical precipitation is effective and by far the most used process in the treatment of industrial wastewater. In the precipitation process, the chemicals react with heavy metal ions to form insoluble precipitates, which can be easily separated from water by filtration or sedimentation. Two conventional chemical precipitation processes are hydroxide precipitation and sulfide precipitation, which are commonly used in industrial wastewater treatment. Hydroxide precipitation is often used using NaOH and  $\text{Ca}(\text{OH})_2$  for precipitating heavy

metal ions from wastewater, such as Pb(II) [38]. The minimum solubilities of various metal hydroxide are obtained in the pH range of 8.0 – 11. Sulfide precipitation is also an effective process with low level of solubilities of metal-sulfide precipitate form. The sulfide precipitation can achieve a high degree of metal removal over a broad pH range. However, there are drawbacks in use of chemical precipitation process. Industrial wastewater often in acid condition, which can result in the evolution of toxic H<sub>2</sub>S fumes in the sulfide precipitation [4]. The hydroxide precipitation is also hardly applied due to economic problem when using large amount of reagent for pH adjustment.

Membrane filtration technique with difference types of membrane show capable of removing not only organic compounds but also inorganic contaminant including heavy metal ions. The most common membrane processes for heavy metals removal are low pressure-driven membrane processes (microfiltration (MF) and ultrafiltration (UF)), high pressure-driven membrane processes (nanofiltration (NF) and reverse osmosis (RO)), osmotic pressure-driven membrane process (forward osmosis (FO) and electrodialysis (ED) [39,40]. The pore size, pore distribution, surface charge, degree of hydrophilicity, solution flow, and presence of functional groups, are significantly affect the overall membrane performance in terms of water production rate and heavy metal removal efficiency. Pham *et al.* have reported that removal of arsenic [41] and chromium(VI) [42] could be achieved with high efficiency. However, the disadvantages of membrane filtration technique, such as high cost, process complexity, membrane fouling, and low permeate flux, have limited their use in heavy metal removal.

Solvent extraction appears to have great potential in the field of industrial wastewater treatment, both for the recovery of valuable materials and for removal of toxic heavy metals. Extraction process is the removal of soluble consistent from one liquid (aqueous phase) into another (organic phase). The advantages of this technique include high selectivity, low energy consumption, fast action, easy continuous operation, and ease of automation. Venkateswaran *et al.* have reported that the removal and recovery of Cr(VI) from real chrome-plating wastewater was achieved by solvent extraction method with high efficiency [43].

Oxidation/reduction techniques is considered as a pretreatment step, which are often used together with other method such as precipitation and adsorption. Pentavalent arsenic (As(V)) and trivalent chromium (Cr(III)) are more less toxic than trivalent arsenic (As(III)) and hexavalent chromium (Cr(VI)), respectively, and thus the oxidation of As(III) to As(V) and reduction of Cr(VI) to Cr(III) are considered as detoxification method. In previous studies, chelate fiber adsorbent has high affinity for As(V) but not As(III), Kuraoka *et al.* have used

manganese dioxide for oxidation of As(III) to As(V), together with adsorption of As(V) by chelate fiber [44]. Cr(VI) species is hardly precipitated, while Cr(III) species are possible precipitated at alkali region as Cr(OH)<sub>3</sub> form. Thus, the reduction of Cr(VI) to Cr(III) is importance step for removal of Cr(VI) by precipitation technique.

Adsorption technique is now recognized as an effective and economic technique for treatment of heavy metal from water/wastewater. Adsorption technique does not require chemical addition and is easily used in the developing countries that are lack of skilled personnel. Adsorption has the benefits of having a range of potential sources, low costs, simple operation, a large adsorption capacity, being effective for a variety of metals, having no secondary pollution implications and a vast range of potential biochar materials. Therefore this technique is a promising research direction, with simultaneous multifarious adsorbents and modification techniques also gaining many recent research attentions [45]. The details of adsorption technique are shown in section 1.2.

## 1.2. Adsorption technique

Adsorption is known as a separation process, which is widely applied in the chemical engineering and in our daily life [46]. The adsorption is the phenomenon by which molecules from gas or liquid phase (adsorbate) are fixed preferentially on the surface of a solid (adsorbent) [47]. Thus, by contacting fluids with such solids, the desired objective of purification or separation may be achieved [46]. The adsorption mechanisms include physical adsorption (London – van der Waals forces of intermolecular attraction) and chemical adsorption (electrostatic attraction and/or chemical affinity). Physical adsorption is reversible, low selectivity, and low level of energy, while chemical adsorption is not reversible, may be high selectivity and release heat [47]. Adsorption process can be operated in two main modes: batchwise system and column system.

### 1.2.1. Batchwise Adsorption

Batchwise adsorption is a systematic process that solution is mixed with solid material for determined of length time, after which the two phases (solid phase and liquid phase) are separated. The required time for reaction between adsorbent and adsorbate to reach equilibrium state is fundamentally dependent on the process variables such as temperature, pH value, initial adsorbate concentration, adsorbent dose, type/characteristic of adsorbent, etc. The adsorption efficiency is also affected by various factors as mentioned above. Adsorption performance models describing the dynamic behavior of adsorption processes are based on the adsorption

equilibrium relationship, the solute uptake mechanisms and uptake expression, and the convention equations of solute species and adsorbent.

In adsorption-based water/wastewater treatment operation, information on adsorption isotherms and adsorption kinetics are very important, which are required to get insight into the reaction pathways and underlying mechanisms of the adsorption processes. The adsorption kinetics describes the rate of adsorbate uptake, which ultimate controls the contact time of an adsorbate uptake at the batchwise system [35,45]. In addition, the prediction of the rate of reaction between adsorbent and adsorbate is important to ensure appropriate design of an adsorption-based water treatment system.

Adsorption isotherm is used to describe the interaction mechanisms between the adsorbate species and the surface of adsorbent. Among many adsorption isotherms models, the classical Langmuir and Freundlich isotherm equations provide the fundamental principle on which the derivations of modern isotherm equations are premised [48]. Both of isotherm models are found to be more suitable to describe the relationship between adsorption amount loaded on adsorbent and adsorbate concentration remained at equilibrium state.

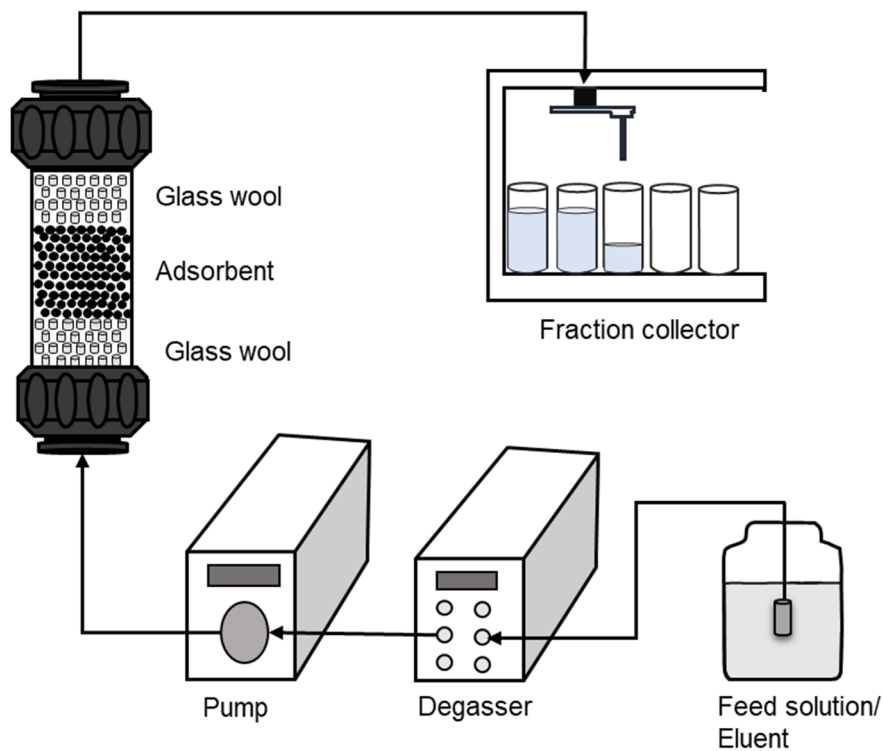


Figure 1.2 Fixed bed column experiment diagram.

### 1.2.2. Column adsorption

The adsorption process is performed by feeding the liquid stream through a column packed adsorbent, which is commonly applied for eliminating trace contaminants from a liquid solution. The operation consists of two phases, feed solution and adsorbent. The process is seen as continuous with respect to the mobile phase (feed solution) but discontinuous with respect to the stationary phase (adsorbent). Adsorption in columns can be treated as a multistage separation process. The efficiency of separation is thus better than that of batchwise operation. Furthermore, both the contacting and separation steps as well as the regeneration of the adsorbent are carried out in the same equipment. The fixed bed column diagram is shown in Figure 1.2. The feed solution is introduced from either bottom or top, and then the adsorbent of the inlet side become saturated with adsorbate. Good column design, having near-ideal conditions, enables a wide range of chromatography in the column, facilitating an easy operation and repeated used [49]. In the column adsorption, the ratio between flow rate and wet volume of adsorbent is an importance parameter and is called a “space velocity”.

### 1.2.3. Adsorbents

The efficiencies of adsorption technique were mainly decided by adsorbent. In principle, an adsorbent may be selected based on numbers of factors, including adsorption capacity, selectivity, regeneration ability, compatibility with operating condition, and cost. Moreover, the adsorbent characteristics, such as adsorbent size, density, porosity, pore size and size distribution, and specific surface area, are important parameters, since the adsorption efficiency is affected by the characteristics. There are organic and inorganic adsorbents to be applied for the water/wastewater treatment.

In recent year, many researchers have used natural biological matrices as adsorbents for removal of toxic heavy metal, due to their wide distribution, low toxicity, chemical stability, and biodegradability. Agricultural waste and residual plant have been applied as adsorbent material for treatment of metal contaminated water/wastewater [49-52]. Zhu *et al.* reported that approximate proportions of adsorbent types and found that bio-adsorbents are the most common adsorbents applied (approximately 58% of studies) [45]. The conventional bio-adsorbent as activated carbon is widely applied in water/wastewater treatment. In addition, bio-adsorbent is considered for detoxification of metal contaminated in water. Zhong *et al.* have demonstrated that As(III) is oxidized to As(V) and adsorbed by bio-adsorbent [54]. Kobya *et al.* used activated carbon for reduction and adsorption of Cr(VI) [53], which Cr(VI) was adsorbed by activated carbon, then reduced to Cr(III).

Iron oxides has been widely studied due to their novel property and functionality, such as easy synthesis, non-toxicity, great biocompatibility, small size, reusability for further application, magnetic property, easily separation in external magnetic field, relatively high surface area, ease of manipulate in complex multiphase systems and comparatively cost-effective. The most common iron oxides adsorbents are goethite (FeOOH), magnetite (Fe<sub>3</sub>O<sub>4</sub>), hematite (Fe<sub>2</sub>O<sub>3</sub>), which can effectively adsorb heavy metal. Goethite and hematite show high adsorption capacity for removal of heavy metal [55,56]. Magnetite shows high affinity for certain metals as lead and chromium [57,58].

Polymer resins adsorbents, which are prepared from polymerizing styrene and divinyl benzene or acrylic esters for adsorbing nonpolar organics from aqueous solutions or polar solutes, respectively. Strong-base polymer resins that contain special functional groups attached to a polymeric matrix have been extensively studied for their ability to remove heavy metal ions. The functional group such as *N*-methyl-*D*-glucamine has been shown to exhibit a higher affinity for boron and arsenic [59]; iminodiacetic acid group has high selectivity for metal cations such as chromium(III), lead(II), copper(II), and zinc(II) [60]. The adsorption mechanisms often occur as ion exchange mechanism between metal ion and H<sup>+</sup>/OH<sup>-</sup> in functional groups. The polymer resins adsorbents are however more expensive than other adsorbents.

### 1.3. Objective

In this dissertation, the adsorptive separation of heavy metals from aquatic environment was investigated. Various adsorbents including commercial adsorbents, ion exchange resins, and low-cost adsorbents such as activated carbon, magnetite, and goethite, are employing for decontamination, detoxification, and separation of heavy metals from aqueous environment. The contents and purpose of this dissertation were as follow:

- i) The adsorptive removal of As(III) and As(V) from aqueous environment has been investigated, employing Diaion CRB05, with *N*-methyl-*D*-glucamine functional group, and Lewatit FO36, with FeOOH functional group. The adsorption performance of two adsorbents was systematic compared follow batchwise adsorption and chromatographic operation. The selectivity of adsorbents is considered in column operation, by using feed solution of As(III)/As(V) binary. The regeneration ability of the adsorbents was also investigated, by three times repeated use of adsorbents in column operation.

- ii) Reductive adsorption of Cr(VI) from aquatic environment was investigated using coal-based activated carbon. Adsorption technique is the best way for removal of Cr(VI), while reduction technique is considered as detoxification. Activated carbon is known as an excellent adsorbent for removal of Cr(VI). In addition, activated carbon have large amount of functional groups such as phenolic, lactic and carboxylic group, which groups play role as reductant for reduction of Cr(VI). The adsorptive removal of Cr(VI) was investigated. The desorption/regeneration of activated carbon should be considered. The adsorption-reduction mechanisms of Cr(VI) during reaction with activated carbon, was also investigated.
- iii) The selective adsorption of Pb(II) from aqueous solution, containing Pb(II), Cu(II), Zn(II) and Cd(II), has been investigated using three adsorbents, chelating resin with iminodiacetic acid group, goethite, and magnetite. The adsorption of heavy metal ions from single solution shows high adsorption amount, while multicomponent system is required to develop separation of Pb(II) from wastewater pollution. The selective adsorption of Pb(II) from multicomponent system was investigated with both of batchwise adsorption and chromatographic separation. After adsorption, elution processes were performed to confirm the selective separation of Pb(II) of the adsorbents.

## Chapter 2. Adsorptive Removal of Arsenic from Aquatic Environment

### 2.1. Introduction

Arsenic (As) is one of the most toxic elements and has been confirmed as a carcinogen for human health. At the same time, arsenic is the most significant chemical contaminant in drinking water globally. Naturally occurring arsenic contamination of groundwater has been detected in 70 countries and could affect more than 140 million people. For example, in Bangladesh, about 33 million people have been exposed to arsenic levels higher than 50  $\mu\text{g/L}$  [61]. Besides, the significant level of arsenic in groundwater and geothermal water have been reported in many areas, including USA, China, Japan, and Vietnam [62,63]. According to Japan Ministry of the Environment recommend, the effluent standard of arsenic and its compound should be lower than 0.1  $\text{mg L}^{-1}$  (1.33  $\mu\text{mol L}^{-1}$ ) [20]. WHO defined the maximum concentration level of arsenic in drinking water at 0.01  $\text{mg L}^{-1}$  (0.133  $\mu\text{mol L}^{-1}$ ) [64].

Several technologies for arsenic removal from water environment have been reported, such as oxidation and filtration [62,65], chemical precipitation and coagulation [35,62], membrane technology [40,41], and adsorption and ion exchange [36,55,66]. Among these possible treatment techniques, the adsorption process has been the most extensively studied, due to its high removal efficiency, flexibility, and simple processing [66]. Various adsorbents, such as red mud [67,68], iron compounds [55,69], chitosan goethite [70], polymer-clay with *N*-methyl-*D*-glucamine [59,71], ion exchange resins having FeOOH group [72], and biopolymer chitosan [73], have also been reported. Among the adsorbents, adsorptive removal of arsenic by ion exchange resins having *N*-methyl-*D*-glucamine group and FeOOH group, have been studied to evaluate the removal efficiency, due to their high selectivity and adsorption capacity [18,55,71,72]. The selectivity of *N*-methyl-*D*-glucamine for arsenate was reported by Dambies *et al.* [74], and adsorption amount of arsenate was 0.807  $\text{mmol g}^{-1}$ . However, adsorption of arsenite using *N*-methyl-*D*-glucamine was rarely considered. Adsorption material containing FeOOH group has high adsorption capacity for arsenic (0.343  $\text{mmol g}^{-1}$  for As(V) and 0.459  $\text{mmol g}^{-1}$  for As(III)) [75]. Although these adsorbents are expected as stable adsorbents with high adsorption capacity of arsenic, systematic comparison of the adsorbents as well as adsorption ability of As(III) and As(V) are rarely performed.

In this chapter, the adsorptive removal of arsenic from water environment was investigated, using the two types of adsorbents, Diaion CRB05 with *N*-methyl-*D*-glucamine group

(abbreviated CRB05, hereafter) and Lewatit FO36 with FeOOH group (abbreviated FO36, hereafter). Comparison of adsorption parameters for both As(III) and As(V), such as pH, adsorption isotherm, adsorption kinetic and desorption, have been investigated in batchwise adsorption system. Chromatographic studies for the arsenic removal were then conducted using the packed columns of the adsorbents to investigate the effect of space velocity and repeated operation.

## 2.2. Experimental

### 2.2.1. Reagents

CRB05 was supplied from Mitsubishi Chemical Co. (Tokyo, Japan) and FO36 was supplied from LANXESS (Tokyo, Japan). CRB05 was conditioned by shaking with 2 mol L<sup>-1</sup> HCl, followed by washing with deionized water, and then was dried. FO36 were used without any pretreatment. Functional group density was calculated from density of nitrogen for *N*-methyl-*D*-glucamine and iron for FeOOH. Nitrogen density was determined by CHN elemental analyzers (MT-6; Yanaco Technical Science). In the case determining iron, 20 mg of FO36 was added in 5 mL H<sub>2</sub>O<sub>2</sub> 9.8 mol L<sup>-1</sup> and 15 mL H<sub>2</sub>SO<sub>4</sub> 18.4 mol L<sup>-1</sup>, then stirring at 50°C for 12 h. After filtration, Fe concentration was analyzed by an inductively coupled plasma atomic emission spectrometer (ICP-AES; Shimadzu ICPE-9000). Na<sub>2</sub>HAsO<sub>4</sub>·7H<sub>2</sub>O was supplied from Alfa Aesar (Lancashire, United Kingdom). NaAsO<sub>2</sub> and all other reagents were supplied by FUJIFILM Wako Pure Chemical Corporation (Osaka, Japan) as analytical grade reagents.

### 2.2.2. Batchwise adsorption

Aqueous feed solutions were prepared by dissolving NaAsO<sub>2</sub> or Na<sub>2</sub>HAsO<sub>4</sub>·7H<sub>2</sub>O in deionized water for aqueous solutions of As(III) and As(V), respectively. Batchwise adsorption was carried out by shaking adsorbent (20 mg) and the aqueous feed solution (10 mL) of As(III) or As(V) for 24 h at 25°C. In the case of experiments of pH influences on the adsorption of As, initial pH was adjusted by adding HCl solution or NaOH solution, which arsenic concentration was fixed at 0.13 mmol L<sup>-1</sup>. In the case of adsorption isotherm, initial arsenic concentration was varied from 0.13 to 26.67 mmol L<sup>-1</sup>. After filtration, the equilibrium pH was measured. The arsenic concentration was determined by ICP-AES. The adsorption amount,  $q$  (mmol g<sup>-1</sup>), was determined by Eq (2-1):

$$q = \frac{([As]_{\text{feed}} - [As]_{\text{eq}})V}{m} \quad (2-1)$$

where  $[As]_{\text{feed}}$  and  $[As]_{\text{eq}}$  are initial and equilibrium concentrations of arsenic in aqueous solution ( $\text{mmol L}^{-1}$ ),  $V$  is the volume of solution (L), and  $m$  is weight of adsorbent (g).

Desorption was also performed by batch experiment. The adsorbents (600 mg) were first contacted with  $13.33 \text{ mmol L}^{-1}$  As(III) or As(V) solution (100 mL) to be shaken for 24 h at  $25^\circ\text{C}$ . The loaded adsorbent was then filtered and dried in a vacuum oven (EYELA VOS-301SD). The loaded adsorbent (20 mg) was added to 10 mL of HCl solution ( $0 - 3 \text{ mol L}^{-1}$ ) or NaOH solution ( $0 - 3 \text{ mol L}^{-1}$ ), and the mixture was shaken for 24 h at  $25^\circ\text{C}$  to elute arsenic. After filtration, arsenic concentration was analyzed by ICP-AES.

### 2.2.3. Column adsorption

Chromatographic operation of arsenic removal was conducted using the column system, shown in Figure 1.2. The adsorbent was packed into a column to be sandwiched by glass wool. Wet volume of the adsorbent was changed as 1.4 mL, 2.3 mL, and 4.1 mL for CRB05 and as 1.5 mL, 2.4 mL, and 4.4 mL for FO36, while the flow rate was fixed at  $0.2 \text{ mL min}^{-1}$ , so that the space velocity (S.V.) was changed as  $\text{S.V.} = 8.5 \text{ h}^{-1}$ ,  $5.2 \text{ h}^{-1}$ , and  $2.9 \text{ h}^{-1}$  for CRB05, and as  $\text{S.V.} = 8 \text{ h}^{-1}$ ,  $5 \text{ h}^{-1}$ ,  $2.7 \text{ h}^{-1}$  and for FO36. In the case of single solution system, feed solution containing either As(V) or As(III) ( $[As]_{\text{feed}} = 0.047 \text{ mmol L}^{-1}$ ,  $\text{pH} = 7.0$ ) was used, while in the case of As(III/V) mixed solution system, ( $[As(\text{III})]_{\text{feed}} = [As(\text{V})]_{\text{feed}} = 0.024 \text{ mmol L}^{-1}$ ,  $\text{pH} = 7.0$ ) was used. The feed solution was fed into the column at flow rate of  $0.2 \text{ mL min}^{-1}$  using a dual plunger pump (Flom KP-21), and the effluent was collected by a fraction collector (EYELA DC-1500). After adsorption, the column was washed with deionized water, and then elution was performed by using HCl or NaOH as an eluent. Bed volume (B.V.) was calculated by Eq (2-2):

$$\text{B.V.} = \frac{vt}{L} \quad (2-2)$$

where  $v$  is volumetric flow rate of solution ( $\text{mL min}^{-1}$ ),  $t$  is time for which the feed solution was applied (min),  $L$  is wet volume of adsorbent (mL). The arsenic concentration in the effluent was measured by ICP-AES.

## 2.3. Results and discussion

### 2.3.1. Batchwise adsorption

#### 2.3.1.1. Effect of pH on arsenic adsorption

The pH parameter plays an important role to determine the adsorption performance [71], since species distribution of arsenic in an aqueous solution is strongly affected by pH of aqueous solution. Figure 2.1 shows the effect of equilibrium pH on the adsorption amount of As(III) and As(V) by CRB05 and FO36. The adsorption amount of As(III) with both adsorbents is increased with pH in acidic region, and then is decreased in  $\text{pH}_{\text{eq}} > 8.5$  for both adsorbents. In the case of As(V), the adsorption amounts were sharply depended on the pH and high adsorption amounts were observed in  $\text{pH}_{\text{eq}} = 3.0 - 4.5$ . Figure 2.2 shows species distribution of As(III) and As(V) calculated by  $\text{p}K_{\text{a}}$  values which are presented in Eqs. (1-1) – (1-6) [18]. In the case of As(III), As(III) exists in nonionic form of  $\text{H}_3\text{AsO}_3$  in the acidic region  $\text{pH} < 6$ , and other ionic forms of  $\text{H}_2\text{AsO}_3^-$ ,  $\text{HAsO}_3^{2-}$ , and  $\text{AsO}_3^{3-}$  appeared at  $\text{pH} > 6$ , the predominant species were  $\text{H}_3\text{AsO}_3$  and  $\text{H}_2\text{AsO}_3^-$ . In the case of As(V), different species were appeared at various pH, the predominant species was monovalent  $\text{H}_2\text{AsO}_4^-$  at  $\text{pH} < 6$  and divalent  $\text{HAsO}_4^{2-}$  at  $\text{pH} > 6$ . Therefore, the adsorbents with *N*-methyl-*D*-glucamine group and FeOOH group show the affinity for monovalent anionic species, and the different adsorption amount is likely depended on the distribution of arsenic species in aqueous solution [55,59].

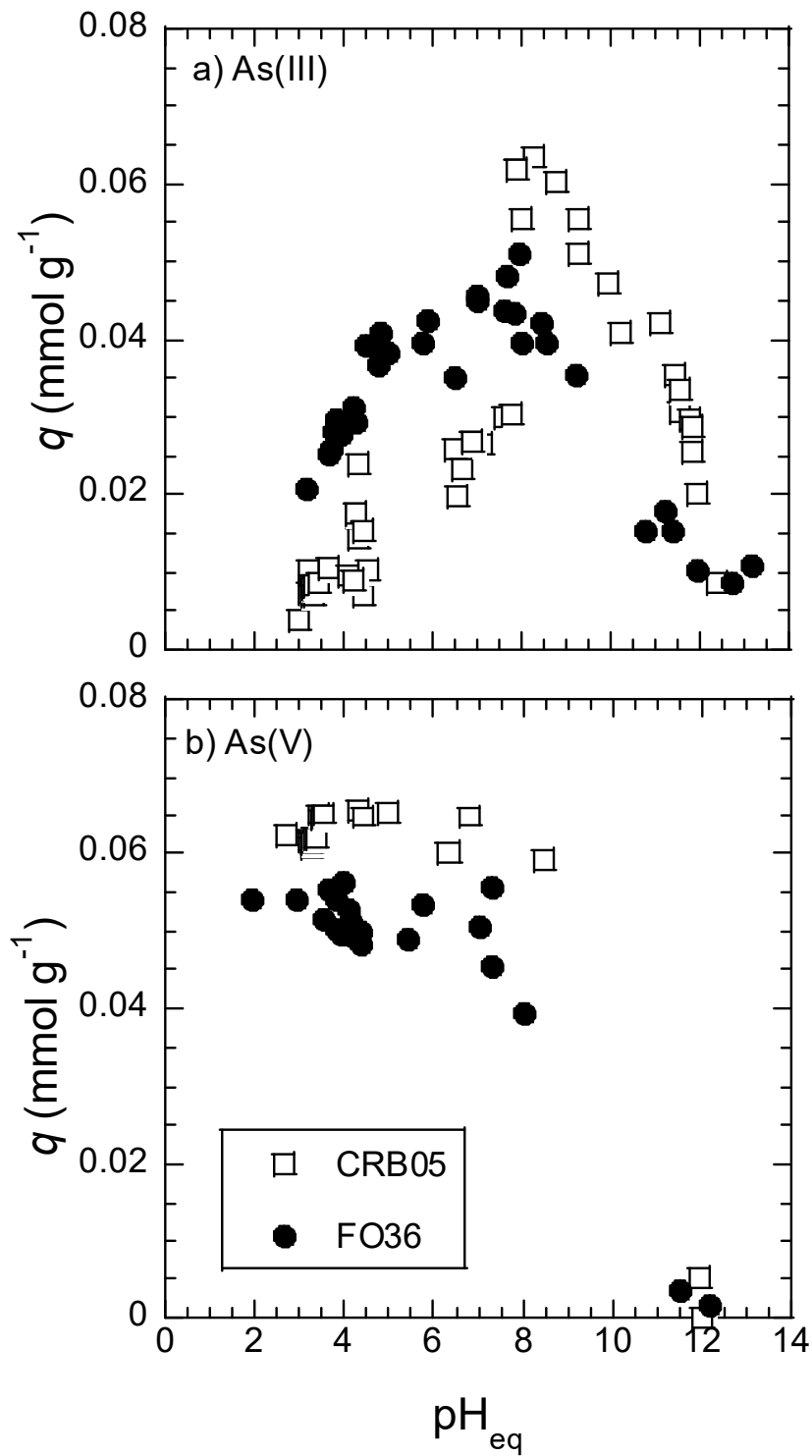


Figure 2.1 Effect of equilibrium pH on removal percentage of (a) As(III) and (b) As(V) by CRB05 and FO36.  $[\text{As}]_{\text{feed}} = 0.13 \text{ mmol L}^{-1}$ .

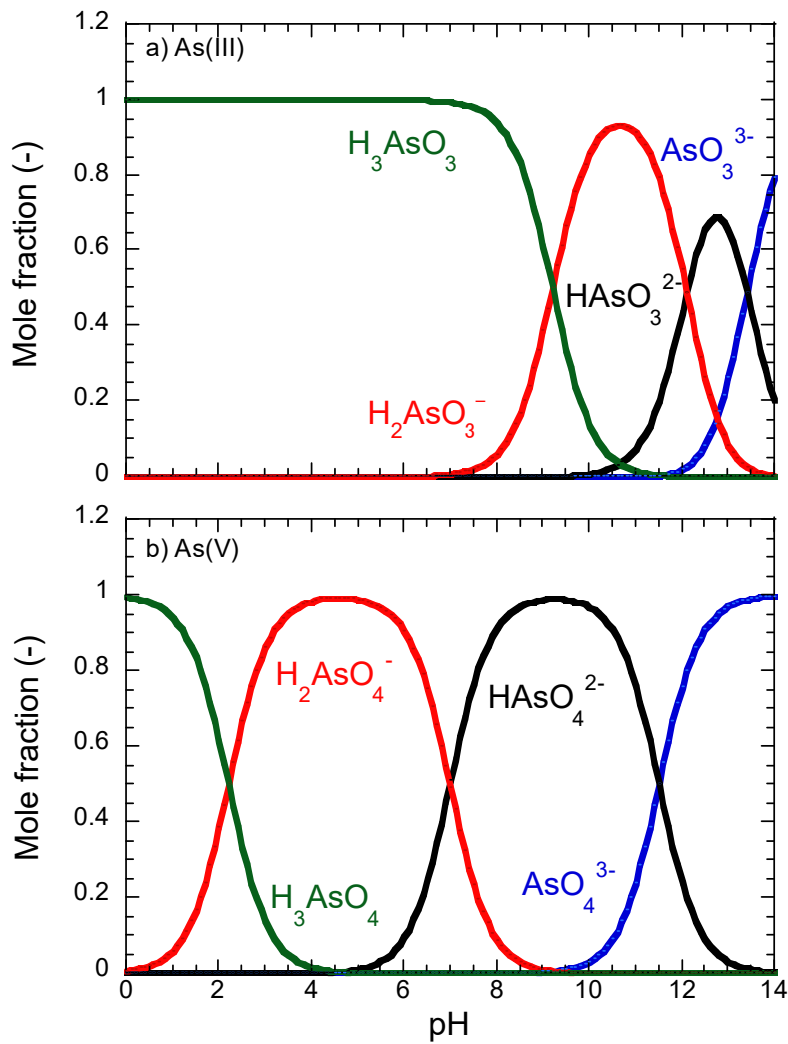


Figure 2.2 Species distribution of (a) As(III) and (b) As(V) in aqueous solution.

#### 2.3.1.2. Adsorption isotherm

The adsorption isotherm of arsenic was investigated, adsorption data were analyzed using the Langmuir isotherm model, as shown in Eq.(2-3), assuming that the maximum adsorption capacity corresponded to the formation of a saturated monolayer of adsorbate on the adsorbent surface [76].

$$q_{\text{eq}} = \frac{q_{\text{max}} \cdot K_L \cdot [\text{As}]_{\text{eq}}}{1 + K_L \cdot [\text{As}]_{\text{eq}}} \quad (2-3)$$

where  $[As]_{eq}$  is the equilibrium concentration ( $mmol L^{-1}$ ),  $q_{eq}$  is the adsorption amount ( $mmol g^{-1}$ ),  $q_{max}$  is the maximum adsorption capacity ( $mmol g^{-1}$ ), and  $K_L$  is the adsorption constant ( $L mmol^{-1}$ ). Figure 2.3 shows the adsorption isotherms of As(III) and As(V) with all of adsorbents at fixed equilibrium pH values as shown in Table 2.1. All of adsorption isotherms were followed by Langmuir isotherm model, indicating the adsorption is limited to monolayer adsorption. The calculated lines of the adsorption isotherms of As(III) and As(V) base on the Langmuir constants are also shown in Figure 2.3 The regression coefficient ( $R^2$ ) values as shown in Table 2.1 are good enough to consistent with Langmuir adsorption mechanism The maximum adsorption amount ( $q_m$ ) and the adsorption constant ( $K_L$ ) calculated with the linear relationship of Langmuir adsorption mechanism was summarized in Table 2.1. The adsorption capacity of As(V) is greater than that of As(III) with all of adsorbents. Also, FO36 has the highest adsorption capacities for both As(III) ( $1.307 mmol g^{-1}$ ) and As(V) ( $1.627 mmol g^{-1}$ ). The adsorption constant ( $K_L$ ) represents the affinity of adsorbate with the binding sites of adsorbent [71], and the dimensionless equilibrium parameter,  $R_L = 1/(1+[As]_{feed}K_L)$  can predict whether the adsorption is favorable or unfavorable [71]. The  $R_L$  value for any concentration of arsenic in aqueous solution shall be found to lie between 0.01 – 0.99, indicating the adsorption of As(III) and As(V) by both adsorbents are favorable. The adsorption performances of arsenic of CRB05 and FO36 have been compared on the basis of the Langmuir parameters ( $q_m$  and  $K_L$  with several previous reported data as shown in Table 2.2 [59,70,75]. The present adsorbents have higher affinity for both of As(III) and As(V).

Table 2.1 Maximum adsorption capacities, adsorption constants of As(III) and As(V), and functional group density of adsorbents.

	As(III)		As(V)	
	CRB05	FO36	CRB05	FO36
pH <sub>eq</sub>	7.76 ± 0.05	6.54 ± 0.04	3.49 ± 0.05	4.06 ± 0.04
$q_m$ ( $mmol g^{-1}$ )	0.945	1.307	1.269	1.627
$K_L$ ( $L mmol^{-1}$ )	0.5325	1.118	32.17	0.030
$R^2$	0.999	0.999	0.997	0.996
Functional group density ( $mmol g^{-1}$ )	2.385	2.854	2.385	2.854

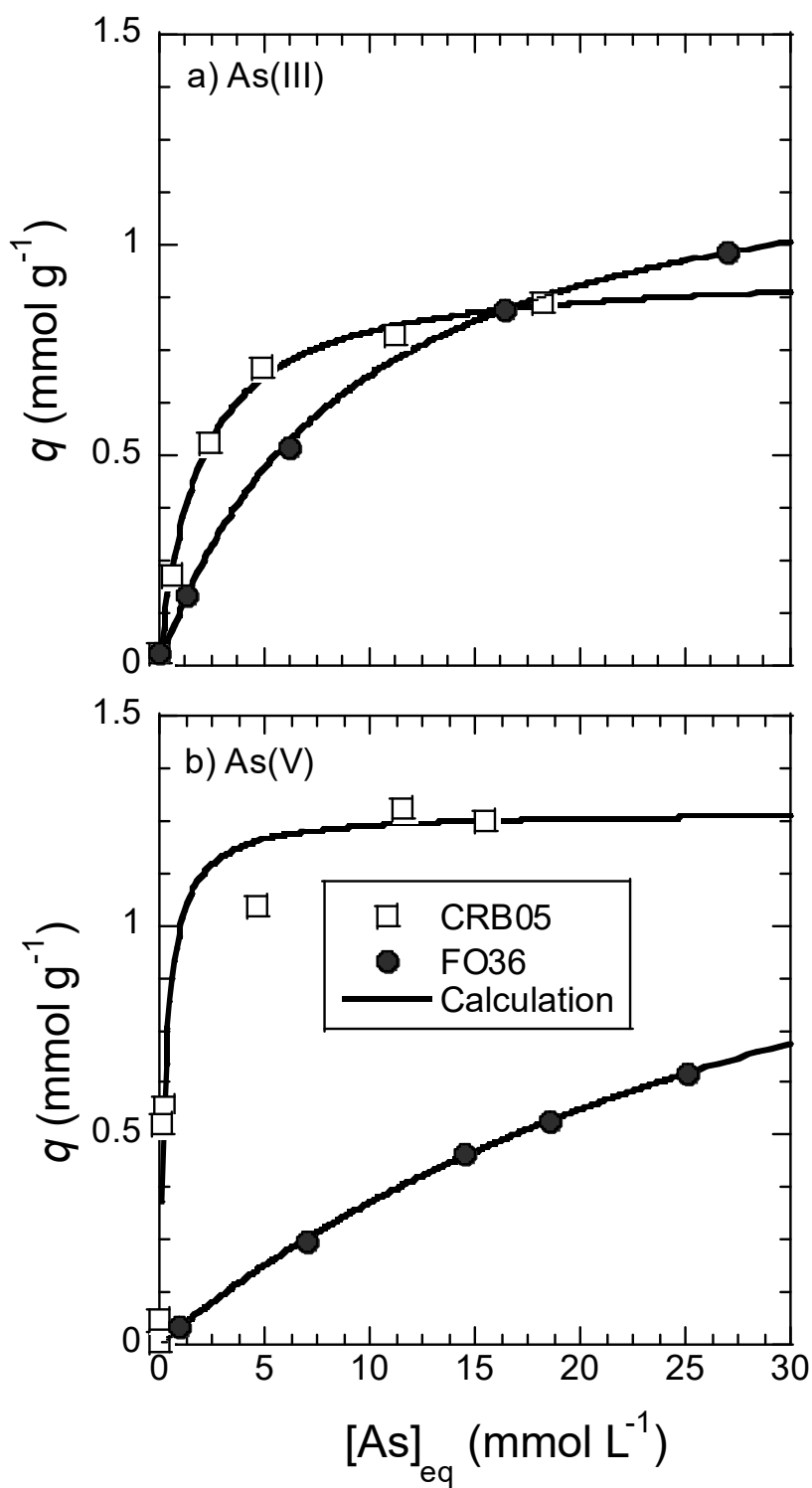


Figure 2.3 Adsorption isotherms of (a) As(III) and (b) As(V) with CRB05 and FO36 at equilibrium pH shown in Table 2.1. Lines are calculated results by Langmuir adsorption mechanisms.

Table 2.2 Comparison of adsorption capacities and adsorption constants for As(III) and As(V) by various adsorbents

Functional group	Adsorbents	As(III)			As(V)			References
		pH <sub>eq</sub>	$q_{\max}$ (mmol g <sup>-1</sup> )	$K_L$ (L mmol <sup>-1</sup> )	pH <sub>eq</sub>	$q_{\max}$ (mmol g <sup>-1</sup> )	$K_L$ (L mmol <sup>-1</sup> )	
FeOOH	FO36	6.54	1.307	1.118	4.06	1.627	0.030	Present work
	BT9	3.5	0.107	60	3.50	0.377	37.5	[74]
	MnBT9	3.5	0.459	253	3.50	0.343	146	
	CGB	5.0	0.0964	33.6	5.00	0.146	8.43	[69]
<i>N</i> -methyl- <i>D</i> -glucamine	CRB05	7.76	0.945	0.5325	3.49	1.269	32.17	Present work
	PVbNMDG	-	-	-	6.00	0.736	967	[59]

CGB: Chitosan goethite bionanocomposite;

PVbNMDG: Poly[*N*-(4-vinyl benzyl)-*N*-methyl-*D*-glucamine];

BT9:  $\alpha$ -FeOOH (waste goethite); MnBT9: akhtenskite coated waste goethite

### 2.3.1.3. Kinetic study

The adsorption of metal ions depends on the interactions between the solution and functional groups on the surface of adsorbent. The specific time is needed to maintain the equilibrium interactions to ensure that the adsorption process is complete. Figure 2.4 shows the effect of contact time on adsorption of arsenic by CRB05 and FO36. The adsorption amount of both adsorbents was increasing when time was passing. In the case of As(III), CRB05 is equilibrated after 10 h, while FO36 requires 24 h to equilibrium. Also, adsorption amount of As(III) with CRB05 is greater than that of FO36. In the case of As(V), the adsorption systems were equilibrated at 14 h and 24 h for CRB05 and FO36, respectively. Adsorption amount obtained with CRB05 was larger than that of FO36 and much greater than adsorption of As(III).

The kinetic models have been used to determine the rate constants of different systems. Widely used kinetic models are those based on the decrease of available active sites to interact with solute (adsorption capacity) and have been successfully used to determine rate constants and characteristics of the sorption process. proposed the pseudo-first order model for describing the adsorption process of solid-liquid systems as Eq. (2-4) and its linear form is formulated as Eq. (2-5) [77].

$$\frac{dq}{dt} = k_1(q_{eq} - q_t) \quad (2-4)$$

$$\ln(q_{eq} - q_t) = \ln q_{eq} - k_1 t \quad (2-5)$$

where  $k_1$  is the rate constant ( $\text{min}^{-1}$ ),  $q_{eq}$  is the metal ions adsorption amount at equilibrium, and  $q_t$  is the metal ions adsorption amount at time  $t$  (min). The pseudo-second order equation has been widely used due the excellent fit of experimental data for the entire sorption period of many systems [78]. Pseudo-second-order model is derived as expressed in Eq. (2-6), and stated in the linear form as Eq. (2-7).

$$\frac{dq}{dt} = k_2(q_{eq} - q_t)^2 \quad (2-6)$$

$$\frac{t}{q_t} = \frac{1}{k_2 q_{eq}^2} + \frac{1}{q_{eq}} t \quad (2-7)$$

where  $k_2$  is the rate constant ( $\text{g mmol}^{-1} \text{min}^{-1}$ ).

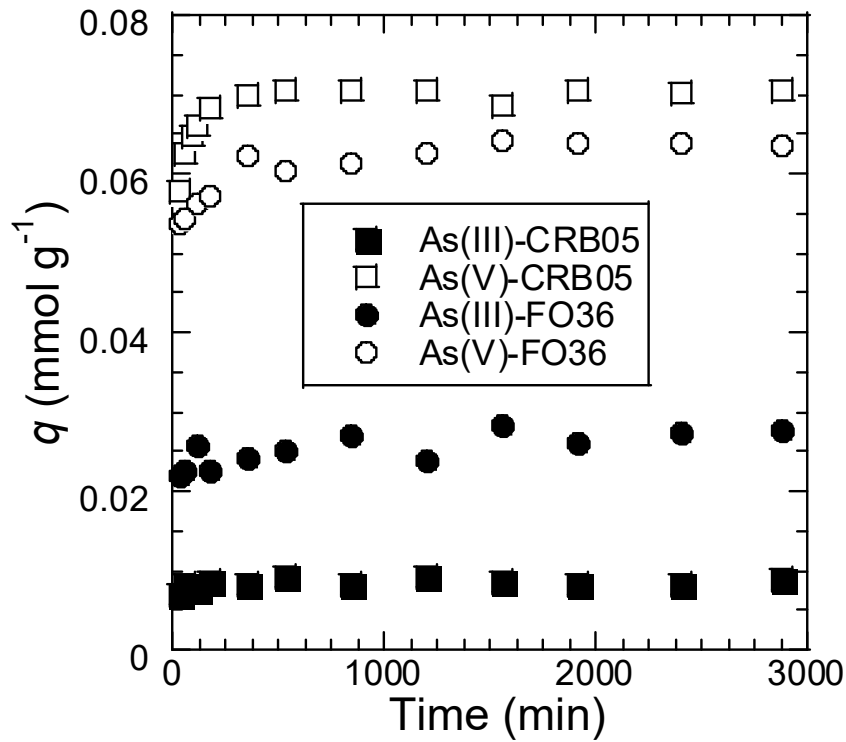


Figure 2.4 Effect of contact time on adsorption of arsenic by CRB05 and FO36.

Figure 2.5 and Figure 2.6 show the pseudo-first-order and pseudo-second-order kinetics for arsenic adsorption using CRB05 and FO36. The rate constants determined were summarized in Table 2.3, together with equations of the regression lines and correlation coefficients ( $R^2$ ). The correlation coefficients for two models indicated that the pseudo-second-order kinetic is considered more consistent to represent the kinetic data in the adsorption systems. This trend indicates that the rate-controlling step of the adsorption of metals are chemical-adsorption involving valence forces by the sharing or exchange of electron between adsorbent and metal ions, and complexation. The rate constant,  $k_2$ , of CRB05 was much greater than those of FO36 for both of As(III) and As(V).

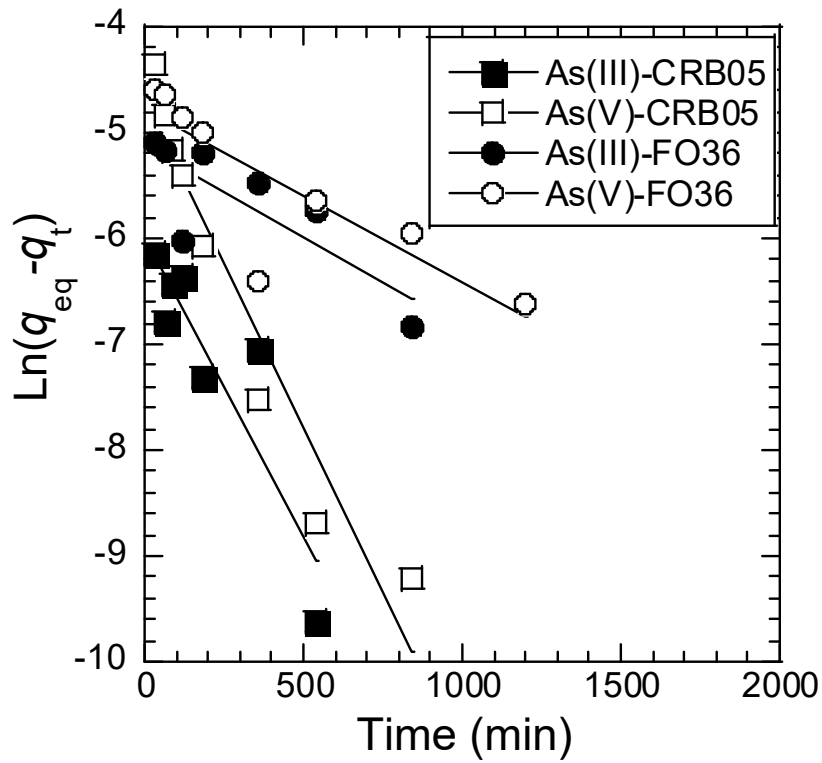


Figure 2.5 Pseudo-first-order kinetics for adsorption of arsenic by CRB05 and FO36.

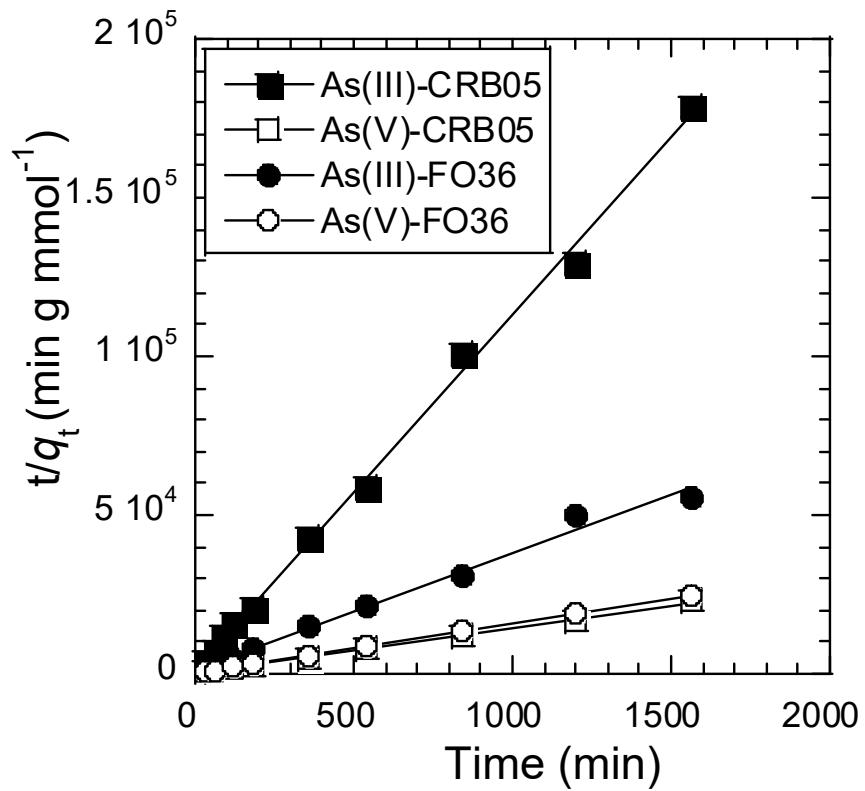


Figure 2.6 Pseudo-first-order kinetics for adsorption of arsenic by CRB05 and FO36.

Table 2.3 Equilibrium adsorption amounts and kinetic constants

	Adsorbents	$q_{\text{exper.}}$ (mmol g <sup>-1</sup> )	$K_1$ (min <sup>-1</sup> )	$R_1^2$	$K_2$ (g mmol <sup>-1</sup> min <sup>-1</sup> )	$R_2^2$
As(III)	CRB05	0.0093	0.0057	0.66	9.07	1.00
	FO36	0.0282	0.0017	0.80	1.34	0.99
As(V)	CRB05	0.0705	0.0062	0.72	5.35	1.00
	FO36	0.064	0.0016	0.93	0.92	1.00

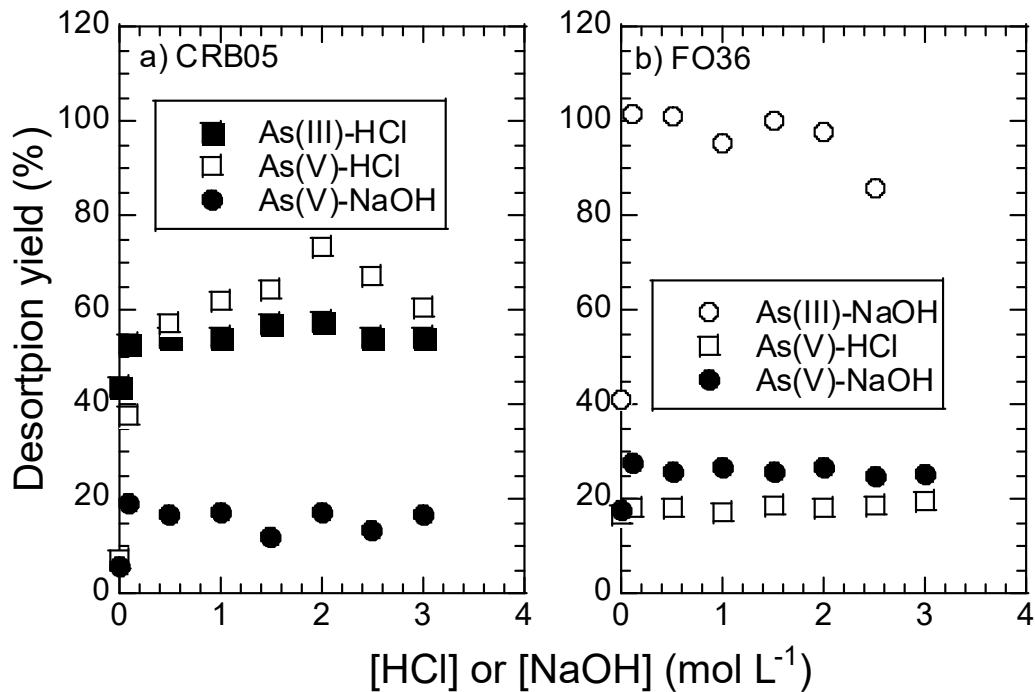


Figure 2.7 Desorption of As(III) and As(V) from loaded (a) CRB05 and (b) FO36.

#### 2.3.1.4. Desorption process

Desorption of arsenic loaded on the adsorbents was investigated. Figure 2.7 shows the desorption percentage of arsenic from the adsorbents. The As-loaded adsorbent was prepared with loaded amount 1.15 mmol g<sup>-1</sup> (As(V) with CRB05), 0.537 mmol g<sup>-1</sup> (As(III) with CRB05), 0.752 mmol g<sup>-1</sup> (As(V) with FO36), and 0.331 mmol g<sup>-1</sup> (As(III) with FO36). In the case of CRB05, both of As(V) and As(III) were desorbed by 1.5 – 2.5 mol L<sup>-1</sup> of HCl. However, the desorption efficiencies were incomplete, and the desorption yields were 70% for As(V) and

58% for As(III). In the case of FO36, As(III) could be effectively desorbed by NaOH, with desorption percentage of 95% by NaOH 0.1 – 2.0 mol L<sup>-1</sup>, however, the desorption of As(V) is not effective to suppress to desorption yield 28%. Low desorption yield of As(V) is caused by precipitation reaction of FeAsO<sub>4</sub>·nH<sub>2</sub>O. The desorption yield in batchwise system is expected to be improved by increasing volume of eluent or number of elution times.

### 2.3.2. Chromatographic removal of arsenic

#### 2.3.2.1. Removal of arsenic from single solution and mixed solution

Chromatographic operation of arsenic removal was finally investigated. Figure 2.8a shows the breakthrough curves of As(V), As(III), and As(III/V) with CRB05 at S.V. = 5.2 h<sup>-1</sup>, along with the pH of the effluent (pH<sub>effluent</sub>). Complete adsorption was achieved until B.V. = 3100 for As(III), B.V. = 2000 for As(V), and B.V. = 2400 for As(III/V), respectively. These results were not consistent with the results of adsorption isotherms, shown in Table 2.1. This is caused by that the equilibrium pH for adsorption isotherm of As(V) was 3.49 and that of As(III) was 7.76, while the pH<sub>effluent</sub> was in the range of 6.5 – 7. Higher adsorption amount for As(III) with CRB05 rather than for As(V) is due to the pH difference. Figure 2.8b shows breakthrough curves of As(V), As(III), and As(III/V) with FO36 at S.V. = 2.7 h<sup>-1</sup>. In the case of As(III) single system, the adsorption was broken through at B.V. = 240, while in the case of As(V) single system, the adsorption was broken through at B.V. = 820. The result was consistent with the adsorption capacity of FO36, because the adsorption capacity of As(V) are higher than that of As(III). In addition, the pH<sub>effluent</sub> was in the range of 3.0 – 5.0, and the results were also consistent with those shown in Figure 2.1. In the case of As(III/V) mixed system, the breakthrough point of As(III/V) was at B.V. = 410. Comparison between two kinds of adsorbents, CRB05 has larger adsorption amount rather than FO36 in column system. In addition, the adsorption amount of CRB05 for As(III) is larger than that of As(V) in column system.

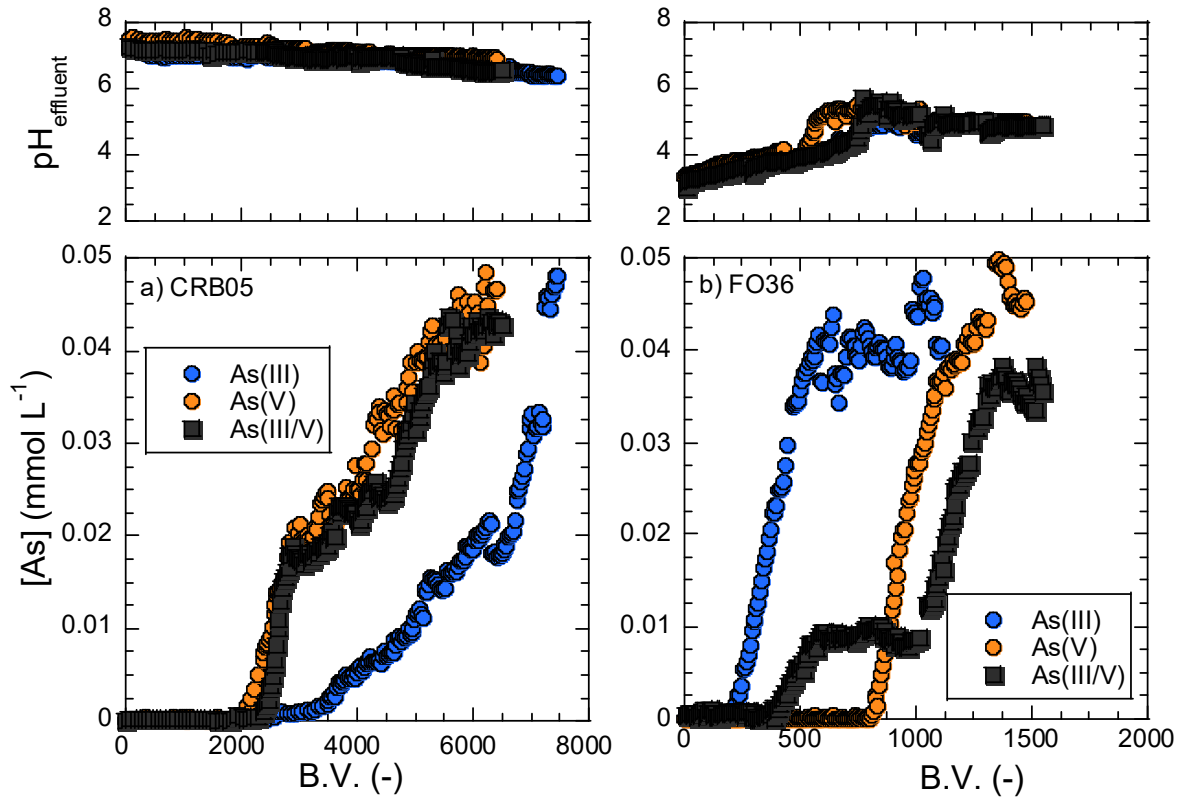


Figure 2.8 Breakthrough curves of arsenic removal with single solution and mixed solution by (a) CRB05 (S.V. = 5.2 h<sup>-1</sup>) and (b) FO36 (S.V. = 2.7 h<sup>-1</sup>).

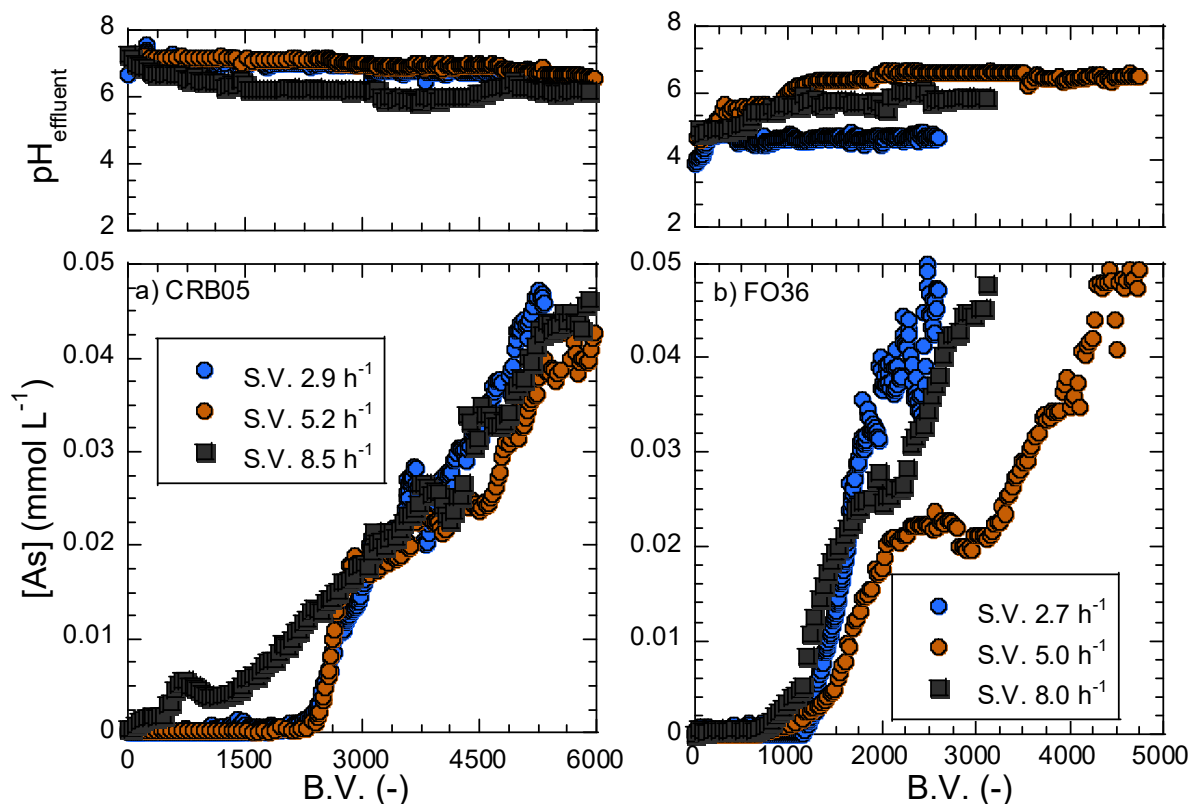


Figure 2.9 Breakthrough curves of As(III/V) removal with difference S.V. by (a) CRB05 and (b) FO36.

### 2.3.2.2. Effect of space velocity on arsenic removal

The effect of S.V. on the removal efficiency of As(III/V) was also investigated, by changing S.V. =  $2.9 \text{ h}^{-1}$ ,  $5.2 \text{ h}^{-1}$ , and  $8.5 \text{ h}^{-1}$  for CRB05 and S.V. =  $2.7 \text{ h}^{-1}$ ,  $5 \text{ h}^{-1}$ , and  $8 \text{ h}^{-1}$  for FO36. The breakthrough curves obtained are shown in Figure 2.9. In the case of CRB05, however, arsenic was broken immediately at B.V. = 200 with high S.V. =  $8.5 \text{ h}^{-1}$ , although arsenic was broken at high breakthrough point B.V. = 2400 and 2800 with low S.V. ( $2.9 \text{ h}^{-1}$  and  $5.2 \text{ h}^{-1}$ ). In the case of FO36, arsenic was broken at a similar breakthrough point (B.V. = 800, 900, and 1000), even when S.V. was increased. This suggests that FO36 could be applied to arsenic removal under the high S.V. condition. Among two adsorbents, arsenic removal by CRB05 is better than that by FO36. This consistent that the adsorption constants of arsenic ( $K_L$ ) of CRB05 is higher than those of FO36 for As(III) and As(V).

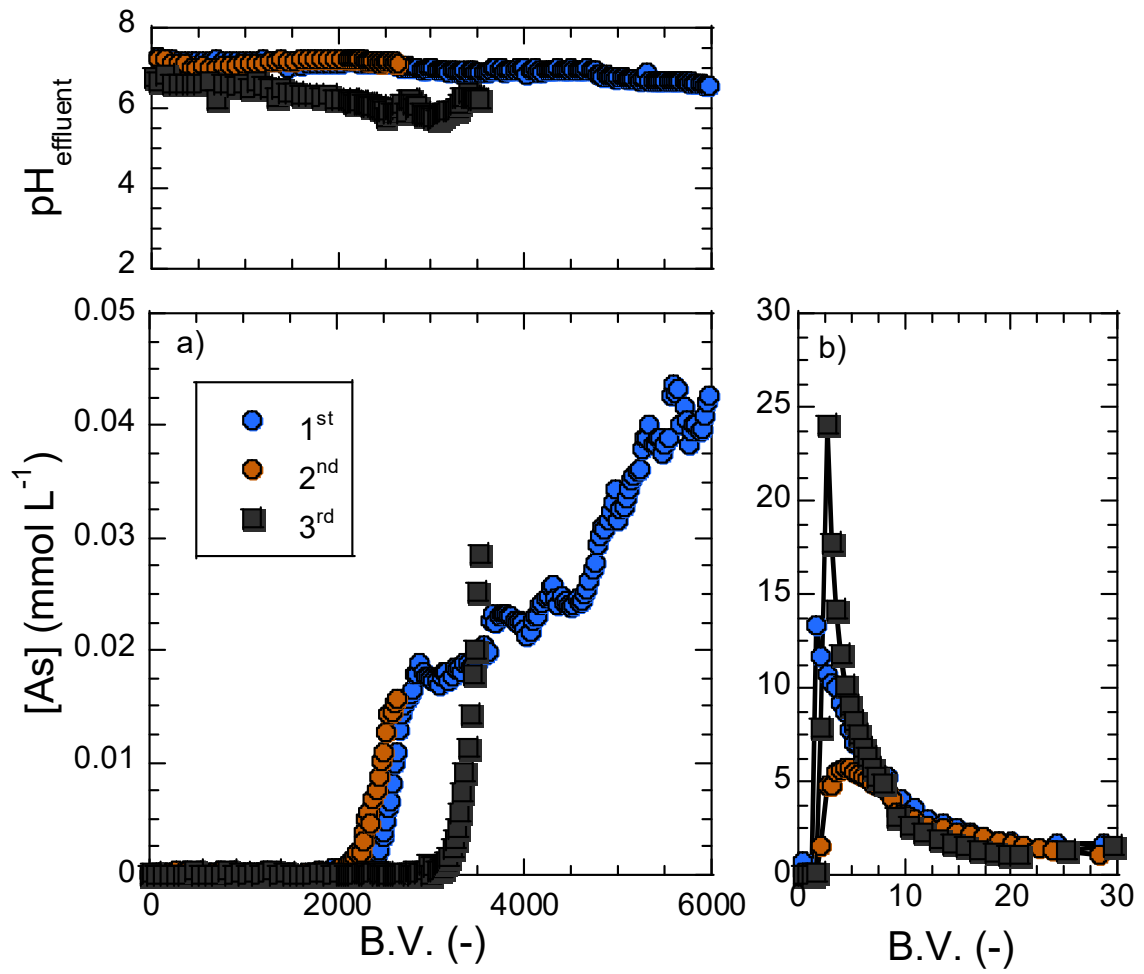


Figure 2.10 Breakthrough curve (a) and elution curve (b) for repeated use column with CRB05.

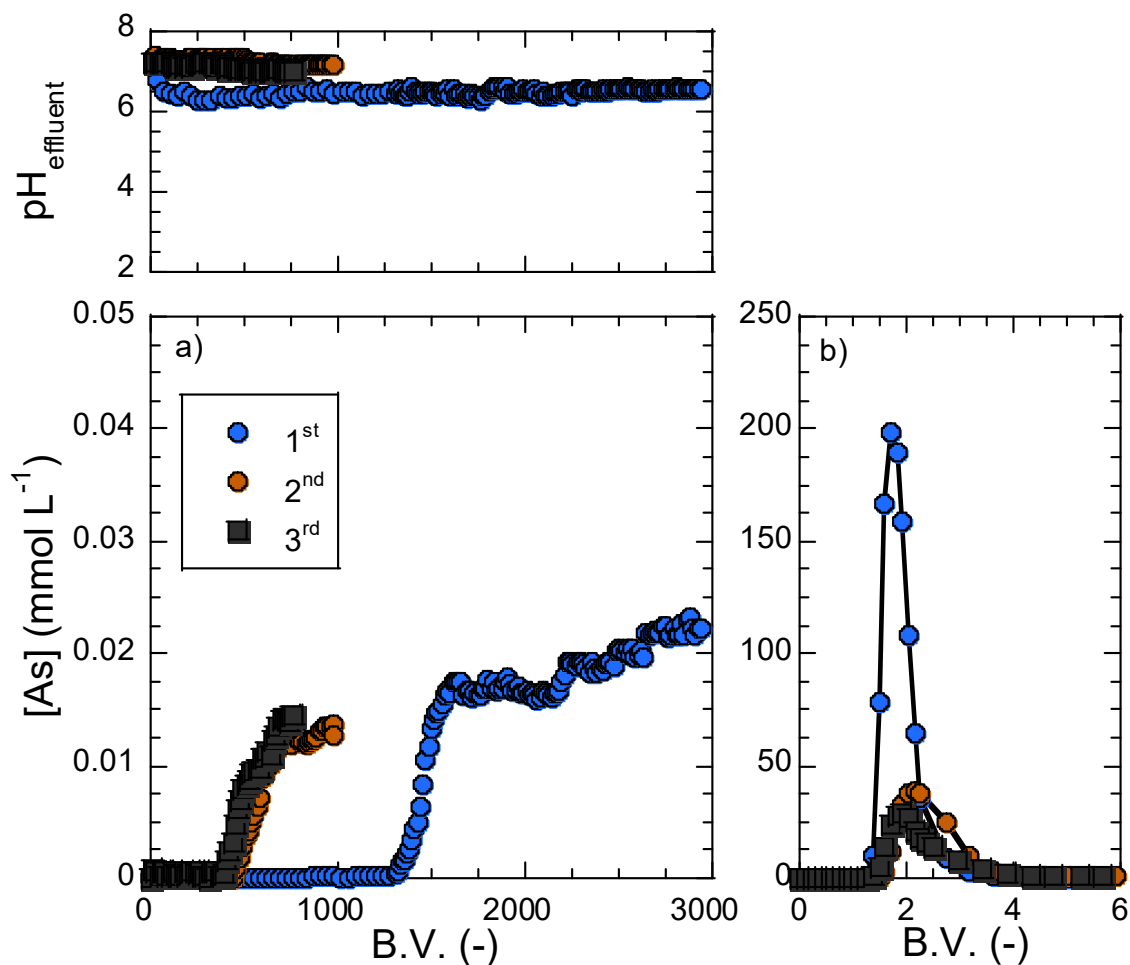


Figure 2.11 Breakthrough curve (a) and elution curve (b) for repeated use column with FO36.

### 2.3.2.3. Repeated use of adsorption column

Figure 2.10 shows the breakthrough and elution curves of arsenic with CRB05. Elution was carried out with  $2 \text{ mol L}^{-1}$  HCl at  $\text{S.V.} = 5.2 \text{ h}^{-1}$ . Arsenic loaded in CRB05 was completely eluted by  $2 \text{ mol L}^{-1}$  HCl. In three times iteration, the breakthrough points were slightly decreased to  $\text{B.V.} = 2800$ . Figure 2.11 shows the breakthrough and elution curves of repeated processing of FO36. Elution was carried out with NaOH at  $\text{S.V.} = 2.7 \text{ h}^{-1}$ . In every adsorption – elution processing, complete elution of the loaded arsenic could be achieved. Breakthrough point was however decreased from  $\text{B.V.} = 1300$  to 500 after 1st cycle. Decrease in the adsorption capacity might be due to the decomposition of the FeOOH functional group on FO36 by high concentration of NaOH. Therefore, elution of FO36 should be performed with low concentration of NaOH. From 2nd cycle, eluent concentration was changed from  $0.5 \text{ mol}$

$L^{-1}$  to low level concentration of NaOH to  $0.1 \text{ mol L}^{-1}$ , then breakthrough point was kept at B.V. = 500 in 3rd cycle. Therefore, FO36 is expected to be repeated used in column operation when using regenerant of  $0.1 \text{ mol L}^{-1}$  NaOH.

#### 2.4. Conclusion

Removal of arsenic contaminated in water environment by adsorption was investigated using the adsorbents of CRB05 and FO36. Batchwise adsorption shows that adsorptive removal of arsenic is highly pH depended, and optimal pH was determined in range 3.0 – 4.5 for removal of As(V) and 7.0 – 9.0 for removal of As(III). Adsorption isotherm data fit with Langmuir models, both of adsorbents have high adsorption capacity, and FO36 is the better adsorbent with higher adsorption capacity,  $1.307 \text{ mmol g}^{-1}$  for As(III) and  $1.627 \text{ mmol g}^{-1}$  for As(V). However, adsorption of arsenic with CRB05 is faster than with FO36.

In the case of chromatography study, FO36 has a higher selectivity for As(V) rather than As(III), while CRB05 possess higher selectivity for As(V) rather than As(III). Removal of arsenic by CRB05 is better than by FO36. However, CRB05 should be used low S.V., while FO36 could be operated with high S.V.. In addition, repeated use column adsorption with CRB05 is more stable than that of FO36.

## Chapter 3.Reductive Adsorption of Chromium(VI) by Coal-based Activated Carbon

### 3.1. Introduction

Recently, chromium (Cr) has been widely used in diverse areas, such as electroplating, metal plating, and leather tanning, which tends to be a major cause of Cr contamination in the water environment [79]. As mentioned in Chapter 1, Cr exists mainly in Cr(III) and Cr(VI) oxidation states in aqueous solution. Cr(VI) species are considered among the top 16 hazardous substances, according to The Agency for Toxic Substances and Diseases Registry classifications, owing to their toxic and carcinogenic profiles [32]. Cr(VI) species are about 100 times more toxic than Cr(III) species, because Cr(VI) is easily adsorbed in the stomach and accumulated in the kidney and liver [80]. Alternatively, low Cr(III) levels are essential to mammalian life, as mentioned in Chapter 1. According to Japan Ministry of the Environment, the limitation of Cr(VI) in effluent wastewater has defined at  $0.5 \text{ mg L}^{-1}$  ( $9.62 \text{ }\mu\text{mol L}^{-1}$ ) [20]. The World Health Organization (WHO) has regulated the maximum concentration of Cr(VI) in drinking water at  $0.05 \text{ mg L}^{-1}$  ( $0.962 \text{ }\mu\text{mol L}^{-1}$ ) [64].

Various methods and techniques have been studied for Cr(VI) removal from water environment, including adsorption [53,81], reduction [80], ion exchange [82], membrane filtration [83], and solvent extraction [43]. Among these techniques, adsorption processes have been the most extensively studied owing to their high removal efficiency, flexibility, and simple and easy processing. Activated carbon (AC) is one of the excellent adsorbents, since the AC possesses several advantages as an adsorbent, such as high pore volume, large specific surface area, and high adsorption capacity [84]. Studies on the adsorption of Cr(VI) with different type of the ACs, such as Hazelnut shell [53], corncob [50], and mango [51], have been reported. In addition to the feasible adsorption properties, Park *et al.* reported that the phenolic functional group on the surface of the AC can reduce Cr(VI) to Cr(III) [85]. Chen *et al.* found that Cr(III) existed on surface of the AC, after adsorption of Cr(VI) [80]. The coal-based AC with high specific surface area and large amount of phenolic functional group [84], was selected for reduction – adsorption of Cr(VI). Although reduction of Cr(VI) to Cr(III) is considered to be effective for detoxification of Cr(VI), the mechanisms of reductive adsorption of Cr(VI) is still not clearly understood.

In this chapter, the reductive adsorption of Cr(VI) from water environment has been investigated employing coal-based AC. Equilibrium and kinetic studies have been first carried out in batchwise system to reveal both adsorption and reduction performances. The column studies for removal of Cr(VI) were then performed using the packed column of AC to investigate the effect of pH and effect of space velocity.

## 3.2. Experimental

### 3.2.1. Reagents

A coal-based AC, M010, was supplied by Mitsubishi Chemical Co. (Tokyo, Japan). The AC was characterized in our previous study [84], including Boehm titration and nitrogen adsorption-desorption to determine functional group, pore volume and specific surface of AC, and further characterized using a zeta potential analyzer (ELSZ-1000, Otsuka Electronics Co., Ltd.), as shown in Table 3.1. All other reagents were supplied by FUJIFILM Wako Pure Chemical Corporation (Osaka, Japan) and were of analytical grade.

Table 3.1 Characterization of coal-based AC [83]

Pore volume (cm <sup>3</sup> g <sup>-1</sup> )	Surface area (m <sup>2</sup> g <sup>-1</sup> )	Surface functional group (mmol g <sup>-1</sup> )				Isoelectric point
		Acidic			Basic	
		Carboxylic	Lactonic	Phenolic		
0.531	1390	N.D.*	N.D.*	0.19	0.040	5.95

\*) Not detected.

### 3.2.2. Batchwise experiment

An aqueous solution of Cr(VI) was prepared by dissolving CrO<sub>3</sub> in deionized water, and the pH was adjusted using NaOH or H<sub>3</sub>PO<sub>4</sub> solutions. In preliminary experiments, H<sub>3</sub>PO<sub>4</sub> and H<sub>2</sub>SO<sub>4</sub> were investigated for use in pH adjustment, indicating that a high adsorption amount was obtained using H<sub>3</sub>PO<sub>4</sub> in the low pH region. Batchwise experiments were conducted by shaking a suspended mixture of AC (50 mg; particle size, 0.5 – 1.0 mm) and aqueous feed solution (10 mL) for 2 h in equilibrium studies, and for between 5 min and 3 h in kinetic studies. For equilibrium studies, the effect of pH was investigated in the pH range of 1.0 – 13.0 at an initial Cr(VI) concentration ([Cr(VI)]<sub>ini</sub>) of 4.3 mmol L<sup>-1</sup>. The effect of initial concentration was investigated in the [Cr(VI)]<sub>ini</sub> range of 2.5 – 50 mmol L<sup>-1</sup> at pH 2.0 – 9.0 and at

temperatures of 288 – 318 K. In all cases, after shaking the suspended mixture, filtration was conducted, and the pH and total Cr concentration in the aqueous solution were measured using a pH meter (Horiba F-74) and inductively coupled plasma atomic emission spectrometry (ICP-AES; Shimadzu ICPE-9000), respectively. Simultaneously, the Cr(VI) concentration ([Cr(VI)]) in the aqueous solution was determined using a UV-vis spectrophotometer (JASCO; UV-660) at 540 nm after reacting with 1,5-diphenylcarbazide (DPC) indicator [83,86]. The Cr(III) concentration ([Cr(III)]) was determined by subtracting [Cr(VI)] from [Cr(total)]. The adsorption amount,  $q_{\text{eq}}$  (mmol g<sup>-1</sup>), was calculated using Eq. (3-1).

$$q_{\text{eq}} = \frac{([\text{Cr}(\text{total})]_{\text{ini}} - [\text{Cr}(\text{total})]_{\text{eq}}) \cdot V}{m} \quad (3-1)$$

where [Cr(total)]<sub>ini</sub> and [Cr(total)]<sub>eq</sub> are the initial and equilibrium total Cr concentrations (mmol L<sup>-1</sup>),  $V$  is the aqueous solution volume (L), and  $m$  is the mass of AC (g).

The valence state of Cr loaded on AC was also measured. Accordingly, the AC was dried after Cr adsorption, and then analyzed by X-ray photoelectron spectroscopy (XPS; Shimadzu/KRATOS AXIS165) using a monochromatic Al K $\alpha$  source. Survey spectra were collected from 0 to 1253.6 eV at a pass energy of 160 eV. The optimum fitting was achieved by deconvolution of the Cr 2*p* spectrum into four peaks. The peaks at 577 and 586 eV were assigned to Cr(III) 2*p*<sub>3/2</sub> and 2*p*<sub>1/2</sub>, respectively, while the peaks at 579 and 589 eV were assigned to Cr(VI) 2*p*<sub>3/2</sub> and 2*p*<sub>1/2</sub>, respectively [80,87,88].

### 3.2.3. Column Experiment

Column experiments were performed using a glass column (inner diameter, 5 mm; outer diameter, 12 mm; length, 10 cm). AC (particle size, 0.5 – 1.0 mm; wet volume, 1.0 mL) was packed into the glass column and sandwiched with glass wool. A feed solution of Cr(VI) ([Cr(VI)]<sub>feed</sub> = 1.0 mmol L<sup>-1</sup>) was prepared at different pH values (2.0, 3.0, 5.0, and 6.0) and fed into the column at a flow rate of 0.2 mL min<sup>-1</sup>, such that the space velocity (S.V. = flow rate/wet volume) was 12 h<sup>-1</sup>. To obtain different S.V. values, the flow rate was varied to 0.1 (S.V. = 6 h<sup>-1</sup>), 0.2 (S.V. = 12 h<sup>-1</sup>), 0.5 (S.V. = 30 h<sup>-1</sup>), and 1 mL min<sup>-1</sup> (S.V. = 60 h<sup>-1</sup>). The feed solution was fed into the column using a dual plunger pump (Flom KP-21) and the effluent was collected using a fraction collector (EYELA DC-1500). The Cr(VI) concentration was analyzed by UV-vis spectrophotometry, while the total Cr concentration was measured by ICP-AES. The bed volume (B.V.) was calculated using Eq. (3-2).

$$B.V. = \frac{vt}{L} \quad (3-2)$$

where  $v$  is the volumetric flow rate of solution ( $\text{mL min}^{-1}$ ),  $t$  is the length of time for which the feed solution was applied (min), and  $L$  is the wet volume of AC (mL).

### 3.3. Results and discussion

#### 3.3.1. Batchwise adsorption

##### 3.3.1.1. Effect of pH on reductive adsorption

The pH of aqueous solution is one of the most important parameters affecting on the adsorption characteristics of ionic adsorbate. Figure 3.1 shows the effect of  $\text{pH}_{\text{eq}}$  on adsorption of Cr(total) with AC. The adsorption amount of Cr(total) was increased in acidic pH region, and then was decreased in  $\text{pH}_{\text{eq}} > 6.0$ . High adsorption amounts were therefore observed in  $\text{pH}_{\text{eq}} = 4.0 - 6.0$ . Cr(VI) occurs as five anionic forms in aqueous solution, as expressed in Eqs. (1-7) – (1-10) [21], and the Cr(VI) species distribution in aqueous solution is shown in Figure 3.1c.

In aqueous solution, various Cr(VI) species ( $\text{H}_2\text{CrO}_4$ ,  $\text{HCrO}_4^-$ ,  $\text{CrO}_4^{2-}$ ,  $\text{Cr}_2\text{O}_7^{2-}$ , and  $\text{HCr}_2\text{O}_7^-$ ) were appeared at various pH, and  $\text{CrO}_4^{2-}$  ( $\text{pH} > 8$ ) and  $\text{Cr}_2\text{O}_7^{2-}$  ( $\text{pH} < 8$ ) are two major species in aqueous solution. Considering the isoelectric point (IP) of the AC is 5.95, the adsorption of Cr(VI) proceeds *via* electrostatic attraction between  $\text{Cr}_2\text{O}_7^{2-}$  and positively charged surface of the AC in the acidic pH region.

Beside the adsorption process, reduction of Cr(VI) to Cr(III) was occurred. Generally, the reduction of Cr(VI) to Cr(III) in aqueous solution requires large amount of proton and electron [89]. The reduction of Cr(VI) in aqueous solution therefore proceeds at low and high pH region, as mentioned in Eqs. (3-3) and (3-4) [90].



The reduction of Cr(VI) is proceeded by the existence of phenol group on the surface of the AC, C-C and C-OH groups was oxidized to C-OH and C=O, respectively [85]. The speciation of Cr(VI) and Cr(III) adsorbed on the AC, determined by XPS analysis, was also shown in Figure 3.1a. The most of Cr existed on the AC was revealed to be Cr(III), indicating the Cr(VI) was reduced to Cr(III). Figure 3.1b shows the fraction of Cr species remained in the

aqueous solution after adsorption. In acidic pH region of  $\text{pH} < 4$ , the most of Cr species remained in the aqueous solution was Cr(III), while the most of Cr species was still Cr(VI) at  $\text{pH} > 4$ . The adsorption – reduction scheme can be therefore considered as follows.

(i)  $\text{pH} < 4$

Cr(VI) ( $\text{Cr}_2\text{O}_7^{2-}$ ) is adsorbed on the AC with positive charge by electrostatic attraction, and then the most of Cr(VI) is reduced to Cr(III). After reduction, a part of Cr(III) is released into the aqueous solution based on distribution of Cr(III), and then Cr(VI) remained in the aqueous solution is adsorbed. Adsorption of Cr(VI) – reduction of Cr(VI) to Cr(III) – release of Cr(III) – adsorption of Cr(VI) is cycled until adsorption of Cr(III) is equilibrated. The most of Cr(VI) in the system was thus finally reduced to Cr(III) in the low concentration region of Cr(VI), while Cr(VI) is observed in the aqueous solution after adsorption in the range of higher concentration of Cr(VI), as shown in Figure 3.2e.

(ii)  $4 < \text{pH} < 6$

$\text{Cr}_2\text{O}_7^{2-}$  is adsorbed as same as  $\text{pH} < 4$ , and then adsorbed Cr(VI) is reduced to Cr(III). The reduced Cr(III) is however hardly released into the aqueous solution, because Cr(III) is precipitated as hydroxide at  $\text{pH} > 4.6$  [22]. Therefore, Cr adsorbed on the AC is existed as precipitates, and the most of Cr remained in the aqueous solution after adsorption is Cr(VI).

(iii)  $\text{pH} > 6$

Major species of Cr(VI) at  $\text{pH} < 8$  is  $\text{Cr}_2\text{O}_7^{2-}$  and that at  $\text{pH} > 8$  is  $\text{CrO}_4^{2-}$ . The adsorption of Cr(VI) in this pH region is dramatically decreased, compared to that in acidic pH region, since the isoelectric point of the AC is 5.95. Although the adsorption amount of Cr(VI) is small, adsorbed Cr(VI) is reduced with the AC and exists as Cr(III) precipitates.

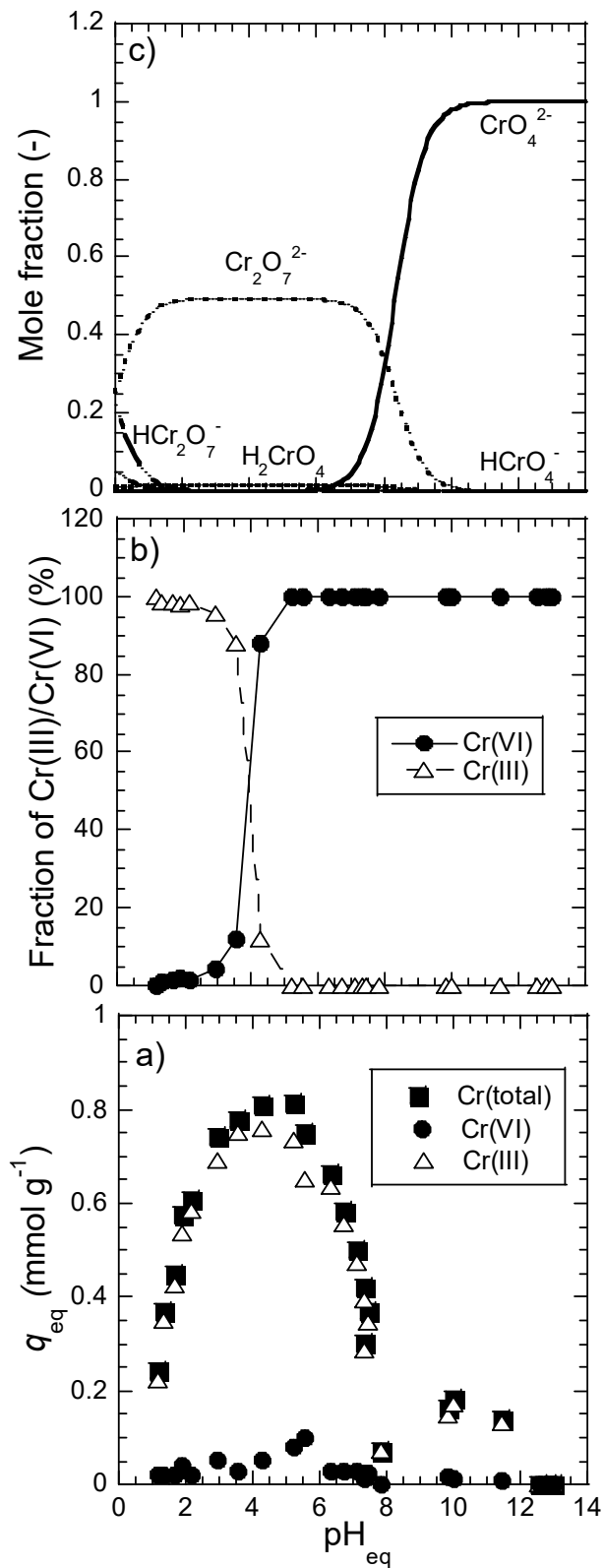


Figure 3.1 Effect of pH on (a) adsorption amount of Cr(total), Cr(VI), and Cr(III), (b) fraction of Cr(VI) and Cr(III) in the aqueous solution after adsorption, and (c) species distribution of Cr(VI);  $[\text{Cr(VI)}]_{\text{ini}} = 4.3 \text{ mmol L}^{-1}$ .

### 3.3.1.2. Adsorption isotherm

The adsorption isotherm of Cr on the AC with changing  $\text{pH}_{\text{eq}}$  and temperature was investigated. Figure 3.2 shows the adsorption isotherms of Cr at 298 K with  $\text{pH}_{\text{eq}} = 2.04 \pm 0.07$ ,  $4.12 \pm 0.09$ ,  $5.92 \pm 0.12$ , and  $8.75 \pm 0.11$ , together with Cr(VI) and Cr(III) speciation on the AC and Cr(VI) and Cr(III) fractions in aqueous solution. At all pH values, most Cr on the AC was Cr(III), as observed for the pH effect (Figure 3.1). Cr remaining in aqueous solution after adsorption at  $\text{pH}_{\text{eq}} > 4.12$  was mostly Cr(VI), which was also consistent with the data in Figure 3.1. However, at  $\text{pH}_{\text{eq}} = 2.04$ , the Cr(VI) fraction of total Cr remaining in aqueous solution increased with the increasing Cr concentration in the feed solution. Therefore, the adsorption – reduction – release cycle stopped when Cr(III) adsorption was equilibrated.

The adsorption isotherm data for total Cr were analyzed using the Langmuir isotherm model, as shown in Eq. (3-5), assuming that the maximum adsorption capacity corresponded to the formation of a saturated monolayer of adsorbate on the adsorbent surface [76].

$$q_{\text{eq}} = \frac{q_{\text{max}} \cdot K_L \cdot [\text{Cr}(\text{total})]_{\text{eq}}}{1 + K_L \cdot [\text{Cr}(\text{total})]_{\text{eq}}} \quad (3-5)$$

where  $[\text{Cr}(\text{total})]_{\text{eq}}$  is the equilibrium concentration ( $\text{mmol L}^{-1}$ ),  $q_{\text{eq}}$  is the adsorption amount ( $\text{mmol g}^{-1}$ ),  $q_{\text{max}}$  is the maximum adsorption capacity ( $\text{mmol g}^{-1}$ ), and  $K_L$  is the adsorption constant ( $\text{L mmol}^{-1}$ ). At all  $\text{pH}_{\text{eq}}$  values, the adsorption isotherms fitted well with the Langmuir mechanism, and the maximum adsorption capacities and adsorption constants were determined, as shown in Table 3.2. The highest adsorption capacity of  $3.43 \text{ mmol g}^{-1}$  was obtained at  $\text{pH}_{\text{eq}} = 2.04$ , although the total Cr adsorption amount at  $\text{pH} \approx 4$  was lower than that at  $\text{pH} \approx 2$ , as shown in Figure 3.1. This difference was attributed to the adsorption constant at  $\text{pH}_{\text{eq}} = 4.12$  being higher than that at  $\text{pH}_{\text{eq}} = 2.04$ , resulting in a higher adsorption amount being obtained from dilute solution, as shown in Figure 3.1. As mentioned in section 3.3.1.1, the adsorption equilibria of both Cr(VI) and Cr(III) exist in the system at  $\text{pH} < 4$ , while the adsorption equilibrium of Cr(III) is not existed at  $\text{pH} > 4$  due to precipitation of Cr(III). This difference may correspond the highest adsorption capacity at  $\text{pH}_{\text{eq}} = 2.04$ .

The adsorption performance of Cr(VI) of AC has been compared on the Langmuir parameters ( $q_{\text{max}}$  and  $K_L$ ) with several previously published data as shown in Table 3.3 [53,58,79,91,92]. The adsorption constant,  $K_L$  is related to the free adsorption energy and the affinity of adsorbent for Cr(VI) in aqueous solution. The present adsorbent has highest affinity for Cr(VI) among the adsorbents reported, because both  $q_{\text{max}}$  and  $K_L$  are highest. In addition, the adsorption capacity of the present AC is larger than 3 times other activated carbon such as

Corn cob ( $1.09 \text{ mmol g}^{-1}$ ) [91], Rice husk ( $0.93 \text{ mmol g}^{-1}$ ) and saw dust ( $1.03 \text{ mmol g}^{-1}$ ) [92]. The adsorption constants represent the affinity of the adsorbate for the adsorbent binding site, and the dimensionless constant separation factor,  $R_L$ , indicates whether the adsorption is favorable or not. The  $R_L$  was calculated as Eq. (3-6).

$$R_L = \frac{1}{1 + K_L \cdot [\text{Cr}(\text{total})]_{\text{ini}}} \quad (3-6)$$

where  $R_L > 1$  indicates unfavorable adsorption,  $R_L = 1$  indicates linear adsorption,  $0 < R_L < 1$  indicates favorable adsorption, and  $R_L = 0$  indicates irreversible adsorption [89]. At all  $\text{pH}_{\text{eq}}$  values, the  $R_L$  values obtained were between 0 and 1, demonstrating that the AC used was favorable for Cr(VI) adsorption.

Table 3.2 Adsorption isotherm parameters obtained for Cr(VI) adsorption onto AC

$\text{pH}_{\text{eq}}$	$q_{\text{max}}$ ( $\text{mmol g}^{-1}$ )	$K_L$ ( $\text{L mmol}^{-1}$ )	$R^2$
$2.04 \pm 0.07$	3.43	0.352	1.00
$4.12 \pm 0.09$	2.12	1.13	1.00
$5.92 \pm 0.12$	1.43	0.660	1.00
$8.75 \pm 0.11$	0.102	0.448	0.97

Table 3.3 Comparison maximum adsorption capacity and adsorption constants between various adsorbents.

Adsorbents	pH <sub>eq</sub>	$q_{\max}$ (mmol g <sup>-1</sup> )	$K_L$ (L mmol <sup>-1</sup> )	References
Coal-based AC	2.04 ± 0.07	3.43	0.352	Present work
Rice husk carbon	2.0	0.93	14.04	[91]
Saw dust Carbon	2.0	1.03	29.12	
CHA*	3.0	0.71	1.872	[78]
EHA*	3.0	0.70	25.42	
Hazelnut shell AC	-	3.27	3.697	[53]
Magnetized corn cob AC	2.0	1.10	2.08	[90]
Corn cob AC	2.0	1.09	1.872	
Magnetic magnetite nanoparticle	2.0	0.39	13.312	[58]

\* Undissolved self-extracted peat soil humic acid from Sigma Aldrich (CHA) and from Northeast China (EHA)

### 3.3.1.3. Thermodynamic adsorption

Temperature is another important factor affecting adsorption systems, because temperature influences the adsorption capacity. Therefore, the reductive adsorption of Cr(VI) on the AC at pH<sub>eq</sub> = 2.0 was investigated at different temperatures, and the corresponding adsorption isotherms were obtained, as shown in Figure 3.3. All adsorption isotherms corresponded to the Langmuir model, and the maximum adsorption capacities and adsorption constants are summarized in Table 3.4. Temperature is related to thermodynamic properties, such as enthalpy, entropy, and Gibbs free energy, which are needed to confirm whether an adsorption process is spontaneous, and whether the adsorption system is exothermic or endothermic. Thermodynamic parameters can be estimated from equilibrium constants as functions of temperature *via* the van't Hoff equation, Eqs. (3-7) – (3-8) [36].

$$\ln K = -\frac{\Delta H^\circ}{R_g T} + \frac{\Delta S^\circ}{R_g} \quad (3-7)$$

$$\Delta G^\circ = -R_g T \ln K \quad (3-8)$$

where  $R_g$  is the gas constant ( $8.314 \text{ J mol}^{-1} \text{ K}^{-1}$ ) and  $T$  is temperature (K). Figure 3.4 shows the van't Hoff plot for reductive adsorption of Cr(VI) by the AC. The thermodynamic variables were then calculated, as summarized in Table 3.4. The negative values of  $\Delta G^\circ$  confirmed the feasibility of the process and spontaneous adsorption. The positive  $\Delta H^\circ$  value indicated that the adsorption process was endothermic, while the positive  $\Delta S^\circ$  value suggested increased randomness at the solid–aqueous solution interface during adsorption. The adsorption data were consistent with previous reports[53].

Table 3.4 Thermodynamic parameters for Cr(VI) adsorption by AC

Temperature (K)	pH <sub>eq</sub>	$q_{\max}$ (mmol g <sup>-1</sup> )	$K_L$ (L mmol <sup>-1</sup> )	$\Delta G^\circ$ (kJ mol <sup>-1</sup> )	$\Delta H^\circ$ (kJ mol <sup>-1</sup> )	$\Delta S^\circ$ (J mol <sup>-1</sup> K <sup>-1</sup> )
288	2.06 ± 0.07	3.42	0.32	-13.78	7.10	72.55
298	2.03 ± 0.07	3.43	0.35	-14.53	/	/
308	2.09 ± 0.06	3.67	0.39	-15.28		
408	2.10 ± 0.04	3.82	0.42	-15.94		

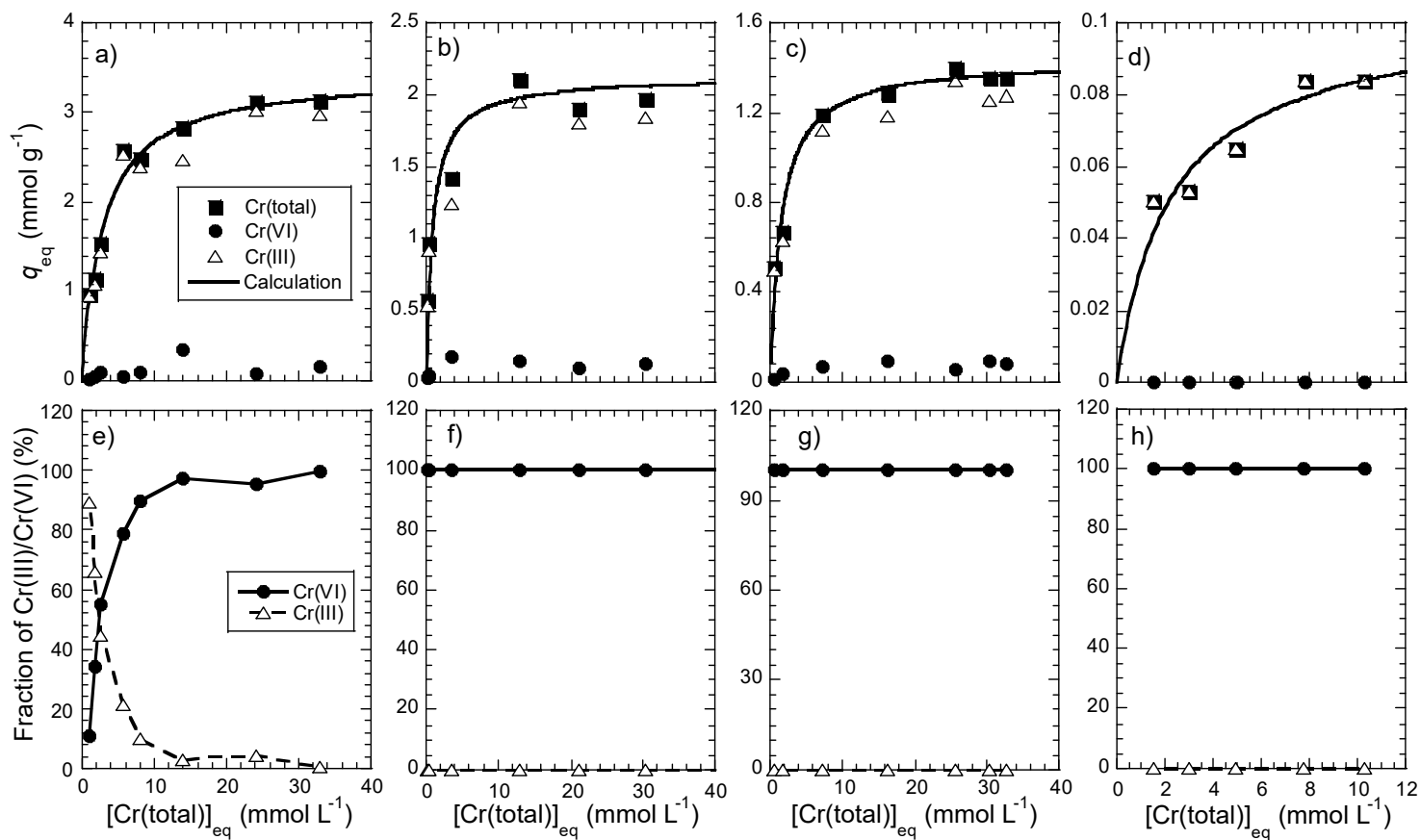


Figure 3.2 Adsorption isotherms of Cr at 298 K, together with speciation of Cr(VI) and Cr(III) on the AC at (a)  $\text{pH}_{\text{eq}} = 2.04$ , (b)  $\text{pH}_{\text{eq}} = 4.12$ , (c)  $\text{pH}_{\text{eq}} = 5.92$ , and (d)  $\text{pH}_{\text{eq}} = 8.75$ . Fraction of Cr(VI) and Cr(III) in the aqueous solution after adsorption are also shown as (e)  $\text{pH}_{\text{eq}} = 2.04$ , (f)  $\text{pH}_{\text{eq}} = 4.12$ , (g)  $\text{pH}_{\text{eq}} = 5.92$ , and (h)  $\text{pH}_{\text{eq}} = 8.75$ . Calculated values of the adsorption isotherms based on Langmuir adsorption mechanism are shown as solid lines in (a) – (d).

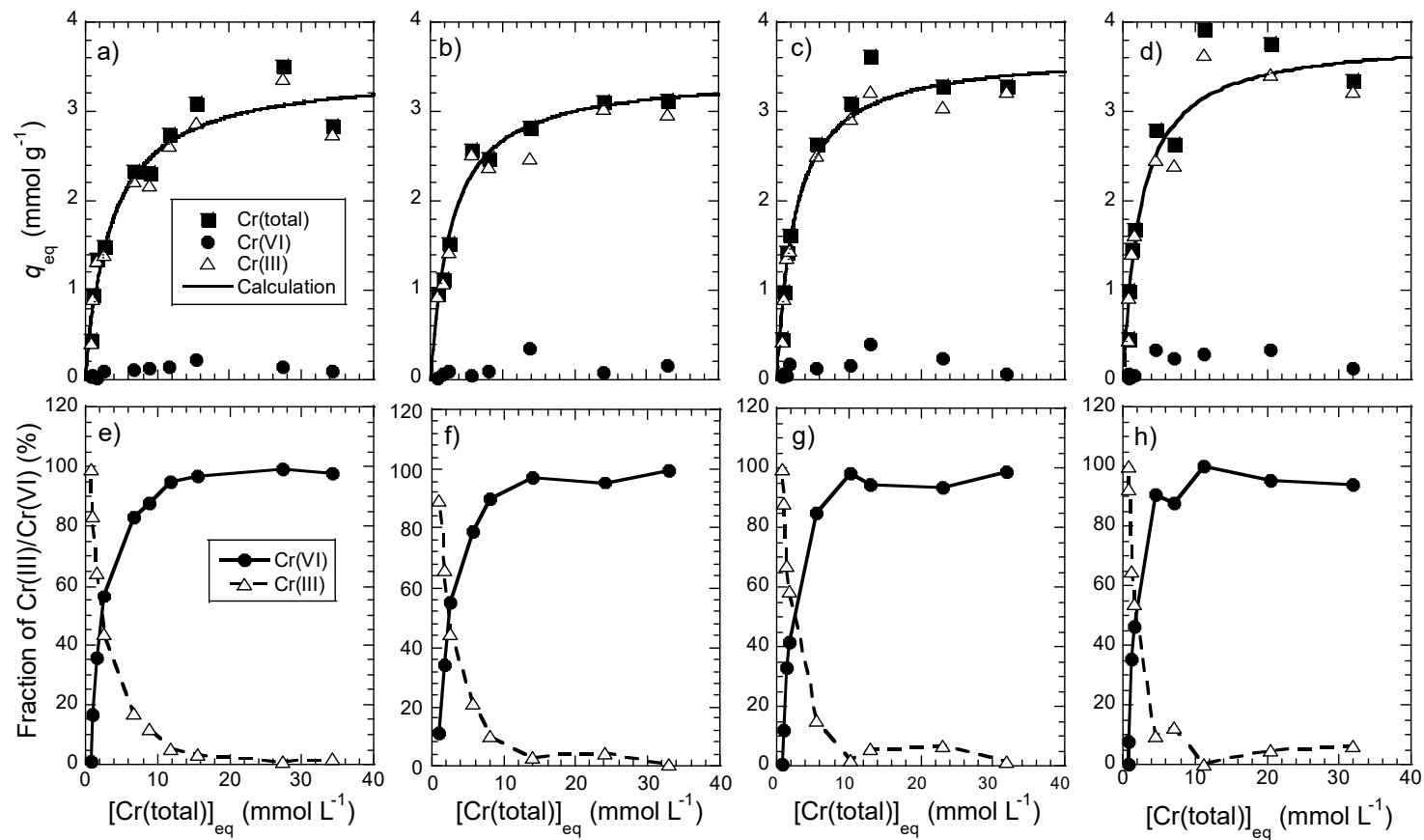


Figure 3.3 Adsorption isotherms of Cr, together with speciation of Cr(VI) and Cr(III) on the AC at temperature of (a) 288 K, (b) 298 K, (c) 308 K, and (d) 318 K. Fraction of Cr(VI) and Cr(III) in the aqueous solution after adsorption are also shown as (e) 288 K, (f) 298 K, (g) 308 K, and (h) 318 K. Calculated values of the adsorption isotherms based on Langmuir adsorption mechanism are shown as solid lines in (a) – (d).

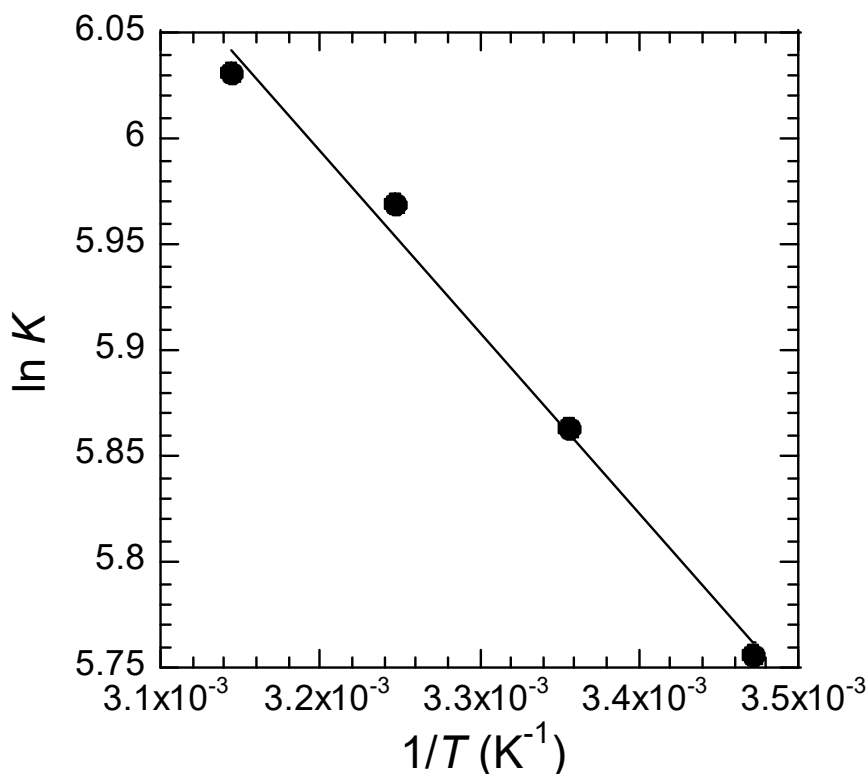


Figure 3.4 Van't Hoff plot for Cr(VI) adsorption by the AC.

#### 3.3.1.4. Kinetic study

Time-course variation of the reductive adsorption of Cr(VI) was investigated at  $\text{pH}_{\text{ini}} = 2.0$ . Figure 3.5 shows the time-course variation of the adsorption amount of total Cr, together with speciation of Cr(VI) and Cr(III), from aqueous Cr(VI) solution of different initial concentration ( $[\text{Cr(VI)}]_{\text{ini}} = 2.5 - 5.5 \text{ mmol L}^{-1}$ ). Although the time to achieve adsorption equilibrium was slightly increased with increase in the initial Cr concentration, the adsorption amount of Cr was almost equilibrated at 40 – 60 min. In addition, the most of adsorbed Cr on the AC was Cr(III), even in the very beginning of the adsorption, indicating the reduction of the Cr(VI) to Cr(III) is quite fast. Figure 3.5 also shows the concentration of total Cr, Cr(VI), and Cr(III) in the aqueous solution. In this concentration range, fraction of Cr(VI) to total Cr was started to be decreased just after adsorption started, and then was completely reduced after 3 h. The results obtained also confirm that the reductive adsorption of Cr(VI) at acidic pH region was based on the adsorption – reduction – release cycle.

The rate-determining step of the reductive adsorption can be considered on the adsorption step, since the rate of reduction was quite fast. The kinetics of reductive adsorption was therefore investigated based on pseudo-first-order and pseudo-second-order adsorption models,

which were generally used for analyzing conventional adsorption system. Pseudo-first-order model can be expressed by Eq. (3-9), where  $k_1$  is the rate constant ( $\text{min}^{-1}$ ),  $q_{\text{eq}}$  is the adsorption amount of Cr at equilibrium, and  $q_t$  is the adsorption amount of Cr at time  $t$  (min), and a linear relationship for the pseudo-first-order model can be obtained as Eq. (3-10) [77].

$$\frac{dq}{dt} = k_1(q_{\text{eq}} - q_t) \quad (3-9)$$

$$\ln(q_{\text{eq}} - q_t) = \ln q_{\text{eq}} - k_1 t \quad (3-10)$$

Pseudo-second-order model can be expressed by Eq. (3-11) where  $k_2$  is the rate constant ( $\text{g mmol}^{-1} \text{min}^{-1}$ ), and a linear relationship for the pseudo-second-order model can be obtained as Eq. (3-12) [78].

$$\frac{dq}{dt} = k_2(q_{\text{eq}} - q_t)^2 \quad (3-11)$$

$$\frac{t}{q_t} = \frac{1}{k_2 q_{\text{eq}}^2} + \frac{1}{q_{\text{eq}}} t \quad (3-12)$$

Based on the analysis of the data shown in Figure 3.5, the present reductive adsorption system agreed with the pseudo-second-order kinetics, as shown in Figure 3.6. The rate constants determined were summarized in Table 3.5., together with equations of the regression lines and correlation coefficients ( $R^2$ ). Although the rate constant is basically not affected by the initial Cr concentration, the present rate constants were slightly different by the initial concentration, especially in low initial Cr concentration. This might be because the reduction of Cr(VI) to Cr(III) and release of the resultant Cr(III) are increased, when initial concentration is increased.

Table 3.5 Pseudo-second-order kinetic parameters

$[\text{Cr(VI)}]_{\text{ini}}$ ( $\text{mmol L}^{-1}$ )	$q_{\text{eq}}$ ( $\text{mmol g}^{-1}$ )	$k_2$ ( $\text{g mmol}^{-1} \cdot \text{min}^{-1}$ )	$R^2$
2.5	0.441	0.992	0.999
4.0	0.755	0.201	0.999
5.5	1.019	0.283	0.999

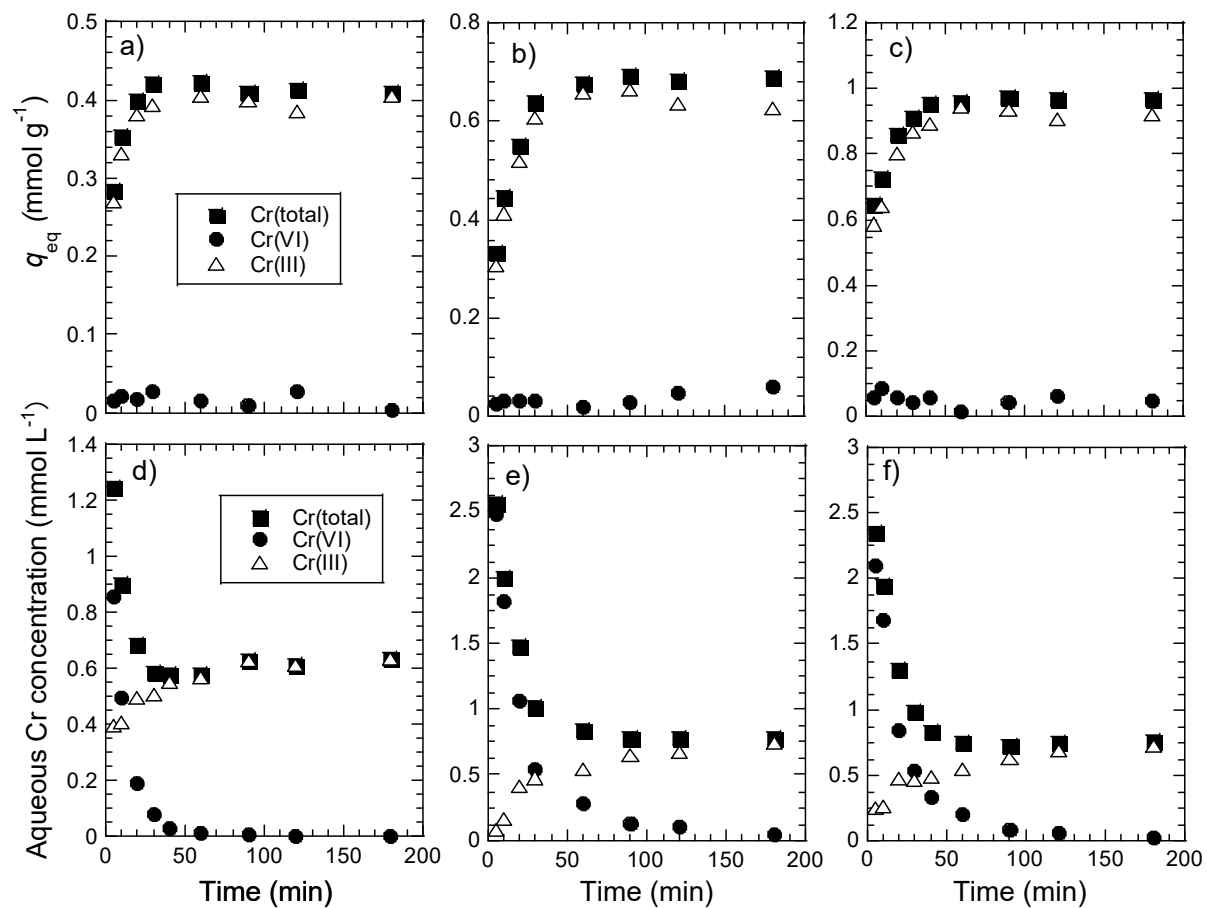


Figure 3.5 Time-course variation of the adsorption amount of total Cr, together with speciation of Cr(VI) and Cr(III) on the AC from aqueous solution of  $[\text{Cr(VI)}]_{\text{ini}} =$  (a)  $2.5 \text{ mmol L}^{-1}$ , (b)  $4.0 \text{ mmol L}^{-1}$ , and (c)  $5.5 \text{ mmol L}^{-1}$ . Fraction of Cr(VI) and Cr(III) in the aqueous solution after adsorption are also shown as (d)  $2.5 \text{ mmol L}^{-1}$ , (e)  $4.0 \text{ mmol L}^{-1}$ , and (f)  $5.5 \text{ mmol L}^{-1}$ .

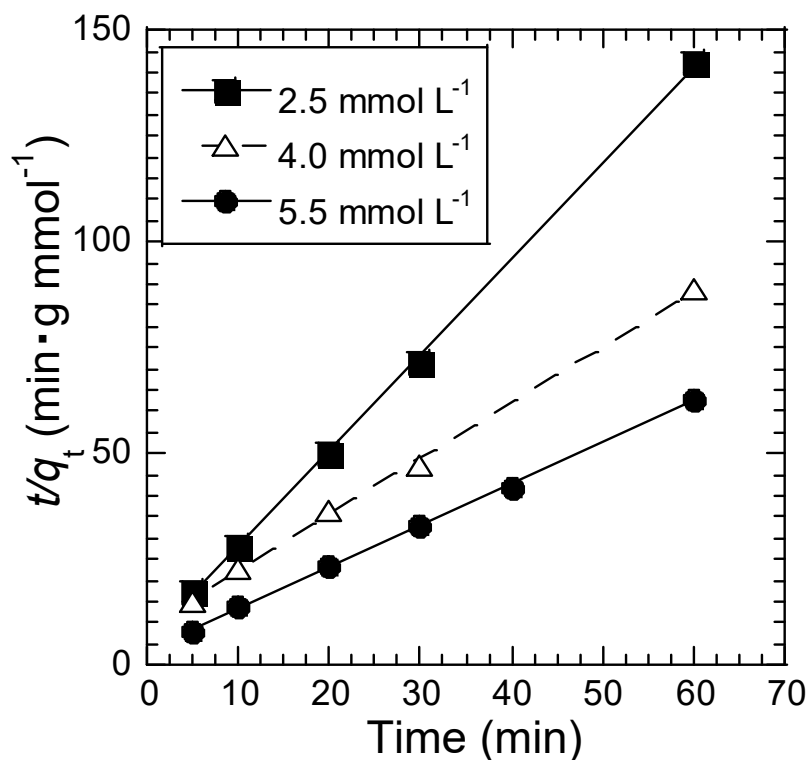


Figure 3.6 Pseudo-second-order kinetic for reductive adsorption of Cr(VI) with various initial concentrations.

### 3.3.2. Chromatographic operation

Finally, the AC was applied for chromatographic operation for removal of Cr(VI) in aqueous solution. Effect of pH value of the feed solution was firstly investigated. Figure 3.7 shows the breakthrough curves of total Cr from different pH at S.V. = 12 h<sup>-1</sup>, together with pH of the effluent. Because the column was carefully washed with deionized water before column operation, the pH of the effluent in the beginning was almost 7 except for the use of feed solution of pH<sub>feed</sub> = 2.0. In the case of pH<sub>feed</sub> = 2.0, the pH of the effluent was decreased immediately after starting the column operation. In this case, Cr was immediately broken through, while the Cr concentration in the effluent was almost constant until B.V. = 700 and then was increased. Low adsorption ability at pH<sub>feed</sub> = 2.0 from dilute solution was consistent with the results of batchwise adsorption, as shown in Figure 3.1, and thus the AC was not suitable for Cr removal in low pH region, even though reduction of Cr(VI) to Cr(III) occurs. In the case of pH<sub>feed</sub> = 5.0 and 6.0, Cr was also broken through immediately. In the case of pH<sub>feed</sub> = 3.0, however, complete adsorption was proceeded until B.V. = 500.

Effect of the S.V. on the Cr removal was then investigated using feed solution of  $\text{pH}_{\text{feed}} = 3.0$ . Figure 3.8 shows the breakthrough curves of Cr, together with the speciation of Cr(VI) and Cr(III) in the effluent. Complete removal of Cr could be achieved when  $\text{S.V.} = 6$  and  $12 \text{ h}^{-1}$ , while Cr was immediately broken through when  $\text{S.V.} > 30 \text{ h}^{-1}$ . The most of Cr remained in the effluent was Cr(VI), because adsorption amount of Cr applied to the AC was quite high compared with the condition for the batchwise adsorption.

Elution of Cr from the AC after adsorption was however difficult due to the reduction of Cr(VI) to Cr(III) on the adsorbent, since Cr(III) reduced might be converted as  $\text{Cr}_2\text{O}_3$ . When elution of the loaded Cr after adsorption was carried out with  $2 \text{ mol L}^{-1} \text{ H}_2\text{SO}_4$  solution, elution yield was only 18.9%. Elution of Cr loaded should be considered in the future to reuse the AC.

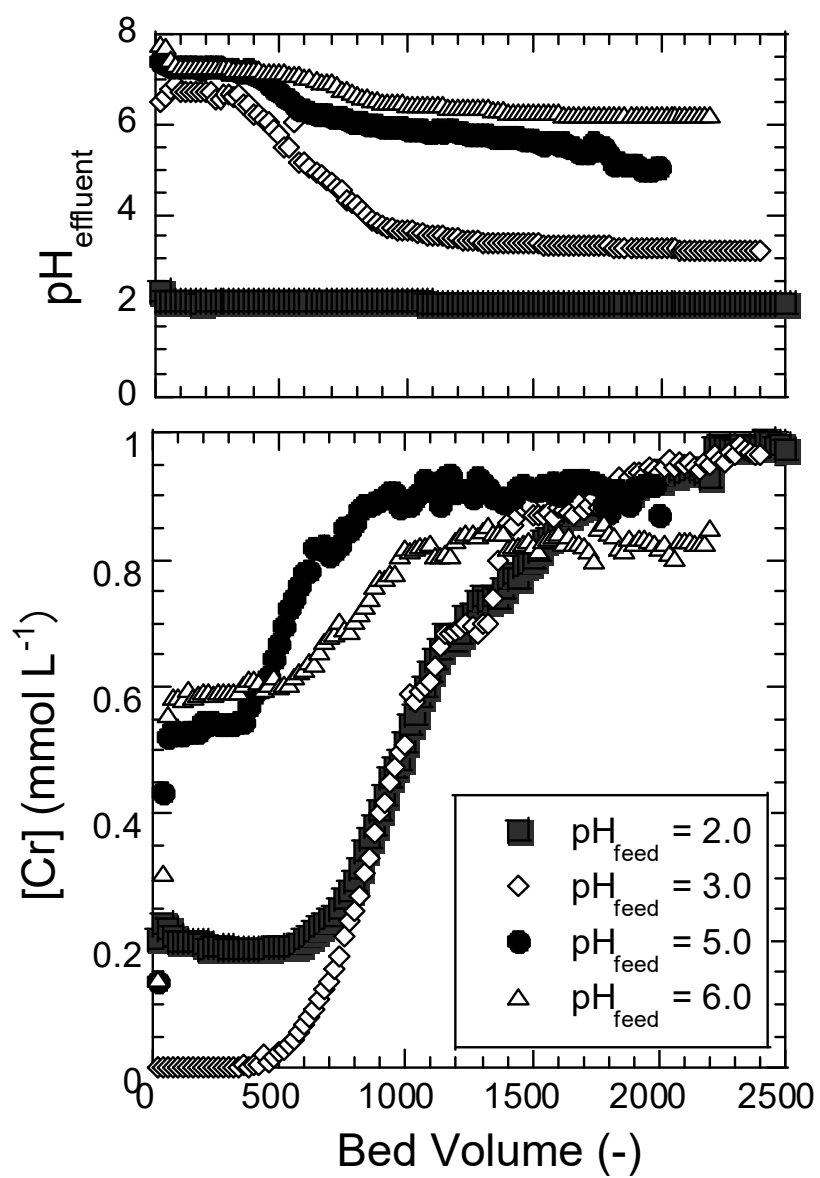


Figure 3.7 Breakthrough curves of Cr(total) by the AC with various  $\text{pH}_{\text{feed}}$ ;  $[\text{Cr(VI)}]_{\text{feed}} = 1.0 \text{ mmol L}^{-1}$  and  $\text{S.V.} = 12 \text{ h}^{-1}$ .

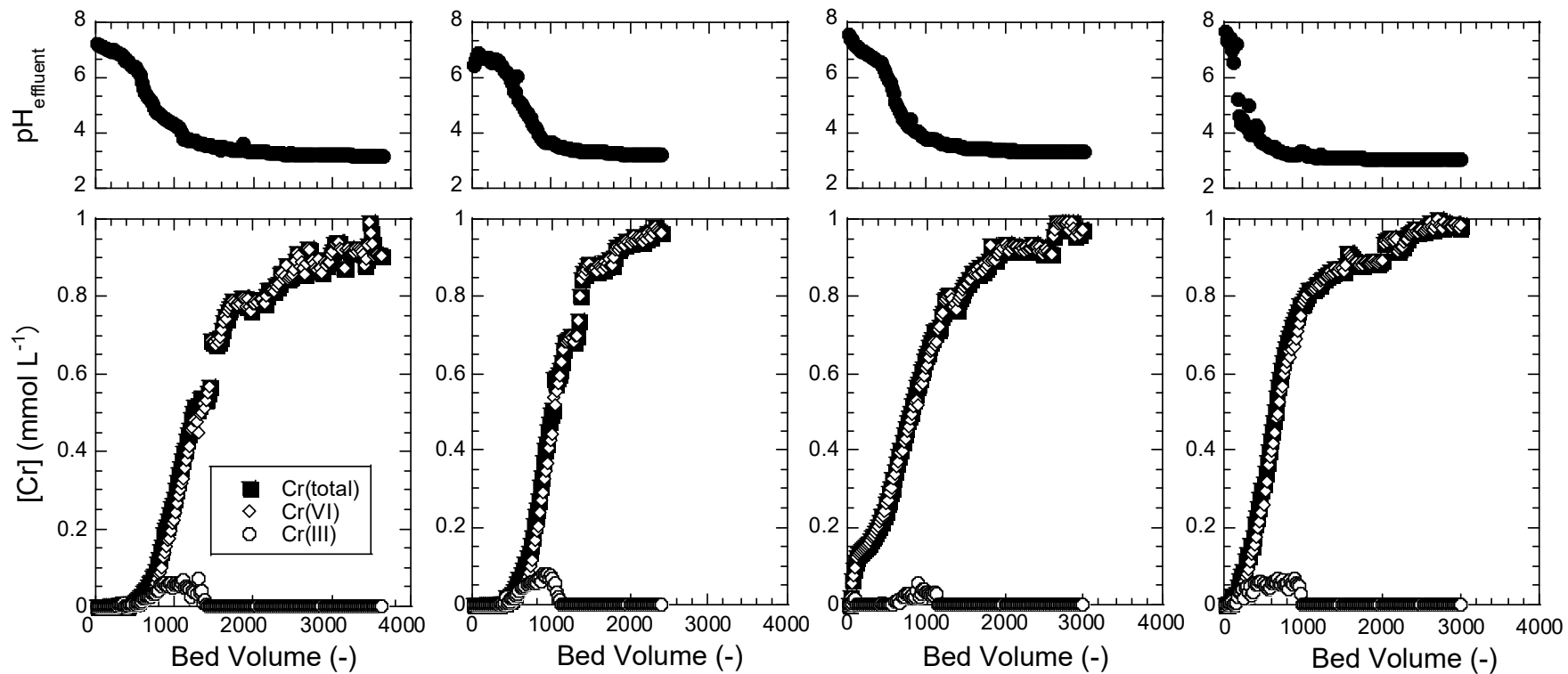


Figure 3.8 Breakthrough curves of Cr(total) by the AC with S.V. = (a)  $6 \text{ h}^{-1}$ , (b)  $12 \text{ h}^{-1}$ , (c)  $30 \text{ h}^{-1}$ , and (d)  $60 \text{ h}^{-1}$ , together with speciation of Cr(VI) and Cr(III) on effluent;  $[\text{Cr(V)}]_{\text{feed}} = 1.0 \text{ mmol L}^{-1}$  and  $\text{pH}_{\text{feed}} = 3.0$ .

### 3.4. Conclusion.

Reductive adsorption of Cr(VI) with the AC was investigated, with the following results obtained:

- i) Cr adsorption proceeded effectively at  $\text{pH}_{\text{eq}} = 4.0 - 6.0$ . Over the entire pH range, Cr adsorbed on the AC existed as Cr(III), while the fraction of Cr(VI) and Cr(III) remaining in aqueous solution was affected by pH. Cr(III) loaded on AC was hardly released at  $\text{pH} > 4$ , while Cr(III) was released to aqueous solution in acidic region.
- ii) The adsorption isotherm at 298 K followed the Langmuir mechanism, and a high maximum adsorption amount ( $q_{\text{max}} = 3.43 \text{ mmol g}^{-1}$ ) was obtained at  $\text{pH}_{\text{eq}} = 2.04$ , despite the adsorption constant at this pH being lower than that at  $\text{pH}_{\text{eq}} = 4.12$ . The maximum adsorption capacity and the adsorption constant of the AC are higher than other adsorbents previously reported.
- iii) The present reductive adsorption was an endothermic reaction, with  $\Delta H^\circ = +7.10 \text{ kJ mol}^{-1}$ . The entropy change of the present process was  $+72.55 \text{ kJ mol}^{-1} \text{ K}^{-1}$ , resulting in the Gibbs free energy of the present reductive adsorption process having a negative value, which indicated that the reaction was spontaneous.
- iv) The rate-determining step of this reductive adsorption was likely to be the adsorption step, which followed pseudo-second-order kinetics.
- v) The AC was applied to chromatographic operation for Cr removal, and Cr was completely removed from the aqueous solution at  $\text{pH}_{\text{feed}} = 3.0$  after approx. 500 bed volumes.

## Chapter 4. Selective Adsorption of Lead(II) from Aqueous Environment

### 4.1. Introduction

Lead (Pb) is one of hazardous metals, although Pb has many application in industrial activities, such as battery manufacturing, paints, smelting, and paper industries [24]. Industrial wastewater discharged from battery manufacturing is considered as a major anthropogenic Pb source, and thus the industrial wastewater is known as a potential source of Pb(II) pollution. The Japan Ministry of the Environment has set the limitation level of Pb in effluent wastewater as  $0.1 \text{ mg L}^{-1}$  ( $4.83 \text{ } \mu\text{mol L}^{-1}$ ) [20]. The World Health Organization (WHO) has defined the maximum concentration of Pb in drinking water at  $0.01 \text{ mg L}^{-1}$  ( $0.483 \text{ } \mu\text{mol L}^{-1}$ ) [64]. As mentioned in section 1.1.2. other toxic heavy metals are also contaminated in the battery industrial wastewater, such as Cu(II), Zn(II), and Cd(II) at high concentration [25]. Due to their high solubility in water environment, heavy metals are absorbed by living organisms [58,93]. Therefore, removal of these heavy metals should also be considered, together with Pb recovery.

Efficient separation methods for the hazardous metals from water environment are still an active issue, according to the increase in stringent regulations for such metals. Many separation techniques have been reported for removal of Pb(II), such as precipitation [38], ion exchange [60,94], adsorption [95–97], and membrane separation [40]. Adsorption has been gaining more attention due to low cost, efficiency, and high selectivity [96]. Various studies have been performed for adsorption of Pb(II) using various adsorbents, such as activated carbon [25], chelating resins [60,98], cation exchange resin [99], carbon nanotube [100], waterworks sludge [101], magnetite [102,103], hematite [56], zero-valent iron [104], and goethite [96,97,105]. Chelating resins are particularly useful, due to high adsorption capacity and regeneration ability. Liu *et al.* and Dinu *et al.* have synthesized iminodiacetic acid (IDA) chelating resin for removal of Pb(II) and several heavy metals from aqueous solution. The IDA chelating resin has high adsorption capacity for Pb(II), Cu(II), Zn(II), and Cd(II) [60,98]. However, the chelating resins are quite expensive, due to difficulty of synthesis, and adsorption rate was very low [60,98]. Goethite, which is a natural oxyhydroxide, has an isostructural with diaspore which is based on hexagonal close packing and consists of a large amount of reactive surface hydroxyl sites. Mohamed *et al.* and Rahimi *et al.* have prepared goethite *via* precipitation technique and have investigated the adsorption performance of Pb(II) from aqueous solution. Goethite was proved to be effective for removal of Pb(II), although the selective adsorption of Pb(II) from contaminated water was not revealed [97,105]. Magnetite, a ferrite compound with a cubic

inverse spinel structure, has been also recently paid attention. Wang *et al.* have reported that the effective removal of Pb(II) by magnetite nanoparticles could be achieved, due to high specific surface area and the presence of hydroxyl groups as reactive sites [103]. Bagbi *et al.* have prepared magnetite nanoparticle *via* chemical co-precipitation technique and have revealed the magnetite nanoparticles possess high affinity for Pb(II) [102]. Although the adsorption of Pb(II) from water environment has been studied, using magnetite, goethite, and chelating resin, as mentioned above, almost all of the reported works are for a single Pb(II) solution, but not for multi-components system. Adsorption of Pb(II) from multi-components system is required to develop the separation process of Pb(II) from polluted water environment [60]. Accordingly, the low-cost adsorbent with high selectivity for Pb(II) is required. In addition, based on our literature survey, only limited publications have focused on chromatographic separation for adsorption of Pb(II) from multi-components system.

In this chapter, the selective adsorption of Pb(II) from aqueous solution, containing Pb(II), Cu(II), Zn(II), and Cd(II), have been investigated using three adsorbents, chelating resin, goethite, and magnetite. The adsorption equilibrium was investigated both in single Pb(II) system and in multi-components system. Adsorption kinetics of the metals with the adsorbents were then investigated, based on pseudo-first order and pseudo-second order models. Desorption of the loaded metals on the adsorbents was then carried out using different concentration of hydrochloric acid. The chromatographic separation of Pb(II) was finally investigated in multi-components system.

## 4.2. Experimental

### 4.2.1. Reagents

Chelating resin, Diaion CR11 (particle size: 0.56 mm) was supplied by Mitsubishi Chemical Co. (Tokyo, Japan). Before the experiments, CR11 was conditioned by shaking with 2 mol L<sup>-1</sup> HCl and 2 mol L<sup>-1</sup> NaOH solution to remove solvents and other precipitated chemicals. In order to convert resins from Na<sup>+</sup> form to H<sup>+</sup> form, HCl was then used for shaking with resin, followed by washing with deionized water to remove excess Cl<sup>-</sup>. Powdery goethite (P-AMAs, particle size 50 – 75 μm) and granular goethite (AMAs, particle size: 0.5 – 1.0 mm) were supplied by Toda Kogyo Corp. (Hiroshima, Japan). Magnetite (particle size 0.1 – 0.5 mm) and all other reagents were supplied by FUJIFILM Wako Pure Chemical Corporation (Osaka, Japan) and were of analytical grade.

#### 4.2.2. Batchwise adsorption

Aqueous solution was prepared by dissolving  $\text{PbCl}_2$ ,  $\text{CuCl}_2 \cdot 2\text{H}_2\text{O}$ ,  $\text{ZnCl}_2$ , and  $\text{CdCl}_2$  in deionized water. Batchwise adsorption was performed by shaking suspended mixture of adsorbent (50 mg) and aqueous solution (10 mL) at 160 rpm for 2 h to attain equilibration. The effect of pH was investigated in the range of pH from 1.0 to 6.0 at an initial concentration  $[\text{M}]_{\text{ini}} = 1.0 \text{ mmol L}^{-1}$  for both of aqueous single Pb(II) solution and multi-components (Pb(II), Cu(II), Zn(II), and Cd(II)) systems, while the adsorption isotherms were obtained by changing  $[\text{M}]_{\text{ini}}$  from 0.5 to 10  $\text{mmol L}^{-1}$  at fixed equilibrium pH. The pH value of aqueous solution was controlled by adding appropriate amount of NaOH or HCl solution. In all cases, the suspended mixture, after shaking, was filtered, and the pH value and the metal concentration in the aqueous solution were measured using a pH meter (Horiba F-74) and an inductively coupled plasma atomic emission spectrometer (ICP-AES; Shimadzu ICPE-9000), respectively. The adsorption amount  $q_{\text{eq}}$  ( $\text{mmol/g}$ ) was calculated by Eq (4-1).

$$q_{\text{eq}} = \frac{([\text{M}]_{\text{ini}} - [\text{M}]_{\text{eq}}) \cdot V}{m} \quad (4-1)$$

where  $[\text{M}]_{\text{ini}}$  and  $[\text{M}]_{\text{eq}}$  is the initial and equilibrium concentration of cation ( $\text{mmol L}^{-1}$ ),  $V$  is the volume of aqueous solution (L), and  $m$  is weight of adsorbent (g). Dissolution of Fe from P-AMAs and magnetite was determined by material balance based on the concentration of Fe in the aqueous solution, which was determined by ICP-AES. Total amount of Fe of P-AMAs and magnetite was determined by dissolving 20 mg of each adsorbent by mixture of 5 mL of  $\text{H}_2\text{O}_2$  and 15 mL of concentrated  $\text{H}_2\text{SO}_4$  at  $50^\circ\text{C}$  for 12 h, followed by determination of Fe concentration by ICP-AES.

Adsorbents before and after adsorption of metals were characterized using a field emission scanning electron microscope (FE-SEM, JEOL JSM-7800F) and a Fourier transform infrared spectroscopy (FT-IR, JASCO FT/IR-4600). Prior to SEM analysis, all the samples were sputter-coated with an approximately 4 nm thick gold layer to minimize possible surface charge effects.

Desorption studies were also carried out. Metal-loaded adsorbents were prepared by shaking 1 g of adsorbent and 200 mL of multi-components aqueous solution of  $[\text{M}]_{\text{ini}} = 2.5 \text{ mmol L}^{-1}$  at  $25^\circ\text{C}$  for 2 h. After filtration, loaded adsorbents were dried. Desorption was then carried out by shaking dried loaded adsorbent (50 mg) and eluent (10 mL) at  $25^\circ\text{C}$  for 2 h. HCl solution of  $0.5 - 2 \text{ mmol L}^{-1}$  was used for CR11 and HCl solution of  $0.005 - 2 \text{ mmol L}^{-1}$  was used for P-AMAs and magnetite as eluents. Concentration of metal after elution was analyzed by ICP-AES.

### 4.2.3. Column adsorption

In the case of goethite, granular type AMAs was used for chromatographic separation, instead of P-AMAs, to prevent from pressure drop. The chromatographic separation was conducted using a column apparatus setup, as shown in Figure 1.2. A glass column (length 10 cm, inner diameter 0.8 cm) was packed a known amount of adsorbent (wet volume 0.5 mL: 0.50 g of CR11, 3.31 g of magnetite, or 1.11 g of AMAs) between glass wool. The column was washed by deionized water before adsorption of metal ions. A multi-components aqueous solution of  $[M]_{\text{feed}} = 1.0 \text{ mmol L}^{-1}$  and  $\text{pH}_{\text{feed}} = 5.0$  was fed into column at  $0.05 \text{ mL min}^{-1}$ , such that space velocity (S.V. = flow rate/wet volume) was  $6 \text{ h}^{-1}$ , by using a dual plunger pump (Flow KP-21). After adsorption of metals was saturated, the system was washed by deionized water, then elution was performed by feeding eluent of  $2 \text{ mol L}^{-1}$  HCl for CR11 and  $1 \text{ mol L}^{-1}$  HCl for AMAs and magnetite, at  $0.05 \text{ mL min}^{-1}$ . The effluent was collected using a fraction collector (EYELA DC-1500). The pH in effluent were measured by pH meter, and the metal concentration was analyzed ICP-AES. Bed volume (B.V.) was calculated by Eq. (4-2).

$$\text{B.V.} = \frac{v \cdot t}{L} \quad (4-2)$$

where  $v$  is the volumetric flow rate of solution ( $\text{mL min}^{-1}$ ),  $t$  is the time after feeding the feed solution (min), and  $L$  is the wet volume of adsorbent (mL).

## 4.3. Results and discussion

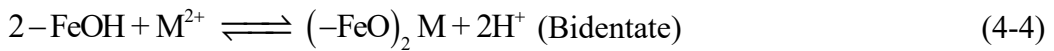
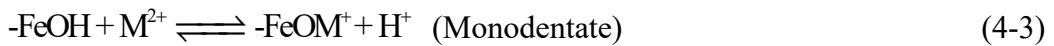
### 4.3.1. Batchwise adsorption

#### 4.3.1.1. Effect of pH

Since pH is one of the most important parameters deciding the complexation of the agent and metal ions [93], the effect of pH on the batchwise adsorption was firstly investigated in single metal system. Figure 4.1 shows the effect of the equilibrium pH ( $\text{pH}_{\text{eq}}$ ) on the adsorption amounts of metals from aqueous solution containing single metal, together with dissolution percentage of Fe from adsorbents in the cases of P-AMAs and magnetite. In the case of CR11, the adsorption amount of all metals is rapidly increased with pH from 1.0 to 3.0, while adsorption amount of Cu was plateau at  $\text{pH} > 3.0$  due to the adsorption percentage of 100%. This could be explained that the IDA groups in resin are protonated in low pH region to compete between protons and metal ions ( $\text{M}^{2+}$ ) at binding sites of the adsorbent. The adsorption is improved at higher pH, since the dissociation of the proton on the adsorbent is promoted. In the cases of P-AMAs and magnetite, adsorption of metals occurs at pH from 3.0 to 6.0, although

adsorption amount of Zn and Cd was still low. By increasing of pH of the aqueous solution, the adsorption amounts of metals are increased to proceed the deprotonation of the adsorbent surface [106]. The dissolution of Fe from P-AMAs and magnetite, during the batchwise adsorption was quite small. The detail of adsorption mechanisms with three kinds of adsorbents could be explained as follows.

- i) CR11: CR11 was proton type of IDA (R-N-(COOH)<sub>2</sub>) on polystyrene support. The low adsorption amount in acidic pH region (pH < 3.0) is due to the lower of dissociation extent of carboxylic group to suppress the complex formation [95]. In the case of pH > 3.0, CR11 could coordinate with metal ions through the nitrogen and oxygen atoms in the IDA group to form stable complexes [98,107].
- ii) P-AMAs: The adsorption is based on the reaction between metal ions and hydroxyl group ( $\alpha$ -Fe(O)OH). At low pH region, since the hydroxyl groups on the surface are closely associated with the oxonium ion (H<sub>3</sub>O<sup>+</sup>), the metal ions hardly approaches to the adsorbent surface due to the repulsive force [108]. The adsorbent surface becomes negatively charged by increasing pH [97]. Since the adsorption of metal ion by P-AMAs accompanied with complex formation, hydroxyl group share their electron pair to bind with metal ions [97].
- iii) Magnetite: Magnetite is known as an amphoteric solid, which can develop charge *via* the protonation and deprotonation of functional groups (-FeOH) site on surface. Adsorption amount of metal ion was increased with increasing pH by rising the electrostatic attraction between active site -FeOH and metal ion (M<sup>2+</sup>). When increasing of pH, the number of surface groups -FeOH are present in more reactive deprotonated form -FeO<sup>-</sup>. The adsorption of metal ion on magnetite can form monodentate and bidentate complexes, as following Eqs.(4-3) and (4-4) [58,102]:



Batchwise adsorption of Pb(II) from multi-components system, containing Pb(II), Cu(II), Zn(II), and Cd(II), was investigated to reveal the selectivity of the adsorbents. Figure 4.2 shows the effect of pH on the adsorption amount of Pb(II) and other metals in multi-components system, together with dissolution percentage of Fe from P-AMAs and magnetite into aqueous solution. CR11 with IDA group shows high adsorption ability for all metals in wide pH range, while the selectivity for metal is little. The adsorption ability of Pb(II) with CR11 is higher

than those of Zn(II) and Cd(II), but less than that of Cu(II). In the cases of P-AMAs and magnetite, the functional group is hydroxyl group, and the adsorption ability is less than IDA group. The adsorption of metal was thus hardly occurred at  $\text{pH} < 3.0$ , as same as the single metal solution, and the adsorption amounts of metals were increased with increase in pH from 3.0 to 6.0. P-AMAs shows high adsorption selectivity for Pb(II) and Cu(II), while Zn(II) and Cd(II) were hardly adsorbed. Magnetite has high selectivity for Pb(II), while adsorption of other three metals were hardly occurred. The adsorption amount of Pb(II) was higher 3 time than that of Cu(II) and 10 time than those of Zn(II) and Cd(II). The adsorption ability and selectivity of the metals with adsorbents are thus strongly affected by the functional group. The results obtained clearly indicate the possibility to use the magnetite for the selective separation of Pb(II) from their mixtures with Pb(II), Cu(II), Zn(II), and Cd(II). In addition, dissolution of Fe from both P-AMAs and magnetite was also quite small, as same as single metal system.

Further confirmation of metal uptake on the adsorbents was carried out using FE-SEM and FT-IR analyses. Surface morphologies of the three adsorbents, before and after adsorption, are shown in Figure 4.3. In all adsorbents, sub-micron size particles are seen, together with pore. The surface morphology is hardly changed by the adsorption of metals, since the size of metal ions are extremely small of Å-order. Figure 4.4 displays the FT-IR spectra of the adsorbents, before and after adsorption. In the case of CR11, peaks near  $3410\text{ cm}^{-1}$  (broad) and  $2921\text{ cm}^{-1}$  are assigned to O-H group and C-H group, while other absorption peaks at  $1727\text{ cm}^{-1}$ ,  $1631\text{ cm}^{-1}$ , and  $1213\text{ cm}^{-1}$  are corresponded to the stretching vibrations of carbonyl groups [95,98]. After adsorption of metals, the absorption band related to carbonyl groups in  $1631\text{ cm}^{-1}$  is shifted to  $1606\text{ cm}^{-1}$ , likely due to the adsorption of metals. In the case of P-AMAs, absorption bands at  $796\text{ cm}^{-1}$  and  $883\text{ cm}^{-1}$ , which are corresponded by Fe-O-OH bending vibrations in  $\alpha\text{-Fe(O)OH}$ , were observed before adsorption [97,103]. These bands were also slightly shifted to  $799\text{ cm}^{-1}$  and  $880\text{ cm}^{-1}$  after adsorption of metals. In addition, strong band at  $1065\text{ cm}^{-1}$  appeared after adsorption of metals, which is assigned to the vibration of hydroxyl group for 2-line ferrihydrite [103]. In the case of magnetite, strong band was observed at  $540\text{ cm}^{-1}$  before adsorption, which is assigned to characteristic Fe-O vibration of magnetite [57,58]. The peak was shifted to  $544\text{ cm}^{-1}$  after adsorption of metals corresponding to formation of Fe-O-M on magnetite surface, as previously reported [58].

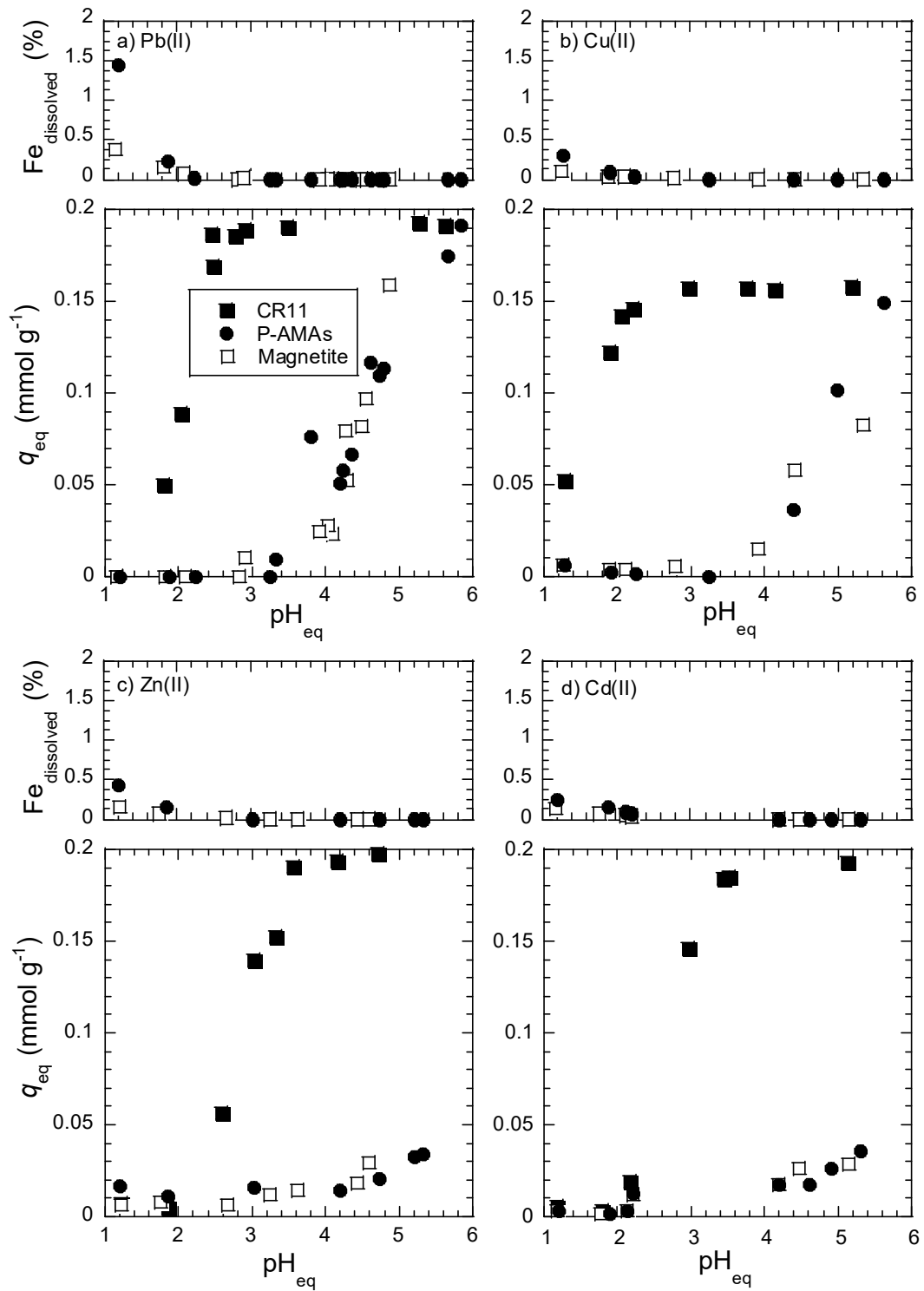


Figure 4.1 Effect of pH on adsorption of (a) Pb(II), (b) Cu(II), (c) Zn(II), and (d) Cd(II) in single metal system with various adsorbents.  $[Pb(II)]_{\text{ini}} = 0.97 \text{ mmol L}^{-1}$ ;  $[Cu(II)]_{\text{ini}} = 0.80 \text{ mmol L}^{-1}$ ;  $[Zn(II)]_{\text{ini}} = 0.98 \text{ mmol L}^{-1}$ ;  $[Cd(II)]_{\text{ini}} = 0.96 \text{ mmol L}^{-1}$ .

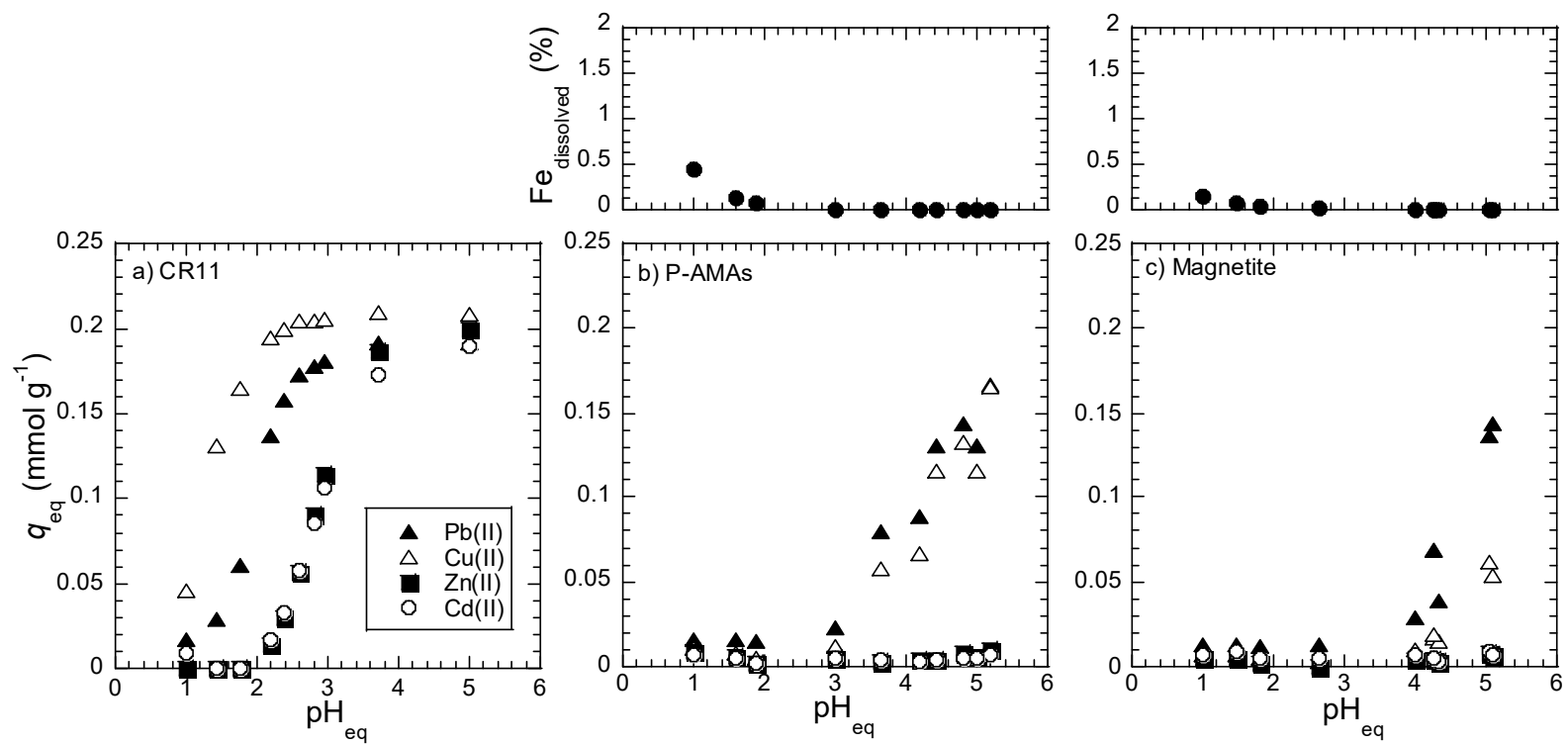


Figure 4.2 Effect of pH on adsorption of Pb(II), Cu(II), Zn(II), and Cd(II) in multi-components system with (a) CR11, (b) P-AMAs, and (c) magnetite.  $[Pb(II)]_{ini} = 0.97 \text{ mmol L}^{-1}$ ;  $[Cu(II)]_{ini} = 1.05 \text{ mmol L}^{-1}$ ;  $[Zn(II)]_{ini} = 1.00 \text{ mmol L}^{-1}$ ;  $[Cd(II)]_{ini} = 0.96 \text{ mmol L}^{-1}$ .

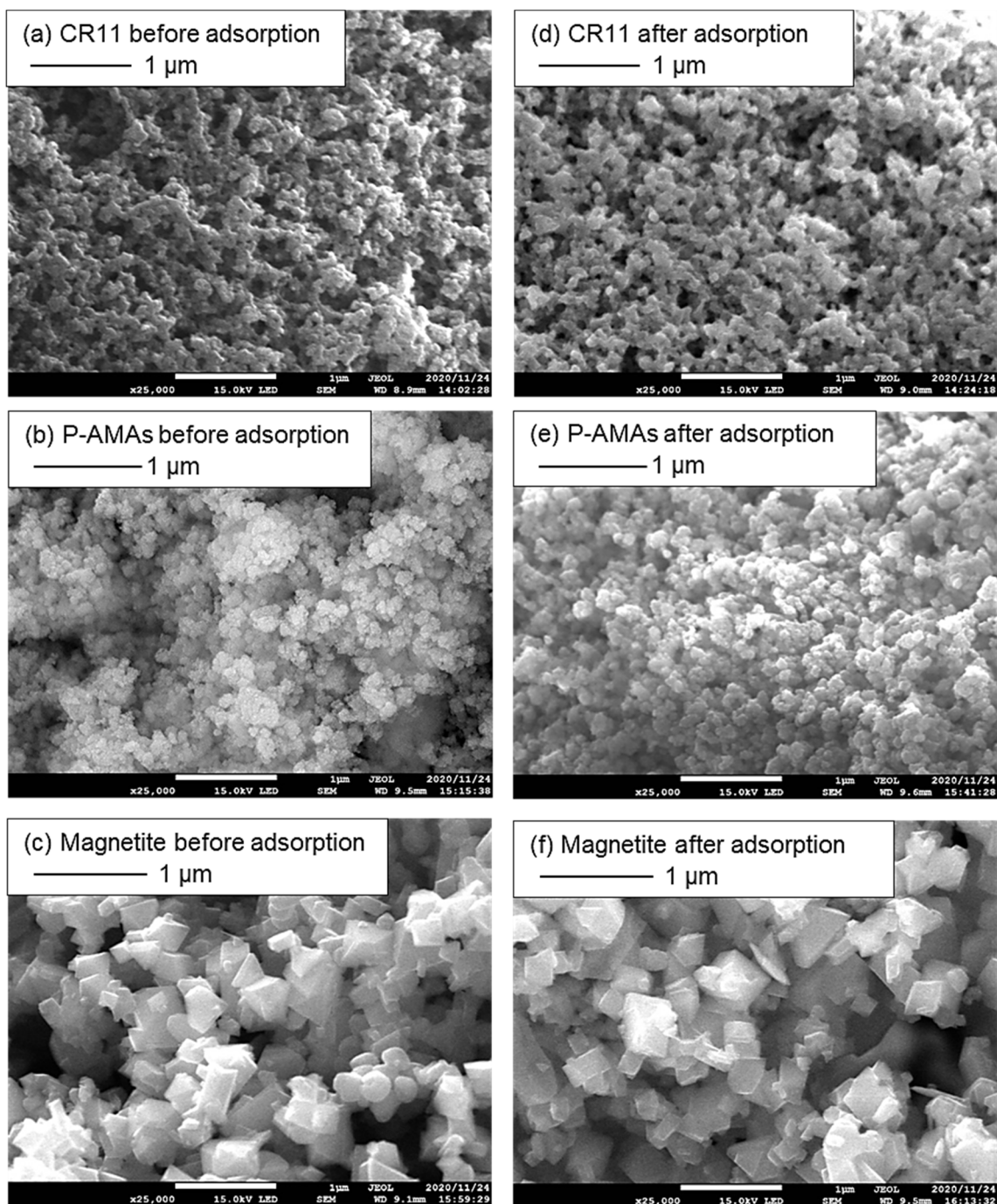


Figure 4.3 SEM micrographs of (a) CR11, (b) P-AMAs, and (c) magnetite before adsorption and (d) CR11, (e) P-AMAs, and (f) magnetite after adsorption. Loaded adsorbents prepared by adsorption for Figure 4.7 were used for (d) – (f).

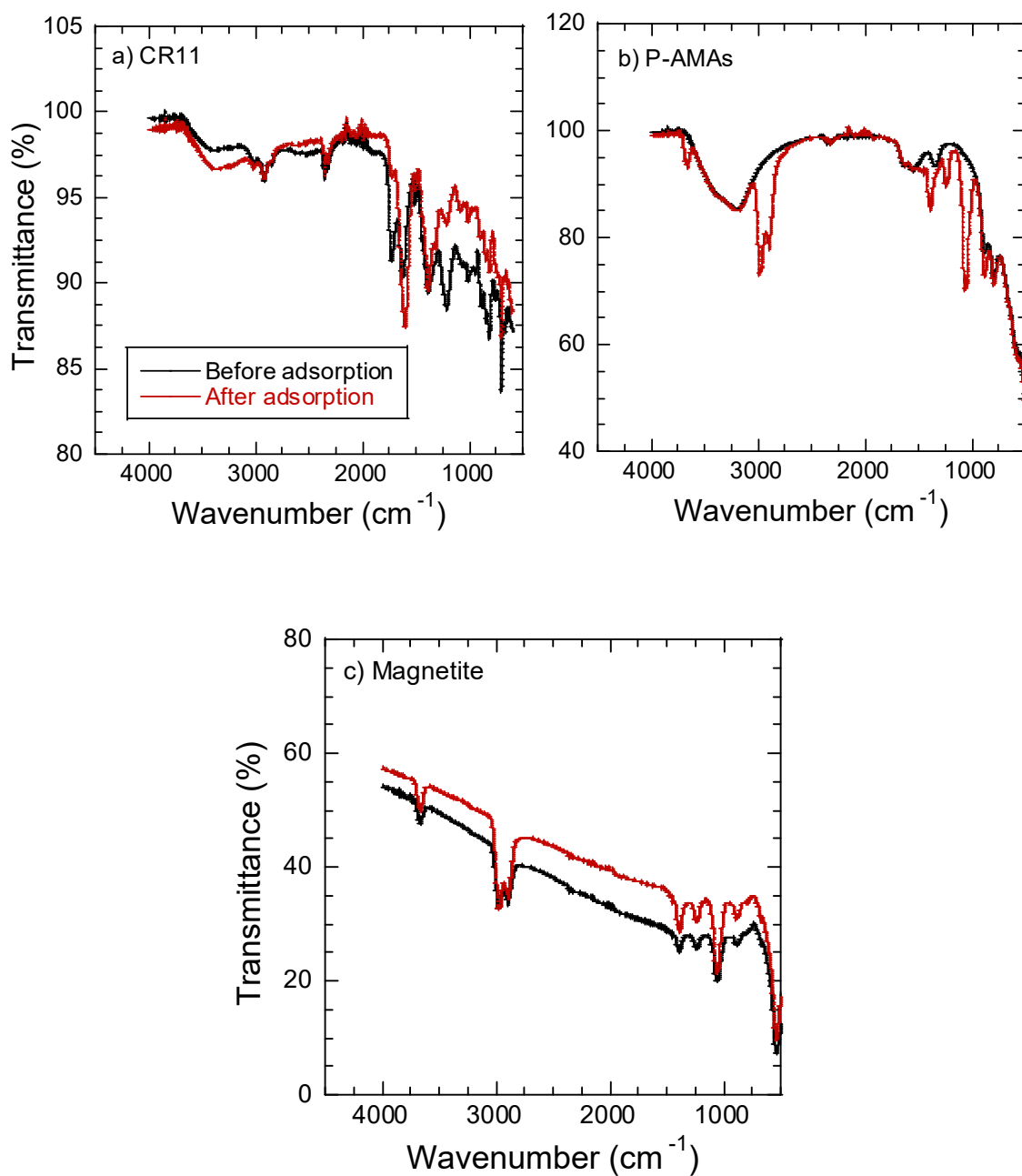


Figure 4.4 FT-IR spectra of (a) CR11, (b) P-AMAs, and (c) magnetite before and after adsorption of metal ions. Loaded adsorbents prepared by adsorption for Figure 4.7 were used for the analyses after adsorption.

#### 4.3.1.2. Adsorption isotherm

The adsorption isotherms of the metals were investigated, and were analyzed using Langmuir isotherm model [76], which assumes adsorption occurs on specific homogeneous sites of adsorbent as a monolayer [109]. The equation of Langmuir model can be expressed as Eq. (4-5) [56,76].

$$q_{\text{eq}} = \frac{q_{\text{max}} \cdot K_L \cdot [M]_{\text{eq}}}{1 + K_L \cdot [M]_{\text{eq}}} \quad (4-5)$$

where  $[M]_{\text{eq}}$  is the equilibrium concentration ( $\text{mmol L}^{-1}$ ),  $q_{\text{eq}}$  is the adsorption amount at equilibrium state ( $\text{mmol g}^{-1}$ ),  $q_{\text{max}}$  is the maximum adsorption capacity ( $\text{mmol g}^{-1}$ ), and  $K_L$  is the adsorption constant ( $\text{L mmol}^{-1}$ ). The essential characteristics of Langmuir isotherm ( $R_L$ ) is defined as:  $R_L = 1 / (1 + [As]_{\text{feed}} K_L)$ . The value of  $R_L$  indicates the type of adsorption isotherm to be either linear ( $R_L = 1$ ), irreversible ( $R_L = 0$ ), favorable ( $0 < R_L < 1$ ) or unfavorable ( $R_L > 1$ ) [56]. Figure 4.5 shows the adsorption isotherms of Pb(II), Cu(II), Zn(II), and Cd(II) with all adsorbents at fixed  $\text{pH}_{\text{eq}}$ , as shown in Table 4.1. The adsorption amounts of all metals with the adsorbents were increased with increase in the concentrations of metals. The adsorption isotherms were then analyzed by Eq. (4-5), and the parameters obtained were summarized in Table 4.1, together with the regression coefficients. The calculated values of the adsorption isotherms were also shown in Figure 4.5 by solid lines. The regression coefficients were closed to unity in all adsorption systems, indicating all adsorption systems were of Langmuir mechanisms. CR11 shows the highest adsorption capacity for all metals and the  $q_{\text{max}}$  obtained for Pb(II) was larger than those for Zn(II) and Cd(II) but smaller than that for Cu(II). These results are consistent with previous reports [60,95,98]. In the cases of P-AMAs and magnetite, the highest adsorption capacity of Pb(II) was obtained and the order of adsorption capacity was  $\text{Pb(II)} > \text{Cu(II)} > \text{Cd(II)} > \text{Zn(II)}$ . The maximum adsorption capacity of CR11 is much larger than those of P-AMAs and magnetite. P-AMAs and magnetite are however considered to possess advantages of selectivity, as shown in Figure 4.2. The essential characteristics of Langmuir isotherm  $R_L$  were calculated and showed that  $R_L$  values were between 0 and 1 at all initial concentrations. Therefore, the adsorption systems were favorable adsorption.

Adsorption parameters, based on Langmuir mechanism, of Pb(II) and several metal ions with chelating resin, goethite, and magnetite, previously reported, are also summarized in Table 4.1 [60,98,105,106,110]. CR11 and P-AMAs adsorbents show good adsorption capacities and adsorption constants, compared with other adsorbents previously reported. In the case of

magnetite, the adsorption capacity was larger than VTM-HA [110], but less than nanoparticle [106]. This indicated that the adsorption capacity of magnetite could be improved by decreasing particle size to increase the surface area.

Table 4.1 Adsorption isotherm parameters of Langmuir model and comparison with previous reports

Adsorbents	Metal	pH <sub>eq</sub>	$q_{\max}$ (mmol g <sup>-1</sup> )	$K_L$ (L mmol <sup>-1</sup> )	$R^2$
CR11	Pb(II)	4.41 ± 0.07	1.46	25.24	0.996
	Cu(II)	4.48 ± 0.12	1.50	10.17	0.996
	Zn(II)	4.43 ± 0.06	1.09	42.59	0.999
	Cd(II)	4.52 ± 0.11	1.11	8.57	0.996
P-AMAs	Pb(II)	4.36 ± 0.08	0.173	2.07	0.989
	Cu(II)	4.44 ± 0.04	0.129	1.91	0.984
	Zn(II)	4.59 ± 0.10	0.037	1.00	0.992
	Cd(II)	4.50 ± 0.08	0.040	1.84	0.998
Magnetite	Pb(II)	4.32 ± 0.03	0.081	4.64	0.996
	Cu(II)	4.48 ± 0.09	0.079	6.11	0.996
	Zn(II)	4.37 ± 0.08	0.028	5.27	0.992
	Cd(II)	4.40 ± 0.11	0.041	2.39	0.996
Adsorbents	Metal	pH	$q_{\max}$ (mmol g <sup>-1</sup> )	$K_L$ (L mmol <sup>-1</sup> )	Ref
VTM-HA	Pb(II)	5.0	0.070	$1.35 \times 10^{-3}$	[109]
Magnetite nanoparticle	Pb(II)	5.5	0.14	24.6	[105]
Chelating resin with iminodiacetic acid (NJC-702)	Pb(II)	5.0	1.18	7.95	[97]
	Cu(II)		2.04	20.98	
	Cd(II)		0.580	3.73	
Chelating resin CR15	Pb(II)	5.5	0.514	$3.12 \times 10^{-4}$	[60]
	Cd(II)		0.992	$6.71 \times 10^{-5}$	
Goethite	Pb(II)	6.0	0.073	$4.51 \times 10^{-3}$	[104]

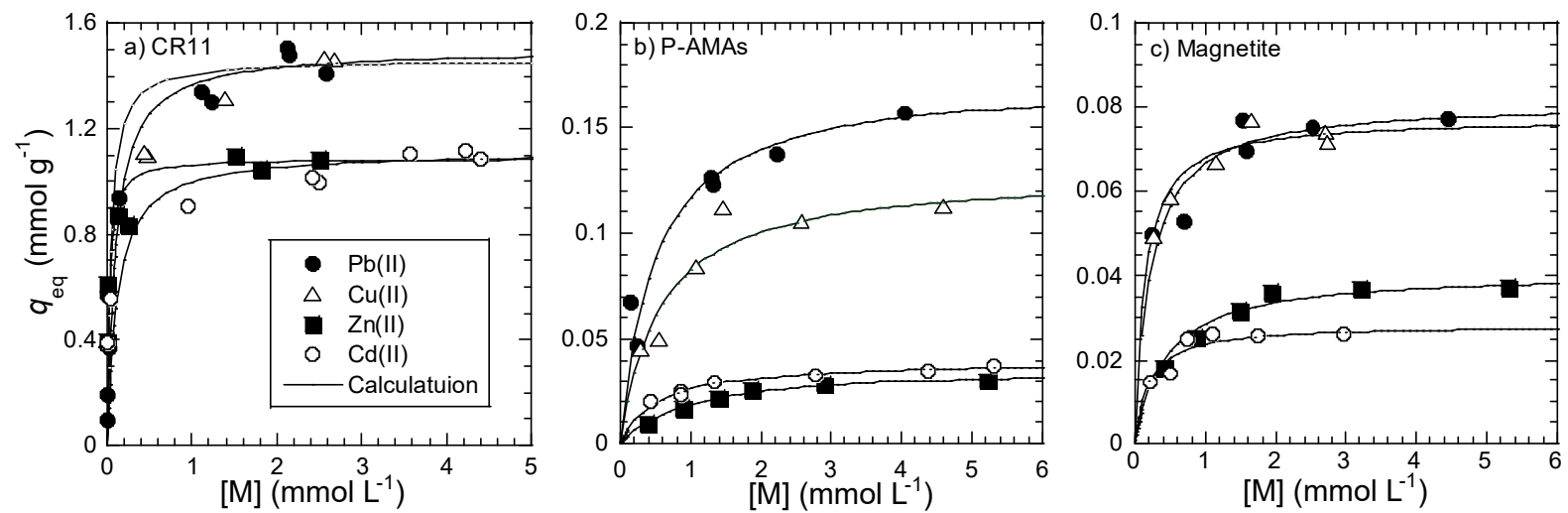


Figure 4.5 Adsorption isotherms of Pb(II), Cu(II), Zn(II), and Cd(II) with (a) CR11, (b) P-AMAs, and (c) magnetite, together with calculated lines based on Langmuir model.  $pH_{eq}$  is shown in Table 4.1.

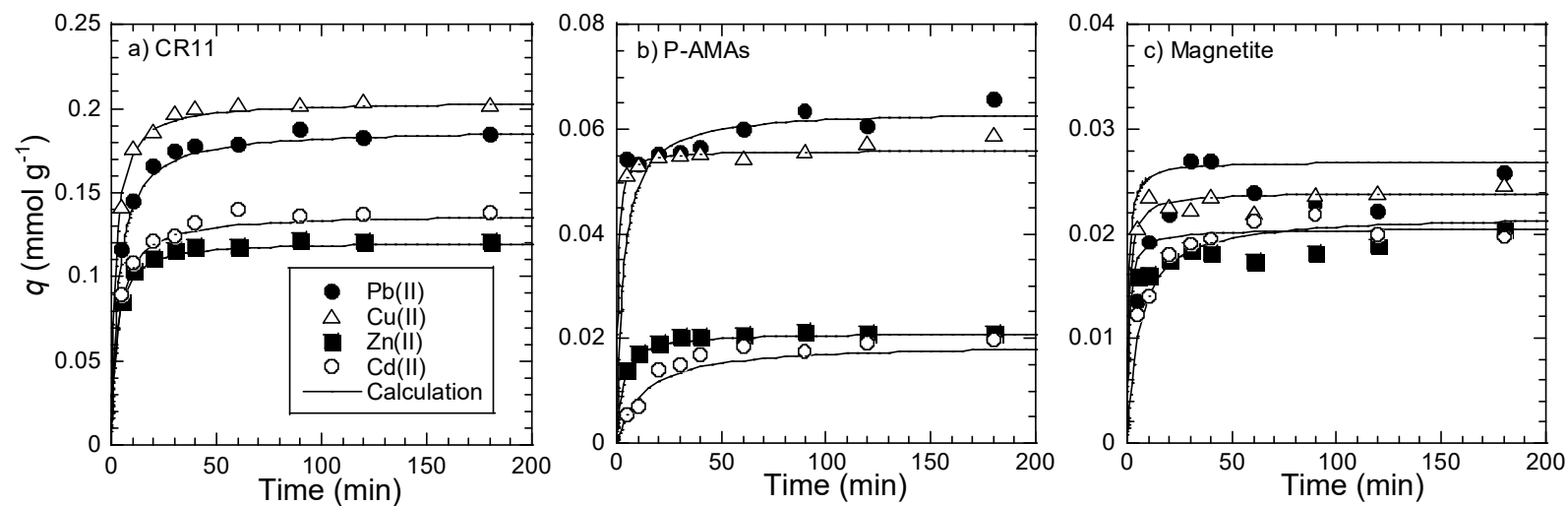


Figure 4.6 Time-course variation of adsorption of metals with (a) CR11, (b) P-AMAs, and (c) magnetite, together with calculated lines based on pseudo-second-order kinetic model.  $[\text{Pb(II)}]_{\text{ini}} = 1.05 \text{ mmol L}^{-1}$ ;  $[\text{Cu(II)}]_{\text{ini}} = 1.04 \text{ mmol L}^{-1}$ ;  $[\text{Zn(II)}]_{\text{ini}} = 0.92 \text{ mmol L}^{-1}$ ;  $[\text{Cd(II)}]_{\text{ini}} = 1.04 \text{ mmol L}^{-1}$ .  $\text{pH}_{\text{ini}} = 5.0$ .

#### 4.3.1.3. Adsorption kinetics

Figure 4.6 shows the time-course variation of the adsorption of metal ions by CR11, P-AMAs, and magnetite in single metal system at  $\text{pH}_{\text{ini}} = 5.0$ . The results indicated that adsorption of metals with CR11 was reached to equilibrium at 120 min, while the equilibrium times for P-AMAs and magnetite were 90 min and 60 min, respectively. P-AMAs and magnetite have therefore advantage in fast adsorption kinetics. The adsorption kinetics were investigated to reveal the rate-controlling step, including mass transport and chemical reaction processes [111]. The adsorption kinetics are expressed as the removal rate of adsorbate, and two general adsorption kinetic models, pseudo-first order and pseudo-second order models, have been established to understand the adsorption kinetic and rate-controlling step [77,78]. The pseudo-first order model is expressed as Eq. (4-6) and stated in the linear form as Eq. (4-7).

$$\frac{dq}{dt} = k_1(q_{\text{eq}} - q_t) \quad (4-6)$$

$$\ln(q_{\text{eq}} - q_t) = \ln q_{\text{eq}} - k_1 t \quad (4-7)$$

where  $k_1$  is the rate constant ( $\text{min}^{-1}$ ),  $q_{\text{eq}}$  is the metal ions adsorption amount at equilibrium, and  $q_t$  is the metal ions adsorption amount at time  $t$  (min). Pseudo-second order model is derived as expressed in Eq. (4-8) and stated in the linear form as Eq. (4-9).

$$\frac{dq}{dt} = k_2(q_{\text{eq}} - q_t)^2 \quad (4-8)$$

$$\frac{t}{q_t} = \frac{1}{k_2 q_{\text{eq}}^2} + \frac{1}{q_{\text{eq}}} t \quad (4-9)$$

where  $k_2$  is the rate constant ( $\text{g mmol}^{-1} \text{min}^{-1}$ ).

The adsorption rates were analyzed by the two models, and the kinetic parameters calculated by fitting the experimental data are summarized in Table 4.2. Correlation coefficients for two models indicates that the pseudo-second order kinetic is considered more consistent to represent the kinetic data in the adsorption systems. This trend indicates that the rate-controlling step of the adsorption of metals is chemical-adsorption involving valence forces by the sharing or exchange of electron between adsorbent and metal ions, and complexation [110]. The calculated lines of the adsorption kinetics based on pseudo-second-order constants are also shown in Figure 4.6. According to Table 4.2, the rate constant,  $k_2$ , of magnetite was much higher than those of other adsorbents. Especially, the rate constant of

magnetite for Pb(II) ( $k_2 = 59.8 \text{ g mmol}^{-1} \text{ min}^{-1}$ ) was 37 times higher than that of CR11 ( $k_2 = 1.59 \text{ g mmol}^{-1} \text{ min}^{-1}$ ) and 11 times higher than that of P-AMAs ( $k_2 = 5.20 \text{ g mmol}^{-1} \text{ min}^{-1}$ ).

Table 4.2 Adsorption kinetic parameters

Adsorbents	Metals	$q_{\text{eq}}$ (mmol $\text{g}^{-1}$ )	Pseudo-first order		Pseudo-second order	
			$k_1$ ( $\text{min}^{-1}$ )	$R_1^2$	$k_2$ ( $\text{g mmol}^{-1} \text{ min}^{-1}$ )	$R_2^2$
CR11	Pb(II)	0.186	0.0376	0.852	1.59	1.00
	Cu(II)	0.204	0.0831	0.963	2.67	1.00
	Zn(II)	0.121	0.0669	0.955	3.79	1.00
	Cd(II)	0.137	0.0479	0.969	2.41	0.999
P-AMAs	Pb(II)	0.0636	0.0179	0.875	5.20	0.999
	Cu(II)	0.056	0.210	0.808	35.2	1.00
	Zn(II)	0.0210	0.0908	0.986	17.8	1.00
	Cd(II)	0.0189	0.0450	0.957	4.30	0.981
Magnetite	Pb(II)	0.0269	0.0623	0.927	59.8	0.987
	Cu(II)	0.0240	0.351	0.936	53.3	0.997
	Zn(II)	0.0206	0.164	0.749	58.4	0.998
	Cd(II)	0.0219	0.104	0.992	8.12	0.999

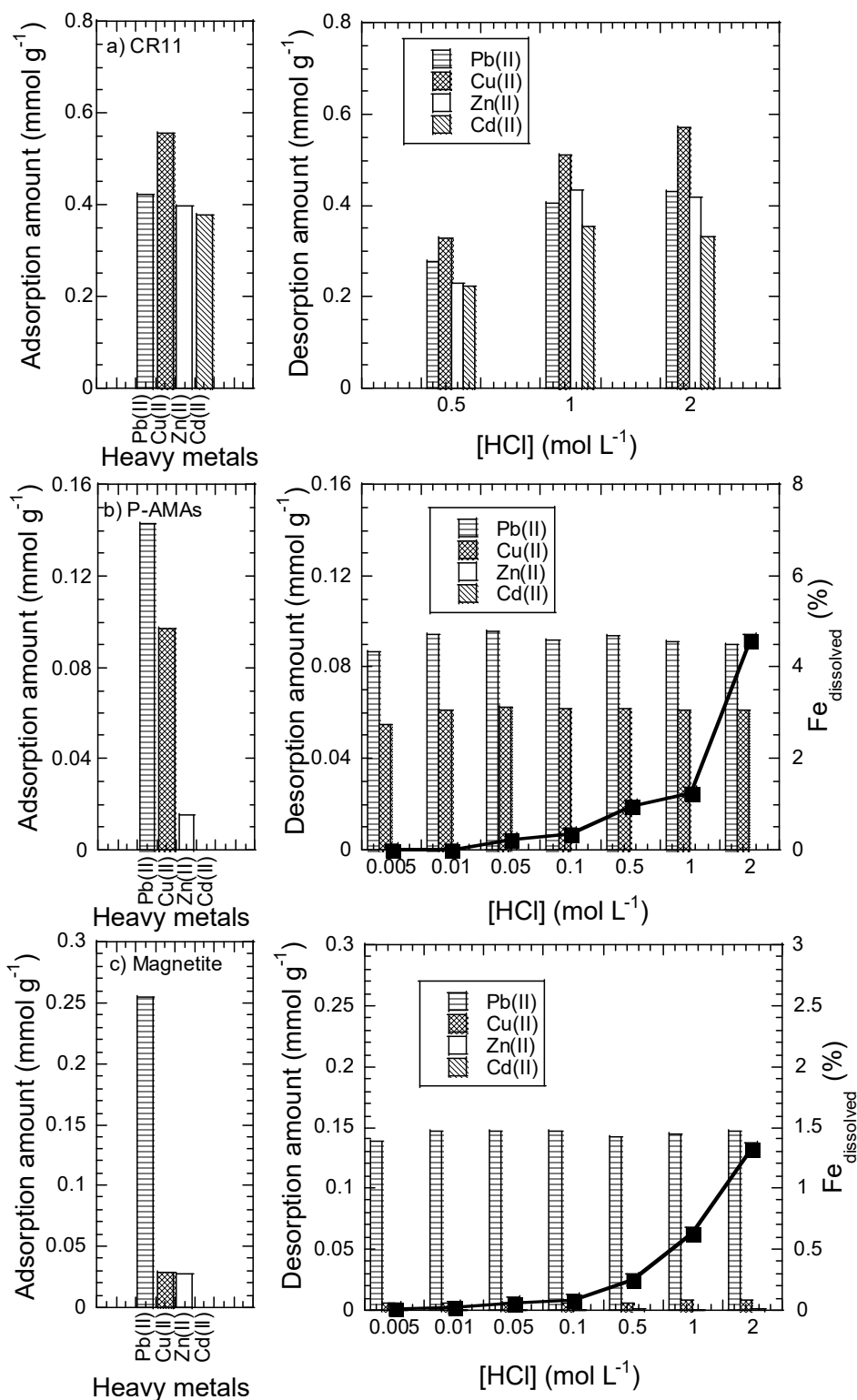


Figure 4.7 Adsorption and desorption amounts of metals with (a) CR11, (b) P-AMAs, and (c) magnetite. Adsorption was carried out in multi-components system containing  $[\text{Pb(II)}]_{\text{ini}} = 2.44 \text{ mmol L}^{-1}$ ;  $[\text{Cu(II)}]_{\text{ini}} = 2.90 \text{ mmol L}^{-1}$ ;  $[\text{Zn(II)}]_{\text{ini}} = 2.96 \text{ mmol L}^{-1}$ ;  $[\text{Cd(II)}]_{\text{ini}} = 2.71 \text{ mmol L}^{-1}$ .  $\text{pH}_{\text{eq}} =$  (a) 3.20, (b) 4.44, and (c) 4.20.

#### 4.3.1.4. Desorption process

Desorption of metals from loaded adsorbent was investigated in batchwise system. The adsorption was performed with multi-components solution, and the desorption of the loaded metals was then carried out by HCl of different concentration as an eluent. Figure 4.7 shows the adsorption and desorption amounts of CR11, P-AMAs, and magnetite with Pb and other metal ions in multi-components system, together with dissolution percentage of Fe from adsorbents in the cases of P-AMAs and magnetite. Desorption yields of the metals from CR11 were increased with increase in HCl concentration, while those from P-AMAs and magnetite were hardly affected by HCl concentration in the range of 0.005 – 2 mol L<sup>-1</sup>. In addition, desorption amount of Cd(II) was 0 mmol g<sup>-1</sup> in all HCl concentrations for P-AMAs and magnetite, since adsorption of Cd hardly occurs with these adsorbents. In the case of CR11, most of metals could be eluted by using 2 mol L<sup>-1</sup> HCl, with desorption yields of 100 % for Pb(II), Cu(II), and Cd(II), and 88% for Zn(II). Therefore, CR11 is available for regeneration. In the case of P-AMAs, desorption yields were in range of 57 – 67% for Pb(II) and Cu(II) and 0% for Zn(II). The regeneration of P-AMAs is therefore impossible. In the case of magnetite, the highest desorption yield was obtained 58% for Pb(II), while Cu(II) and Zn(II) were 31% and 0%, respectively. The magnetite is impossible for regeneration, though the possibility for adsorptive separation of Pb(II) from multi-component system, due to high selectivity toward Pb(II) ion in both of adsorption and desorption processes. The dissolution of Fe from P-AMAs and magnetite was increased with increase in HCl concentration, although the dissolution percentage is low at HCl concentration of lower than 1 mol L<sup>-1</sup>.

#### 4.3.2. Chromatographic separation

The three adsorbents were finally applied for chromatographic separation of Pb(II) in multi-component system. Figure 4.8 shows the breakthrough and elution curves of metals with CR11 at S.V. = 6 h<sup>-1</sup>. The results indicated that adsorption of Pb(II) and Cu(II) were proceeded effectively, while Zn(II) and Cd(II) were hardly adsorbed. Complete adsorption of Pb(II) and Cu(II) could be achieved until B.V. = 300 and B.V. = 900, respectively. The displacement of Pb adsorbed and Cu(II) in the aqueous solution was occurred at B.V. > 900, and large amount of Pb(II) adsorbed in the beginning of adsorption was displaced into effluent by adsorption of Cu(II). After displacement, Pb(II) is slightly remained on CR11 (uptake amount 0.137 mmol g<sup>-1</sup>). Metals loaded on CR11 could be eluted by HCl 2 mol L<sup>-1</sup>. As shown in Figure 4.8b, most of metals observed in the eluent was Cu(II), due to displacement of Pb(II) by Cu(II). The selective separation of Pb with CR11 is therefore hardly achieved. When CR11 is to be used

for removal of Pb(II), the adsorption should be stopped at B.V. = 300. When CR11 is to be considered for recover of Pb(II) from aqueous solution containing Cu(II), the adsorption should be stopped before displacement occurs (B.V. = 900). For instance, when the adsorption is stopped at B.V. = 900, the adsorption amounts were of order of Cu(II) ( $0.84 \text{ mmol g}^{-1}$ ) > Pb(II) ( $0.52 \text{ mmol g}^{-1}$ ) > Cd(II) ( $0.0074 \text{ mmol g}^{-1}$ ) > Zn(II) ( $0.0044 \text{ mmol g}^{-1}$ ), which is consistent with the results in adsorption isotherm.

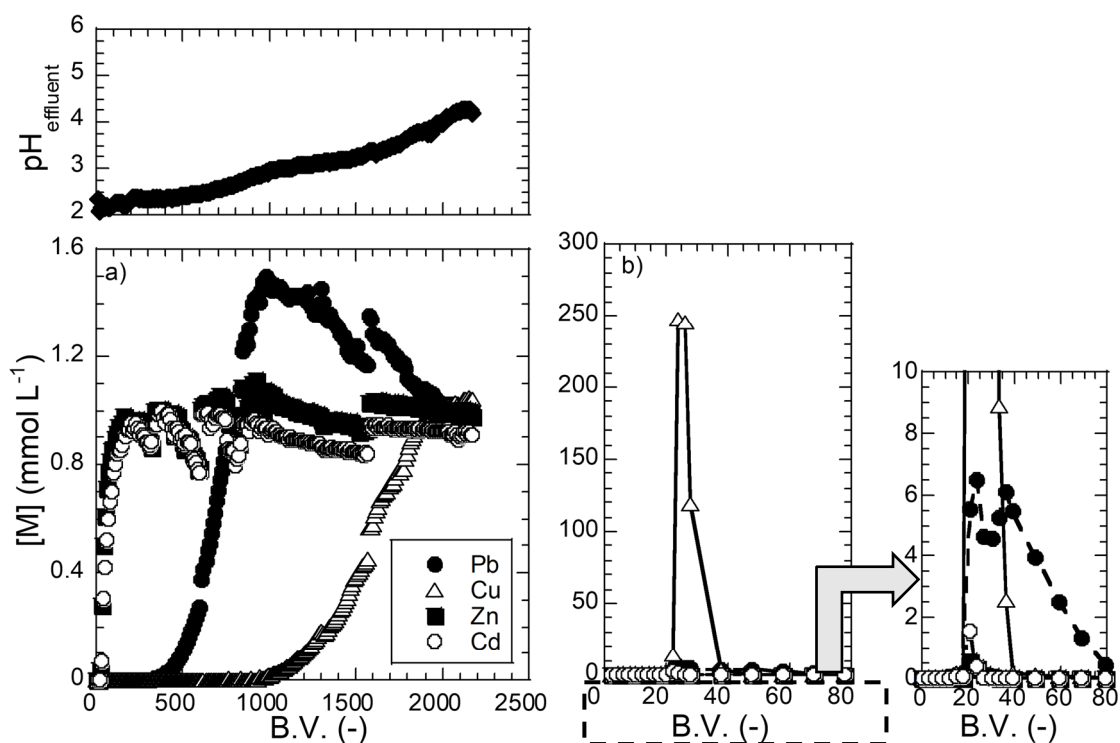


Figure 4.8 (a) Breakthrough and (b) elution curves of metals with CR11 at S.V.  $6 \text{ h}^{-1}$ .  
 $[\text{Pb}]_{\text{ini}} = 0.90 \text{ mmol L}^{-1}$ ;  $[\text{Cu}]_{\text{ini}} = 0.94 \text{ mmol L}^{-1}$ ;  $[\text{Zn}]_{\text{ini}} = 0.90 \text{ mmol L}^{-1}$ ;  
 $[\text{Cd}]_{\text{ini}} = 0.83 \text{ mmol L}^{-1}$ ;  $\text{pH}_{\text{ini}} = 5.0$ . Eluent  $2 \text{ mol L}^{-1} \text{ HCl}$ .

Figure 4.9 shows the breakthrough and elution curves of metals with AMAs. All metals were adsorbed in the beginning of the adsorption, and then Zn(II) and Cd(II) were broken through at B.V. = 30. Pb(II) and Cu(II) were more selectively adsorbed until B.V. = 100 and 80, respectively. In addition, displacement of Zn(II) and Cd(II) adsorbed and Pb(II) and Cu(II) in the aqueous solution was occurred slightly after breakthrough of Zn(II) and Cd(II). Therefore, adsorption amount of Pb(II) and Cu(II) were  $0.052 \text{ mmol g}^{-1}$  and  $0.054 \text{ mmol g}^{-1}$ , while those of Zn(II) and Cd(II) were quite low (less than  $0.005 \text{ mmol g}^{-1}$ ). Elution yields of Pb(II) and Cu(II) were 88% and 78%, respectively. The dissolution of Fe was slightly occurred during

elution, but not adsorption processes, with dissolution percentage of 0.3% in one elution processing. AMAs could be used for removal of Pb(II), together with Cu(II), although selective separation of Pb(II) could not be achieved.

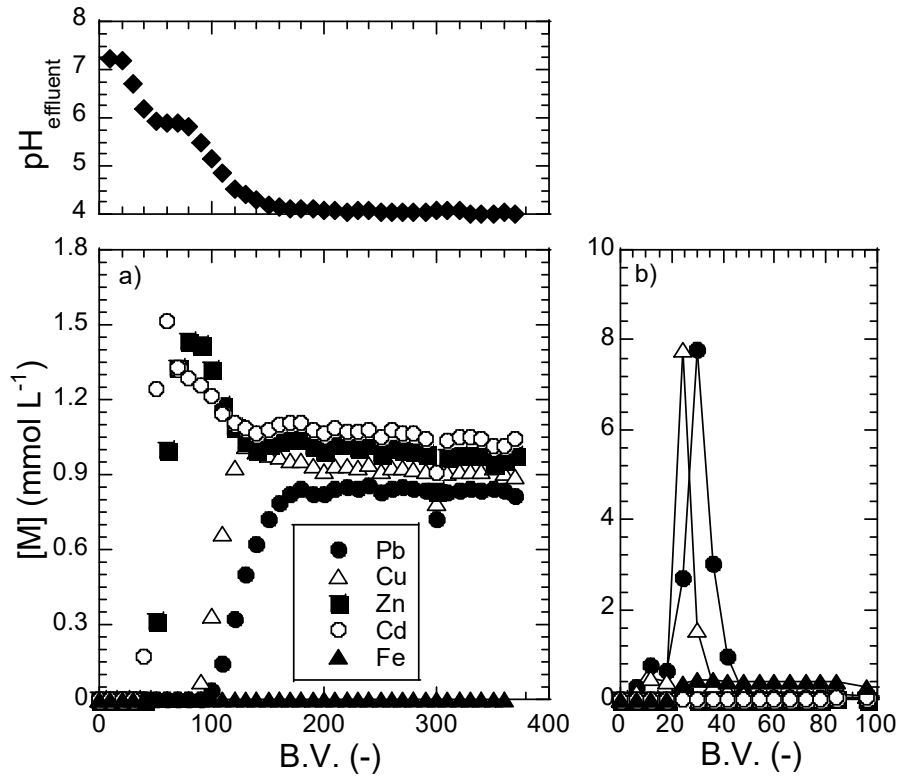


Figure 4.9 (a) Breakthrough and (b) elution curves of metals with AMAs at S.V.  $6 \text{ h}^{-1}$ .  
 $[\text{Pb}]_{\text{ini}} = 0.87 \text{ mmol L}^{-1}$ ;  $[\text{Cu}]_{\text{ini}} = 0.95 \text{ mmol L}^{-1}$ ;  $[\text{Zn}]_{\text{ini}} = 0.94 \text{ mmol L}^{-1}$ ;  
 $[\text{Cd}]_{\text{ini}} = 1.0 \text{ mmol L}^{-1}$ ;  $\text{pH}_{\text{ini}} = 5.0$ . Eluent  $1 \text{ mol L}^{-1} \text{ HCl}$ .

Figure 4.10 shows the breakthrough and elution curves of the metals with magnetite. In this case, Pb(II) was completely adsorbed until B.V. = 70, while other three metals were broken though at B.V. of 30 – 40 and slightly displaced with Pb(II). The adsorption amount of Pb(II) was  $0.013 \text{ mmol g}^{-1}$ , while those of other three metals were less than  $0.005 \text{ mmol g}^{-1}$ , which is consistent with the results obtained by adsorption isotherm. The selective adsorption of Pb(II) is therefore carried out with magnetite, due to its high selectivity for Pb(II). Elution of Pb(II) from magnetite was however difficult, and elution yield of Pb(II) was 59%. The dissolution of Fe(III) was slightly occurred during elution, but not adsorption processes, with dissolution percentage of 0.01% in one elution processing. Among three kinds of adsorbents,

magnetite is thus expected to be used for selective separation of Pb(II) from multi-components system, although complete elution was not achieved.

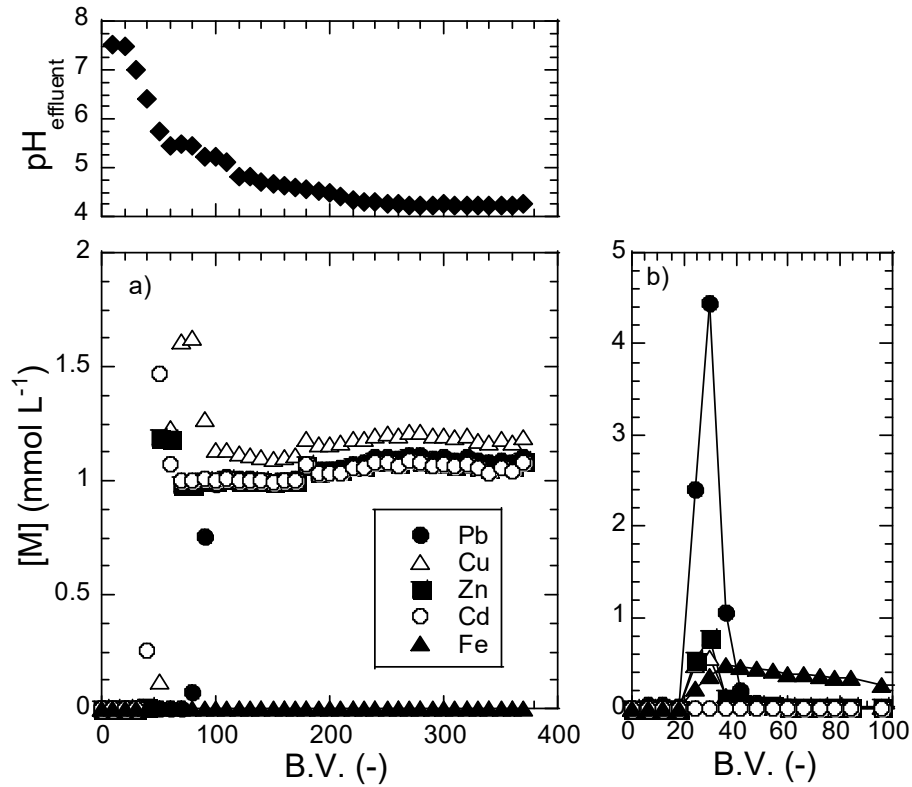


Figure 4.10 (a) Breakthrough and (b) elution curves of metals with magnetite at S.V. 6 h<sup>-1</sup>. [Pb]<sub>ini</sub> = 1.0 mmol L<sup>-1</sup>; [Cu]<sub>ini</sub> = 1.0 mmol L<sup>-1</sup>; [Zn]<sub>ini</sub> = 0.96 mmol L<sup>-1</sup>; [Cd]<sub>ini</sub> = 0.96 mmol L<sup>-1</sup>; pH<sub>ini</sub> = 5.0. Eluent 1 mol L<sup>-1</sup> HCl.

#### 4.4. Conclusion

The selective adsorption of Pb(II) from aqueous solution containing Pb(II), Cu(II), Zn(II), and Cd(II) using CR11, goethite and magnetite was investigated by both of batchwise adsorption and chromatographic separation, with following results.

- i) Adsorption of metals was highly affected by pH, and the adsorption amounts of metals was increased with increase in pH. The selective adsorption of Pb(II) from multi-components system was achieved by magnetite. The adsorption isotherms were of Langmuir model, and CR11 was revealed to possess highest adsorption capacities for the metals.

- ii) Adsorption kinetics of all adsorption systems investigated were well fitted with pseudo-second order kinetic. Magnetite possesses faster kinetic feature than other two adsorbents.
- iii) Desorption of the metals loaded on CR11 could be carried out with 2 mol L<sup>-1</sup> HCl, while quantitative desorption from P-AMAs and magnetite was not achieved.
- iv) The chromatographic separation of metals was performed from aqueous solution containing these metals. The magnetite is feasible for selective separation of Pb(II), although complete elution was not achieved.

## Chapter 5. General Conclusion

This work described the adsorptive separation of heavy metals from aqueous solution. Following conclusions were obtained from research aimed.

In chapter 2, adsorptive removal of arsenic from aqueous environment was investigated, using two ion exchange resins, CRB05 with *N*-methyl-*D*-glucamine functional group and Lewatit FO36 with FeOOH functional group. The systematic comparison of arsenic adsorption behaviors and adsorption performance was performed in batchwise adsorption and chromatographic operation. In batchwise adsorption, the optimal pH values for removal of arsenic were determined as pH 3.0 – 4.5 for As(V) and pH 7.0 – 8.5 for As(III). The adsorption isotherm data were of Langmuir mechanisms and elucidated that FO36 has higher adsorption capacity than that of CRB05, 1.307 mmol g<sup>-1</sup> for As(III) and 1.627 mmol g<sup>-1</sup> for As(V). However, kinetic adsorption followed pseudo-second-order kinetic indicated that adsorption of arsenic with CRB05 was faster than with FO36. In chromatographic operation, FO36 has a higher selectivity for As(V) rather than As(III), while CRB05 possess higher selectivity for As(III) rather than As(V). The elution of arsenic loaded adsorbent could be achieved with high elution yield. The repeated use column adsorption of CRB05 is more suitable than that of FO36.

In chapter 3, the reduction – adsorption of Cr(VI) with coal based activated carbon was investigated. The reaction mechanisms were clearly elucidated, which include adsorption of Cr(VI) – reduction of Cr(VI) to Cr(III) – release of Cr(III) – adsorption of Cr(VI) cycle. Cr(VI) was firstly adsorbed at active site on AC surface; the reduction of Cr(VI) to Cr(III) was occurred due to oxidation of functional groups on AC surface; Cr(III) may release to aqueous solution or kept on AC; Cr(VI) was continuously adsorbed at active site, where released Cr(III); this cycle was continued until all of processes reach equilibrium. In the batchwise system, the optimal pH value for adsorption of Cr(VI) was obtained at pH range of 4.0 – 6.0. The adsorption isotherms were performed in various pH values, and followed Langmuir mechanisms, however, the highest adsorption capacity was obtained at pH<sub>eq</sub> = 2.04 ( $q_{\max} = 3.43 \text{ mmol g}^{-1}$ ). The present reductive adsorption was an endothermic reaction and spontaneous. The rate-determining step of this reductive adsorption was likely to be the adsorption step, which followed pseudo-second-order kinetics. In chromatographic operation, reductive adsorption of Cr(VI) was also affected by pH values. Complete removal of Cr(VI) could be obtained at approx. 500 B.V. with pH<sub>feed</sub> = 3.0. Detoxification of Cr(VI) was also achieved with pH<sub>feed</sub> = 2.0, where Cr(VI) could be adsorbed, reduced, and released Cr(III) to aqueous solution.

In the chapter 4, adsorptive separation of Pb(II) from aqueous solution containing Pb(II) and other heavy metals such as Cu(II), Zn(II) and Cd(II) was investigated, using various adsorbents including iminodiacetic acid chelating resin, goethite and magnetite. Batchwise adsorption of Pb(II) and other metal ions were performed in both of single metal systems and multi-components system. CR11 possesses the highest adsorption ability for these metals, while the selectivity of individual metal is little. Goethite possesses selectivity for Pb(II) and Cu(II), and magnetite possesses selectivity for Pb(II), though the adsorption capacity for the metals is less than those with CR11. The kinetics of the adsorption of metals with all adsorbents is of pseudo-second-order, and the magnetite is revealed to have the fastest adsorption kinetics. Desorption of metals loaded adsorbents were achieved with NaOH or HCl eluent. The three adsorbents can be applied for chromatographic separation for these metals. The magnetite is feasible for selective separation of Pb(II), although complete elution cannot be achieved.

In present work, the initial research aims were achieved, as mentioned above. However, several limitations are remained, which should be improved in the next studies. For applying in large scale, the chromatographic operation should be performed at high space velocity; complete desorption/elution of metal loaded adsorbent is required; regeneration ability of adsorbent is very important; high purity of recovered metal is necessary.

## References Cited

- 1 Tchounwou, P. B., Yedjou, C. G., Patlolla, A. K. and Sutton, D. J. (2012) Heavy Metal Toxicity and the Environment. In *Molecular, Clinical and Environmental Toxicology* (Luch, A., ed.), pp 133–164.
- 2 Srivastava, N. K. and Majumder, C. B. (2008) Novel biofiltration methods for the treatment of heavy metals from industrial wastewater. *J. Hazard. Mater.* **151**, 1–8.
- 3 Ahmaruzzaman, M. (2011) Industrial wastes as low-cost potential adsorbents for the treatment of wastewater laden with heavy metals. *Adv. Colloid Interface Sci.* **166**, 36–59.
- 4 Fu, F. and Wang, Q. (2011) Removal of heavy metal ions from wastewaters: A review. *J. Environ. Manage.* **92**, 407–418.
- 5 Siegel, F. R. (2002) *Environmental Geochemistry of Potentially Toxic Metals*, Springer Berlin Heidelberg, Berlin, Heidelberg.
- 6 Masindi, V. and Muedi, K. L. (2018) Environmental Contamination by Heavy Metals. In *Heavy Metals* (Saleh, H. E.-D. M., and Aglan, R. F., eds.), IntechOpen, Rijeka.
- 7 Choong, T. S. Y., Chuah, T. G., Robiah, Y., Gregory Koay, F. L. and Azni, I. (2007) Arsenic toxicity, health hazards and removal techniques from water: an overview. *Desalination* **217**, 139–166.
- 8 Yoshizuka, K., Nishihama, S. and Sato, H. (2010) Analytical survey of arsenic in geothermal waters from sites in Kyushu, Japan, and a method for removing arsenic using magnetite. *Environ. Geochem. Health* **32**, 297–302.
- 9 Wasserman, G. A., Liu, X., Parvez, F., Ahsan, H., Factor-Litvak, P., van Geen, A., Slavkovich, V., LoIacono, N. J., Cheng, Z., Hussain, I., et al. (2004) Water Arsenic Exposure and Children's Intellectual Function in Araihaazar, Bangladesh. *Environ. Health Perspect.* **112**, 1329–1333.
- 10 Singh, R., Singh, S., Parihar, P., Singh, V. P. and Prasad, S. M. (2015) Arsenic contamination, consequences and remediation techniques: A review. *Ecotoxicol. Environ. Saf.* **112**, 247–270.
- 11 Uddin, R., Saffoon, N. and Alam, M. A. (2011) Arsenic, the poison and poisoned groundwater of Bangladesh: A review. *Int. Curr. Pharm. J.* **1**, 12–17.
- 12 Nordstrom, D. K. (2002) Worldwide Occurrences of Arsenic in Ground Water. *Science* **296**, 2143–2145.
- 13 Shrestha, R. R., Shrestha, M. P., Upadhyay, N. P., Pradhan, R., Khadka, R., Maskey, A., Tuladhar, S., Dahal, B. M., Shrestha, S. and Shrestha, K. B. (2003) Groundwater arsenic contamination in Nepal: A new challenge for water supply sector. In *Arsenic Exposure and Health Effects V*, pp 25–37, Elsevier.
- 14 Berg, M., Tran, H. C., Nguyen, T. C., Pham, H. V., Schertenleib, R. and Giger, W. (2001) Arsenic Contamination of Groundwater and Drinking Water in Vietnam: A Human Health

- Threat. Environ. Sci. Technol. **35**, 2621–2626.
- 15 Sarkar, A. and Paul, B. (2016) The global menace of arsenic and its conventional remediation - A critical review. *Chemosphere* **158**, 37–49.
  - 16 Williams, M., Fordyce, F., Paijitprapapon, A. and Charoenchaisri, P. (1996) Arsenic contamination in surface drainage and groundwater in part of the southeast Asian tin belt, Nakhon Si Thammarat Province, southern Thailand. *Environ. Geol.* **27**, 16–33.
  - 17 Lerda, D. E. and Prosperi, C. H. (1996) Water mutagenicity and toxicology in Rio Tercero (Cordoba, Argentina). *Water Res.* **30**, 819–824.
  - 18 Chiban, M., Zerbet, M., Carja, G. and Sinan, F. (2012) Application of low-cost adsorbents for arsenic removal: A review. *J. Environ. Chem. Ecotoxicol.* **4**, 91–102.
  - 19 Karegar, S., Bhargavi, M. and Divekar, S. V. (2015) Treatment of Wastewater from Chrome Plating Industry by Ion Exchange Method. *Int. J. Res. Eng. Technol.* **04**, 393–401.
  - 20 Japan Ministry of the Environment\_General drainage standards.
  - 21 Sengupta, A. K., Subramonian, S. and Clifford, D. (1988) More on Mechanism and Some Important Properties of Chromate Ion Exchange. *J. Environ. Eng.* **114**, 137–153.
  - 22 Bernardo, G.-R. R., Rene, R.-M. J. and Ma. Catalina, A.-D. la T. (2009) Chromium (III) uptake by agro-waste biosorbents: Chemical characterization, sorption–desorption studies, and mechanism. *J. Hazard. Mater.* **170**, 845–854.
  - 23 Girard, J. E. (2013) *Principles of Environmental Chemistry*, Jones & Bartlett Publishers, USA.
  - 24 Chen, J.-Z., Tao, X.-C., Xu, J., Zhang, T. and Liu, Z.-L. (2005) Biosorption of lead, cadmium and mercury by immobilized *Microcystis aeruginosa* in a column. *Process Biochem.* **40**, 3675–3679.
  - 25 Manjuladevi, M. and Sri, O. M. (2017) Heavy Metals Removal from Industrial Wastewater by Nano Adsorbent Prepared from Cucumis Melo peel Activated Carbon. *J. Nanomedicine Res.* **5**, 00102.
  - 26 Duan, S., Tang, R., Xue, Z., Zhang, X., Zhao, Y., Zhang, W., Zhang, J., Wang, B., Zeng, S. and Sun, D. (2015) Effective removal of Pb(II) using magnetic Co<sub>0.6</sub>Fe<sub>2.4</sub>O<sub>4</sub> micro-particles as the adsorbent: Synthesis and study on the kinetic and thermodynamic behaviors for its adsorption. *Colloids Surf. Physicochem. Eng. Asp.* **469**, 211–223.
  - 27 Azeh Engwa, G., Udoka Ferdinand, P., Nweke Nwalo, F. and N. Unachukwu, M. (2019) Mechanism and Health Effects of Heavy Metal Toxicity in Humans. In *Poisoning in the Modern World - New Tricks for an Old Dog?* (Karcioglu, O., and Arslan, B., eds.), IntechOpen.
  - 28 García-Niño, W. R. and Pedraza-Chaverrí, J. (2014) Protective effect of curcumin against heavy metals-induced liver damage. *Food Chem. Toxicol.* **69**, 182–201.
  - 29 Ratnaike, R. N. (2003) Acute and chronic arsenic toxicity. *Postgrad. Med. J.* **79**, 391–396.
  - 30 Smith, A. H., Lingas, E. O. and Rahman, M. (2000) Contamination of drinking-water by

- arsenic in Bangladesh: a public health emergency. *Bull. World Health Organ.* **78**, 1093–1103.
- 31 Sun, G. (2004) Arsenic contamination and arsenicosis in China. *Toxicol. Appl. Pharmacol.* **198**, 268–271.
  - 32 Gardea-Torresdey, J. L., Tiemann, K. J., Armendariz, V., Bess-Oberto, L., Chianelli, R. R., Rios, J., Parsons, J. G. and Gamez, G. (2000) Characterization of Cr(VI) binding and reduction to Cr(III) by the agricultural byproducts of *Avena monida* (Oat) biomass. *J. Hazard. Mater.* **80**, 175–188.
  - 33 Costa, M. and Murphy, A. (2019) Overview of chromium(III) toxicology. In *The Nutritional Biochemistry of Chromium (III)*, pp 341–359, Elsevier.
  - 34 Rakhunde, R., Deshpande, L. and Juneja, H. D. (2012) Chemical Speciation of Chromium in Water: A Review. *Crit. Rev. Environ. Sci. Technol.* **42**, 776–810.
  - 35 Alka, S., Shahir, S., Ibrahim, N., Ndejiko, M. J., Vo, D.-V. N. and Manan, F. A. (2021) Arsenic removal technologies and future trends: A mini review. *J. Clean. Prod.* **278**, 123805.
  - 36 Abas, S. N. A., Ismail, M. H. S., Kamal, L. and Izhar, S. (2013) Adsorption Process of Heavy Metals by Low-Cost Adsorbent: A Review. *World Appl. Sci. J.* **28**, 1518–1530.
  - 37 Barakat, M. A. (2011) New trends in removing heavy metals from industrial wastewater. *Arab. J. Chem.* **4**, 361–377.
  - 38 Matlock, M. M., Howerton, B. S. and Atwood, D. A. (2002) Chemical Precipitation of Lead from Lead Battery Recycling Plant Wastewater. *Ind. Eng. Chem. Res.* **41**, 1579–1582.
  - 39 Chowdhury, S., Chowdhury, I. R., Kabir, F., Mazumder, M. A. J., Zahir, Md. H. and Alhooshani, K. (2019) Alginate-based biotechnology: a review on the arsenic removal technologies and future possibilities. *J. Water Supply Res. Technol.-Aqua* **68**, 369–389.
  - 40 Abdullah, N., Yusof, N., Lau, W. J., Jaafar, J. and Ismail, A. F. (2019) Recent trends of heavy metal removal from water/wastewater by membrane technologies. *J. Ind. Eng. Chem.* **76**, 17–38.
  - 41 Pham, M. T., Nishihama, S. and Yoshizuka, K. (2020) Arsenic Removal from Aqueous Solutions by Forward Osmosis. *J. Chem. Eng. Jpn.* **53**, 95–99.
  - 42 Pham, M. T., Nishihama, S. and Yoshizuka, K. (2021) Removal of Chromium from Water Environment by Forward Osmosis System. *MATEC Web Conf.* **333**, 04007.
  - 43 Venkateswaran, P. and Palanivelu, K. (2004) Solvent extraction of hexavalent chromium with tetrabutyl ammonium bromide from aqueous solution. *Sep. Purif. Technol.* **40**, 279–284.
  - 44 Kuraoka, A., Umebayashi, T., Nishihama, S. and Yoshizuka, K. (2018) Oxidative Adsorption of Arsenic by *N*-Methylglucamine-modified Chelate Fiber and Manganese Dioxide. *J. Ion Exch.* **29**, 163–165.
  - 45 Zhu, Y., Fan, W., Zhou, T. and Li, X. (2019) Removal of chelated heavy metals from

- aqueous solution: A review of current methods and mechanisms. *Sci. Total Environ.* **678**, 253–266.
- 46 Tien, C. (2019) Introduction. In *Introduction to Adsorption: Basics, Analysis, and Applications*, pp 1–6, Elsevier.
- 47 Berk, Z. (2018) Adsorption and ion exchange. In *Food Process Engineering and Technology*, pp 311–327, Elsevier.
- 48 Unuabonah, E. I., Omorogie, M. O. and Oladoja, N. A. (2019) Modeling in Adsorption: Fundamentals and Applications. In *Composite Nanoadsorbents*, pp 85–118, Elsevier.
- 49 Gebauer, K. and Tschöp, J. (2018) Chromatography Columns. In *Biopharmaceutical Processing*, pp 493–511, Elsevier.
- 50 Njoku, V. O. and Hameed, B. H. (2011) Preparation and characterization of activated carbon from corncob by chemical activation with H<sub>3</sub>PO<sub>4</sub> for 2,4-dichlorophenoxyacetic acid adsorption. *Chem. Eng. J.* **173**, 391–399.
- 51 Rai, M. K., Shahi, G., Meena, V., Meena, R., Chakraborty, S., Singh, R. S. and Rai, B. N. (2016) Removal of hexavalent chromium Cr (VI) using activated carbon prepared from mango kernel activated with H<sub>3</sub>PO<sub>4</sub>. *Resour.-Effic. Technol.* **2**, S63–S70.
- 52 Niazi, N. K., Bibi, I., Shahid, M., Ok, Y. S., Burton, E. D., Wang, H., Shaheen, S. M., Rinklebe, J. and Lüttge, A. (2018) Arsenic removal by perilla leaf biochar in aqueous solutions and groundwater: An integrated spectroscopic and microscopic examination. *Environ. Pollut.* **232**, 31–41.
- 53 Kobya, M. (2004) Adsorption, Kinetic and Equilibrium Studies of Cr(VI) by Hazelnut Shell Activated Carbon. *Adsorpt. Sci. Technol.* **22**, 51–64.
- 54 Zhong, D., Jiang, Y., Zhao, Z., Wang, L., Chen, J., Ren, S., Liu, Z., Zhang, Y., Tsang, D. C. W. and Crittenden, J. C. (2019) pH Dependence of Arsenic Oxidation by Rice-Husk-Derived 3 Biochar: Roles of Redox-Active Moieties. *Environ. Sci. Technol.* **53**, 9034–9044.
- 55 Yang, X., Xia, L., Li, J., Dai, M., Yang, G. and Song, S. (2017) Adsorption of As(III) on porous hematite synthesized from goethite concentrate. *Chemosphere* **169**, 188–193.
- 56 Hashemzadeh, M., Nilchi, A. and Hassani, A. H. (2019) Synthesis of novel surface-modified hematite nanoparticles for lead ions removal from aqueous solution. *Mater. Chem. Phys.* **227**, 279–290.
- 57 Kumari, M., Pittman, C. U. and Mohan, D. (2015) Heavy metals [chromium (VI) and lead (II)] removal from water using mesoporous magnetite (Fe<sub>3</sub>O<sub>4</sub>) nanospheres. *J. Colloid Interface Sci.* **442**, 120–132.
- 58 Rajput, S., Pittman, C. U. and Mohan, D. (2016) Magnetic magnetite (Fe<sub>3</sub>O<sub>4</sub>) nanoparticle synthesis and applications for lead (Pb<sup>2+</sup>) and chromium (Cr<sup>6+</sup>) removal from water. *J. Colloid Interface Sci.* **468**, 334–346.
- 59 Urbano, B. F., Rivas, B. L., Martinez, F. and Alexandratos, S. D. (2012) Water-insoluble polymer–clay nanocomposite ion exchange resin based on N-methyl-d-glucamine ligand

- groups for arsenic removal. *React. Funct. Polym.* **72**, 642–649.
- 60 Dinu, M. V., Dragan, E. S. and Trochimczuk, A. W. (2009) Sorption of Pb(II), Cd(II) and Zn(II) by iminodiacetate chelating resins in non-competitive and competitive conditions. *Desalination* **249**, 374–379.
- 61 Noorani, S. (2013) Arsenic Contamination in Groundwater. *UNICEF Curr. Issues* **2**, 1–4.
- 62 Jain, C. K. and Ali, I. (2000) Arsenic: occurrence, toxicity and speciation techniques. *Water Res.* **34**, 4304–4312.
- 63 Smedley, P. L. and Kinniburgh, D. G. (2002) A review of the source, behaviour and distribution of arsenic in natural waters. *Appl. Geochem.* **17**, 517–568.
- 64 World Health Organization. (2017) Guidelines for drinking-water quality.
- 65 Nicomel, N., Leus, K., Folens, K., Van Der Voort, P. and Du Laing, G. (2016) Technologies for Arsenic Removal from Water: Current Status and Future Perspectives. *Int. J. Environ. Res. Public. Health* **13**, 62.
- 66 Faria, M. C. S., Rosemberg, R. S., Bomfeti, C. A., Monteiro, D. S., Barbosa, F., Oliveira, L. C. A., Rodriguez, M., Pereira, M. C. and Rodrigues, J. L. (2014) Arsenic removal from contaminated water by ultrafine  $\delta$ -FeOOH adsorbents. *Chem. Eng. J.* **237**, 47–54.
- 67 Altundoğan, H. S., Altundoğan, S., Tümen, F. and Bildik, M. (2002) Arsenic adsorption from aqueous solutions by activated red mud. *Waste Manag.* **22**, 357–363.
- 68 Akin, I., Arslan, G., Tor, A., Ersoz, M. and Cengeloglu, Y. (2012) Arsenic(V) removal from underground water by magnetic nanoparticles synthesized from waste red mud. *J. Hazard. Mater.* **235–236**, 62–68.
- 69 Mamindy-Pajany, Y., Hurel, C., Marmier, N. and Roméo, M. (2011) Arsenic (V) adsorption from aqueous solution onto goethite, hematite, magnetite and zero-valent iron: Effects of pH, concentration and reversibility. *Desalination* **281**, 93–99.
- 70 He, J., Bardelli, F., Gehin, A., Silvester, E. and Charlet, L. (2016) Novel chitosan goethite bionanocomposite beads for arsenic remediation. *Water Res.* **101**, 1–9.
- 71 Urbano, B. F., Rivas, B. L., Martinez, F. and Alexandratos, S. D. (2012) Equilibrium and kinetic study of arsenic sorption by water-insoluble nanocomposite resin of poly[N-(4-vinylbenzyl)-N-methyl-d-glucamine]-montmorillonite. *Chem. Eng. J.* **193–194**, 21–30.
- 72 Koseoglu, P., Yoshizuka, K., Nishihama, S., Yuksel, U. and Kabay, N. (2011) Removal of Boron and Arsenic from Geothermal Water in Kyushu Island, Japan, by Using Selective Ion Exchange Resins. *Solvent Extr. Ion Exch.* **29**, 440–457.
- 73 Brion-Roby, R., Gagnon, J., Deschênes, J.-S. and Chabot, B. (2018) Investigation of fixed bed adsorption column operation parameters using a chitosan material for treatment of arsenate contaminated water. *J. Environ. Chem. Eng.* **6**, 505–511.
- 74 Dambies, L., Salinaro, R. and Alexandratos, S. D. (2004) Immobilized N-Methyl-d-glucamine as an Arsenate-Selective Resin. *Environ. Sci. Technol.* **38**, 6139–6146.
- 75 Shih, Y.-J., Huang, R.-L. and Huang, Y.-H. (2015) Adsorptive removal of arsenic using a

- novel akhtenskite coated waste goethite. *J. Clean. Prod.* **87**, 897–905.
- 76 Langmuir, I. (1916) The Constitution and Fundamental Properties of Solids and Liquids. Part I. Solids. *J. Am. Chem. Soc.* **38**, 2221–2295.
- 77 Lagergren, S. (1989) Zur theorie der sogenannten adsorption gelöster stoffe. *K. Sven. Vetenskapsakademiens Handl.* **24**, 1–39.
- 78 Ho, Y. S. and McKay, G. (1999) Pseudo-second order model for sorption processes. *Process Biochem.* **34**, 451–465.
- 79 Barnie, S., Zhang, J., Wang, H., Yin, H. and Chen, H. (2018) The influence of pH, co-existing ions, ionic strength, and temperature on the adsorption and reduction of hexavalent chromium by undissolved humic acid. *Chemosphere* **212**, 209–218.
- 80 Chen, Y., An, D., Sun, S., Gao, J. and Qian, L. (2018) Reduction and Removal of Chromium VI in Water by Powdered Activated Carbon. *Materials* **11**, 269.
- 81 Enniya, I., Rghioui, L. and Jourani, A. (2018) Adsorption of hexavalent chromium in aqueous solution on activated carbon prepared from apple peels. *Sustain. Chem. Pharm.* **7**, 9–16.
- 82 Cavaco, S. A., Fernandes, S., Quina, M. M. and Ferreira, L. M. (2007) Removal of chromium from electroplating industry effluents by ion exchange resins. *J. Hazard. Mater.* **144**, 634–638.
- 83 Çengelöglu, Y., Tor, A., Kir, E. and Ersöz, M. (2003) Transport of hexavalent chromium through anion-exchange membranes. *Desalination* **154**, 239–246.
- 84 Yamaguchi, A., Nishihama, S. and Yoshizuka, K. (2010) Separation of Tetramethyl Ammonium Hydroxide in Waste Water with Ion Exchange Using Activated Carbon Prepared by Bamboo. *J. Ion Exch.* **21**, 375–381.
- 85 Park, S.-J. and Jang, Y.-S. (2002) Pore Structure and Surface Properties of Chemically Modified Activated Carbons for Adsorption Mechanism and Rate of Cr(VI). *J. Colloid Interface Sci.* **249**, 458–463.
- 86 Wiryawan, A., Retnowati, R. and Burhan, R. Y. P. (2018) Method of analysis for determination of the chromium (Cr) species in water samples by spectrophotometry with diphenylcarbazide. *J. Environ. Eng. Sustain. Technol.* **05**, 37–46.
- 87 Biesinger, M. C., Payne, B. P., Grosvenor, A. P., Lau, L. W. M., Gerson, A. R. and Smart, R. St. C. (2011) Resolving surface chemical states in XPS analysis of first row transition metals, oxides and hydroxides: Cr, Mn, Fe, Co and Ni. *Appl. Surf. Sci.* **257**, 2717–2730.
- 88 Biesinger, M. C., Brown, C., Mycroft, J. R., Davidson, R. D. and McIntyre, N. S. (2004) X-ray photoelectron spectroscopy studies of chromium compounds. *Surf. Interface Anal.* **36**, 1550–1563.
- 89 Dubey, R., Bajpai, J. and Bajpai, A. K. (2015) Green synthesis of graphene sand composite (GSC) as novel adsorbent for efficient removal of Cr (VI) ions from aqueous solution. *J. Water Process Eng.* **5**, 83–94.

- 90 Bard, A. J., Parsons, R. and Jordan, J. (2017) *Standard Potentials in Aqueous Solution* 1st ed., Routledge.
- 91 Nethaji, S., Sivasamy, A. and Mandal, A. B. (2013) Preparation and characterization of corn cob activated carbon coated with nano-sized magnetite particles for the removal of Cr(VI). *Bioresour. Technol.* **134**, 94–100.
- 92 Bansal, M., Singh, D. and Garg, V. K. (2009) A comparative study for the removal of hexavalent chromium from aqueous solution by agriculture wastes' carbons. *J. Hazard. Mater.* **171**, 83–92.
- 93 Tang, S.-Y. and Qiu, Y.-R. (2019) Selective separation and recovery of heavy metals from electroplating effluent using shear-induced dissociation coupling with ultrafiltration. *Chemosphere* **236**, 124330.
- 94 Agrawal, A. and Sahu, K. (2006) Separation and recovery of lead from a mixture of some heavy metals using Amberlite IRC 718 chelating resin. *J. Hazard. Mater.* **133**, 299–303.
- 95 Atia, A. A., Donia, A. M. and Yousif, A. M. (2008) Removal of some hazardous heavy metals from aqueous solution using magnetic chelating resin with iminodiacetate functionality. *Sep. Purif. Technol.* **61**, 348–357.
- 96 Kovačević, D., Pohlmeier, A., Özbaş, G., Narres, H.-D. and Kallay, M. J. N. (2000) The adsorption of lead species on goethite. *Colloids Surf. Physicochem. Eng. Asp.* **166**, 225–233.
- 97 Rahimi, S., Moattari, R. M., Rajabi, L., Derakhshan, A. A. and Keyhani, M. (2015) Iron oxide/hydroxide ( $\alpha,\gamma$ -FeOOH) nanoparticles as high potential adsorbents for lead removal from polluted aquatic media. *J. Ind. Eng. Chem.* **23**, 33–43.
- 98 Liu, F., Li, L., Ling, P., Jing, X., Li, C., Li, A. and You, X. (2011) Interaction mechanism of aqueous heavy metals onto a newly synthesized IDA-chelating resin: Isotherms, thermodynamics and kinetics. *Chem. Eng. J.* **173**, 106–114.
- 99 Naushad, Mu., Mittal, A., Rathore, M. and Gupta, V. (2015) Ion-exchange kinetic studies for Cd(II), Co(II), Cu(II), and Pb(II) metal ions over a composite cation exchanger. *Desalination Water Treat.* **54**, 2883–2890.
- 100 Mittal, A., Naushad, Mu., Sharma, G., AlLothman, Z. A., Wabaidur, S. M. and Alam, M. (2016) Fabrication of MWCNTs/ThO<sub>2</sub> nanocomposite and its adsorption behavior for the removal of Pb(II) metal from aqueous medium. *Desalination Water Treat.* **57**, 21863–21869.
- 101 Faisal, A. A. H., Al-Wakel, S. F. A., Assi, H. A., Naji, L. A. and Naushad, Mu. (2020) Waterworks sludge-filter sand permeable reactive barrier for removal of toxic lead ions from contaminated groundwater. *J. Water Process Eng.* **33**, 101112.
- 102 Bagbi, Y., Sarswat, A., Mohan, D., Pandey, A. and Solanki, P. R. (2016) Lead (Pb<sup>2+</sup>) adsorption by monodispersed magnetite nanoparticles: Surface analysis and effects of solution chemistry. *J. Environ. Chem. Eng.* **4**, 4237–4247.

- 103 Wang, X. S., Lu, H. J., Zhu, L., Liu, F. and Ren, J. J. (2010) Adsorption of Lead(II) Ions onto Magnetite Nanoparticles. *Adsorpt. Sci. Technol.* **28**, 407–417.
- 104 Dongsheng, Z., Wenqiang, G., Guozhang, C., Shuai, L., Weizhou, J. and Youzhi, L. (2019) Removal of heavy metal lead(II) using nanoscale zero-valent iron with different preservation methods. *Adv. Powder Technol.* **30**, 581–589.
- 105 Mohamed, R., El-Maghrabi, H. H., Riad, M. and Mikhail, S. (2017) Environmental friendly FeOOH adsorbent materials preparation, characterization and mathematical kinetics adsorption data. *J. Water Process Eng.* **16**, 212–222.
- 106 Nassar, N. N. (2010) Rapid removal and recovery of Pb(II) from wastewater by magnetic nanoadsorbents. *J. Hazard. Mater.* **184**, 538–546.
- 107 Tavakoli, O., Goodarzi, V., Saeb, M. R., Mahmoodi, N. M. and Borja, R. (2017) Competitive removal of heavy metal ions from squid oil under isothermal condition by CR11 chelate ion exchanger. *J. Hazard. Mater.* **334**, 256–266.
- 108 Huang, H., Cheng, G., Chen, L., Zhu, X. and Xu, H. (2009) Lead (II) Removal from Aqueous Solution by Spent *Agaricus bisporus*: Determination of Optimum Process Condition Using Taguchi Method. *Water Air Soil Pollut* **11**.
- 109 Limousin, G., Gaudet, J.-P., Charlet, L., Szenknect, S., Barthès, V. and Krimissa, M. (2007) Sorption isotherms: A review on physical bases, modeling and measurement. *Appl. Geochem.* **22**, 249–275.
- 110 Lu, M., Zhang, Y., Zhou, Y., Su, Z., Liu, B., Li, G. and Jiang, T. (2019) Adsorption-desorption characteristics and mechanisms of Pb(II) on natural vanadium, titanium-bearing magnetite-humic acid magnetic adsorbent. *Powder Technol.* **344**, 947–958.
- 111 Febrianto, J., Kosasih, A. N., Sunarso, J., Ju, Y.-H., Indraswati, N. and Ismadji, S. (2009) Equilibrium and kinetic studies in adsorption of heavy metals using biosorbent: A summary of recent studies. *J. Hazard. Mater.* **162**, 616–645.

## List of Publication

1. Viet Anh HOANG, Syouhei NISHIHAMA and Kazuharu YOSHIZUKA (2019) Adsorptive Removal of Arsenic from Aqueous Environment. Journal of Chemical Engineering of Japan, **52**, 829–834.  
[DOI: 10.1252/jcej.19we084](https://doi.org/10.1252/jcej.19we084)
2. Viet Anh HOANG, Ya Wen CHEN, Syouhei NISHIHAMA, Kazuharu YOSHIZUKA and Ya-Fen WANG (2020) Reductive Adsorption of Chromium(VI) by Coal-Based Activated Carbon. Journal of Chemical Engineering of Japan, **53**, 599–607.  
[DOI: 10.1252/jcej.19we232](https://doi.org/10.1252/jcej.19we232)
3. Viet Anh HOANG, Syouhei NISHIHAMA, and Kazuharu YOSHIZUKA (2021) Selective Adsorption of Lead(II) from Aqueous Solution. Environmental Technology, in press.  
[DOI: 10.1080/09593330.2020.1866088](https://doi.org/10.1080/09593330.2020.1866088)

## Related work

1. Viet Anh HOANG, Ya Wen CHEN, Syouhei NISHIHAMA, Kazuharu YOSHIZUKA and Ya-Fen WANG (2021) Reductive Adsorption of Chromium(VI) with Activated Carbon MATEC Web of Conference, 333, 04004.  
[DOI:10.1051/mateconf/202133304004](https://doi.org/10.1051/mateconf/202133304004)  
The 18<sup>th</sup> Asian Pacific Confederation of Chemical Engineering Congress (APCCChE 2019)

## **Acknowledgement**

First and foremost, I would like to express my deepest appreciation to Professor Syouhei Nishihama, my supervisor, for his dedicated support and guidance. I feel very proud of being his first Ph.D. student. Thank you for always carrying and supporting me in my study as well as my life. His responsive feedbacks and tireless efforts in correcting my manuscripts and dissertation are very meaningful to me.

I would like to extend my sincere gratitude to Professor Kazuharu Yoshizuka for his kind advice and helpful discussion throughout this work. His analytical thinking, enduring enthusiasm for academic science and perseverance have always been an inspiration to me.

My special thanks go to Associate Professor Mitsuharu Terashima and Professor Nobuhiro Okada in jury committee for their valuable comments and suggestions on my research.

I wish to thank my lab-mate in Separation Engineering Laboratory for supporting my experiment. I would like to thank my friends especially Vietnamese group for their sharing and their help during my time in Japan. I wish you achieve all your goals and success in your future research career.

Last but not the least, I am very grateful to my parents and my sister for their love and for always encouraging and trusting my decisions.